PROTEIN PHOSPHATASE 2A METHYLATION AND STABLE LATENCY

By Vitali Stanevich

A dissertation submitted in partial fulfillment of

the requirements of the degree of

Doctor of Philosophy

(Biophysics)

at the

UNIVERSITY OF WISCONSIN-MADISON

2013

Date of final oral examination: 5/24/13

The dissertation is approved by the following members of the Final Oral Committee:

Yongna Xing, Assistant Professor, Oncology

Katrina T. Forest, Professor, Bacteriology

Elaine T. Alarid, Associate Professor, Oncology

Ivan Rayment, Professor, Biochemistry

Janet E. Mertz, Professor, Oncology

Acknowledgements

I would like to thank my advisor, Dr. Yongna Xing, for her support, advice and encouragement in development of my scientific efficiency and critical thinking. I would also like to thank my committee members, Drs. George N. Phillips Jr., Katrina T. Forest, Elaine T. Alarid, Ivan Rayment, and Janet E. Mertz for their time and advice.

I am grateful to all the past and present members of Xing lab for not only providing me with sound advice and helpful insights, but making the lab an enjoyable place to work: Dr. Feng Guo, Dr. Ken Satyshur, Dr. Guanlan Xu, Patrick Menden, Nathan Wlodarchak, Lisa Burdette, Chengyong He, Dr. Xinchang Zhou and Rituparna Sengupta. I would like to especially thank Dr. Li Jiang for providing a good sounding board regarding my research and always being there to help with my experiments. I would also like to thank Dr. Darrell McCaslin, Dr. Gregory A. Barrett-Wilt and all the personnel of the McArdle Laboratory for Cancer Research for their assistance with my experiments.

I would like to thank my friends and family. I am grateful to Ivan and Anastasia Birukou for convincing me to pursue the PhD degree in the USA and providing help with the application process. I am thankful to Patrick Menden for helping me to settle down in Madison and being a reliable friend for all my time here. I would like to thank Christina Warren and her family for making my "afterlab life" memorable and fun. Finally, I would like to thank my parents, grandparents and all other relatives: my current progress is a direct result of their support and understanding during all stages of my life.

Abstract

A structure-based approach was utilized to study the processes involved in maturation and maintenance of protein phosphatase 2A (PP2A).

I used X-ray diffraction to study the interaction between PP2A and leucine carboxyl methyl transferase 1 (LCMT-1). The crystal structure of the complex between the PP2A catalytic subunit (PP2Ac or C-subunit) and LCMT-1 shows that LCMT-1 binding relies on the interaction with two distinct regions of PP2Ac: the carboxy-terminal unstructured region (C-tail) and the active site. Methylation by LCMT-1 is dependent on the active conformation of the PP2A active site. This establishes an important mechanism for the quality control in the process of PP2A holoenzyme assembly: selective binding of LCMT-1 to active PP2Ac ensures that only the active and properly folded PP2Ac molecules are assembled into the functional holoenzyme, and efficiently converts activated PP2Ac molecules into holoenzymes while minimizing the uncontrolled phosphatase activity of free PP2Ac.

I further characterized how different regulatory proteins and factors affect PP2A methylation by LCMT-1. Notably, we showed that the PP2A scaffolding subunit (A-subunit) enhances methylation of PP2Ac by three mechanisms: 1) restriction of PP2Ac C-tail which presumably facilitates entry of C-tail into the active site of LCMT-1; 2) weak charge-charge interactions between the A-subunit N-terminal ridge and a negative surface on LCMT-1; and 3) stabilization of the overall PP2Ac fold that is linked to the central β-sheet and likely prevents allosteric relay of conformational changes via the central β-sheets.

I investigated the interaction between PP2A and α4-protein by X-ray crystallography in combination with biophysical methods. α4 binding requires partial unfolding of PP2Ac involving two structural elements near the active site: helix 120-127 ("helix switch") and loop 183-195 ("loop switch"). Hydrogen/deuterium exchange (HDX) mass spectrometry (MS) confirms crystallographic observations and indicates that the inner surface of PP2Ac becomes exposed upon inactivation and interaction with α4. α4 binding protects PP2Ac from degradation by two mechanisms: it sterically hinders Lys-41 from polyubiquitination and blocks aggregation of the partially folded PP2Ac by shielding the exposed inner surface. The mode of PP2Ac:α4 interaction suggests a mechanism for stable PP2Ac latency.

Elucidating the underlying molecular processes involved in formation of PP2A holoenzymes is crucial for understanding of PP2A regulation in cellular function and provides insights into the multiple pathological states triggered by PP2A deregulation.

Table of contents

List of Abbreviations

PSP	Protein Serine/Threonine Phosphatases
PTP	Protein Tyrosine Phosphatases
PPP	Phosphoprotein Phosphatases
PP1	Protein Phosphatase 1
PP2A	Protein Phosphatase 2A
PP2Ac	Protein Phosphatase 2A C-subunit
PP4	Protein Phosphatase 4
PP6	Protein Phosphatase 6
LCMT-1	Leucine Carboxymethyltransferase 1
PME-1	Phosphatase Methylesterase 1
PPM1	Protein Phosphatase Methyltransferase 1
PTPA	Phosphotyrosyl Phosphatase Activator
TIPRL	TIP41, TOR signaling pathway regulator- like
IGBP1	Immunoglobulin-α4-binding protein 1
TAP42	Two A-associated protein of 42kDa
MID-1	Midline 1
TOR	Target of Rapamycin
C-tail	Carboxyterminal tail of PP2Ac
HEAT-repeat	Huntingtin-Elongation-A subunit-TOR repeat
MT-domain	Methyltransferase domain

nPP2Ac	N-terminal sub-domain of PP2Ac
ITC	Isothermal Titration Calorimetry
HDX-MS	Hydrogen-Deuterium Exchange Mass-Spectrometry
ICP-MS	Inductively Coupled Plasma Mass Spectrometry
CD	Circular Dichroism
PPi	Pyrophosphate
EDTA	Ethylenediaminetetraacetic acid
DTT	Dithiothreitol
pNPP	p-nitrophenyl phosphate
SAM	S-adenosyl methionine
SAH	S-adenosyl homocysteine
GST	Glutathionine S-transferase
MBP	Maltose-binding protein
K_m	Michaelis Constant
V_{max}	Maximum Velocity
K_{cat}	Catalytic Constant
K_d	Dissociation Constant
PDB	Protein Data Bank
APS LS-CAT	Advanced Photon Source Life Sciences Collaboration Access Team

Chapter 1: Introduction

1.1. Phosphorylation and its function in eukaryotic cell.

Post-translational modifications constitute an important layer of enzyme activity regulation and protein-protein interaction. A majority of covalent modifications are reversible and controlled by two groups of enzymes with opposing activities that regulate the level of modifications. Reversible modifications provide cells a quick and efficient way to alter the physico-chemical and functional properties of protein molecules in response to cellular signaling or changes in cellular function. Numerous different covalent modifications have been identified and characterized, and many more are expected to be discovered. Among them, phosphorylation of proteins is one of the most common and well-studied modifications.

Decades of research since initial discovery of protein phosphorylation (1,2) have shown that reversible phosphorylation of proteins, catalyzed by kinases and phosphatases, constitutes a major form of signaling and an essential mechanism of regulation in all living organisms. Phosphorylation mainly occurs in eukaryotic cells on three hydroxyl-containing amino acids: serine, threonine, and tyrosine, of which serine is the predominant target (Fig 1. 1).

The attachment and removal of phosphate groups may have direct or indirect effects on the protein function. Due to obvious reasons, the direct effects, such as control of allosteric conformations or blocking of the catalytic site, were revealed and characterized first (3-5). Later, phosphatases were shown to be involved in the regulation of protein-protein interactions, a process which is fulfilled by phosphate-sensing protein modules. Src-homology domain 2, phospho-tyrosine binding domain, and 14-3-3 proteins are examples of proteins which recognize phosphorylated residues in the context of specific sequences. Almost all cellular processes are regulated by phosphorylation including, but not limited to, metabolic processes, cell cycle

control, organization of cytoskeleton, cell adhesion and gene regulation (5). As a consequence of broad and abundant protein phosphorylation, 30% of eukaryotic proteins are phosphorylated and 3% of higher eukaryotic genome encodes phosphatases and kinases (6).

1.2. Classification and catalytic mechanism of Ser/Thr protein phosphatases

Protein phosphatases are encoded by a small number of gene superfamilies, with each member derived from divergent evolution. This is typical for signaling proteins. Protein phosphatases can be classified based on their substrate specificity into protein serine/threonine phosphatases (PSP), protein tyrosine phosphatases (PTP) and dual-specificity phosphatases. The human genome contains 107 putative PTPs(7) and approximately 30 PSP (8). Whereas the numbers of PTPs and protein tyrosine kinases (PTK) roughly match each other, the number of protein serine/threonine kinases (PSKs) exceeds the number of PSPs by approximately fourteen times (8). As clarified in the discussion below, this difference can be explained by the diverse oligomeric forms of PSPs.

At the moment, PSPs are classified into three distinct families: phosphoprotein phosphatases (PPPs), metal-dependent protein phosphatases (PPMs) and the aspartate-based phosphatases represented by FCP/SCP (TFIIF-associating component of RNA polymerase II CTD phosphatase/small CTD phosphatase) (Fig. 1.2). Some members of PPP family function as holoenzymes and are characterized by the presence of regulatory subunits. Representative members of the PPP family include protein phosphatase 1 (PP1), PP2A, PP2B (commonly known as calcineurin), PP4, PP5, PP6, and PP7, among which PP2A, PP4 and PP6 share a high sequence similarity (60% identity) and are known as PP2A-like phosphatases (Fig. 1.3). The phosphatases in the PPM family are dependent on Mn^{2+}/Mg^{2+} ions, and common members

include PP2C and pyruvate dehydrogenase phosphatase. Although both PPPs and PPMs utilize catalytic metal ions for catalysis, contrary to PPPs, PPMs do not function as oligomeric holoenzymes and control specificity by regulatory domains or sequences. In contrast to other PSPs, FCP/SCP uses an aspartate-based mechanism for catalysis (9,10). The only known substrate for FCP/SCP is the C-terminal domain of RNA polymerase II, which contains tandem repeats of a serine-rich heptapeptide (11). The conserved structural core of aspartate-based phosphatases is the FCPH domain (FCP homology), and SCP also contains a conserved BRCT domain following the FCPH domain (12).

Despite their less conserved primary sequences, all Ser/Thr phosphatases in the PPP family have a highly similar 3D structure and enzymatic mechanism (13). The phosphatases in this family are metalloenzymes with stably bound catalytic metal ions at the active site chelated by six conserved residues (Asp, Asn, and His) (Fig. 1.4). While the identity of proper cellular catalytic metal ions remains to be determined, Mn^{2+}, Fe^{2+}, and Zn^{2+} had been suggested to be potential catalytic metal ions. The sidechain of Asp and a water molecule bridge two metal ions to create a binuclear catalytic center. Dephosphorylation reaction proceeds by S_N2 mechanism with metal-bound water acting as a nucleophile to attack phosphorous atom of the substrate. Mutational and biochemical studies have shown that replacement or removal of residues coordinating catalytic metal ion leads to overproduction of insoluble or inactive protein (14,15). Thus, the metal ions play a dual role in the function of the PPP family of phosphatases: catalyzing dephosphorylation and maintaining the native conformation of the active site and the overall protein fold.

1.3. PP2A phosphatase is an important signaling protein in eukaryotic cells and a pharmaceutical target

The PP2A-like phosphatases of the PPP family consist of PP4, PP6 and PP2A phosphatase itself. The catalytic subunits of these enzymes share a high level of sequence similarity containing approximately 60% identical residues (Fig. 1.3). PP2A is the most ubiquitous and best studied phosphatase among the PP2A-like phosphatases. In some tissues, PP2A may constitute up to 1% of total protein and, together with PP1, a closely related PPP family of phosphatase, contributes up to 90% of Ser/Thr phosphatase activity in cells (16).

PP2A has a well-established role in many important cellular processes, including development (17), cell proliferation and death (18), cell cycle control (19,20), cell mobility (21), DNA repair (22), cytoskeleton dynamics (23) and numerous signaling pathways (24-29). Deregulation of PP2A-like phosphatases has been linked to several types of cancer (16,28,30-33), making them important targets in anticancer therapy (34,35).

The diverse cellular functions of PP2A had caused skepticism about design of efficient drugs targeting the catalytic activity of PP2A. Nonetheless, after decades of research, the PP2A inhibitor, fostriescin, entered Phase I of clinical trials as an anticancer drug (35,36). Further studies revealed that fostriescin acts as an inhibitor of PP2A and PP4, inducing premature entry of cells into mitosis followed by apoptosis (37). In fact, other inhibitors of PP2A, such as okadaic acid and calyculin A, exhibit similar effect to fostriescin, confirming that manipulation of PP2A activity is a promising anti-tumor strategy (36). Another natural product known for its anti-tumor properties via PP2A inhibition is cantharidin. This drug exhibits differential inhibitory

effects toward numerous Ser/Thr phosphatases, with the most potent effect on PP4 and PP2A (38,39).

Inhibition is not the only way for pharmacological manipulation of PP2A function. Due to the involvement of PP2A in many signaling pathways, for certain types of cancer activation of PP2A has more prominent therapeutic effect than does its inhibition (35). The immunodepressant FTY720 is such an example of a PP2A activator, which can be used as a therapeutic drug (40). The exact mechanism of action of this compound is unclear, but there is evidence for its influence on the PP2A holoenzyme formation. Ceramide is another compound with documented positive effect on PP2A activity (41,42).

In overall, due to the involvement of PP2A in multiple cellular processes, understanding the mechanisms of activation and inactivation and looking for new, more precise ways to manipulate its activity is of great importance from both scientific and therapeutic points of view.

1.4. Composition of PP2A phosphatases and functioning as holoenzymes

Cellular PP2A exists in two general forms – a heterodimeric core enzyme and a heterotrimeric holoenzyme (43) (Fig. 1.5). The PP2A core enzyme consists of a scaffolding subunit and a catalytic subunit. Both the scaffolding and catalytic subunits have two isoforms, α and β, with the α-isoform about 10-fold more abundant than the β-isoform. For simplicity, the A- and C-subunits used in this study are the α-isoforms. The third subunit of the holoenzyme is a variable regulatory subunit (B-subunit), which controls substrate specificity and subcellular localization of PP2A. The regulatory subunits are highly diverse, leading to formation of diverse trimeric PP2A holoenzymes.

Similar to other Ser/Thr phosphatases of the PPP family, the catalytic subunit of PP2A contains two central β-sheets with eleven β-strands, flanked by seven α-helices on the one side and a subdomain consisting of three α-helices and three β-strands on the other side (5). The protein loops that emanate from the central β-sheets on the top of the structure form the active site (Fig. 1.4). The active site loops harbor six highly conserved metal-chelating residues that stably chelate two catalytic metal ions (13,44). Despite its high structural similarity to other PPP family of phosphatases, the protein loops of PP2A are significantly different from those of the other phosphatases. Alignment of PP2A and PP1 catalytic subunits showed that these differences result in a relatively high root-mean-square-deviation (RMSD) of 3.38 Å over 284 Cα atoms (8). The deviation in the sequence and structure of these protein loops confers specific physiological function and regulation of PP2A.

The A-subunit of PP2A is a HEAT (huntingtin-elongation-A subunit-TOR) repeat protein containing 15 HEAT repeats and functions as a scaffold protein recruiting both B- and C-subunits for the formation of trimeric PP2A holoenzymes. In each holoenzyme, the C-terminal HEAT repeats 10-15 of the A-subunit interact with the catalytic subunit, while the N-terminal HEAT repeats 1-8 are occupied by a regulatory subunit (45,46). The A-subunit possesses intrinsic structural flexibility, which is important for formation of diverse holoenzymes and for regulation of substrate access to the PP2A active site (45,47). Thus, unlike kinases, PP2A targets broad cellular substrates by the formation of diverse trimeric holoenzymes (43).

The regulatory subunits can be classified into four major families: B, B', B'', and B'''. In total, fifteen genes have been identified that encode at least twenty six different PP2A regulatory subunits via alternative splicing (16). The levels of regulatory subunits are distinctly different in

different tissues, cell types, and different stages of the cell cycle, enabling precise spatial and temporal regulation of PP2A activity. The regulatory subunits of PP2A are highly diverse in their primary sequence and three-dimensional structure, despite their overlapping binding-site on the N-terminal HEAT-repeats of the A-subunit. The crystal structures of PP2A holoenzymes containing representative members from B (48), B′ (45,46), and, recently, B″ (49) have been reported.

1.5. Regulation of PP2A holoenzyme assembly by methylation of the C-subunit

PP2A holoenzyme assembly is a highly regulated process which is the subject of regulation for diverse cellular and environmental signals. The crystal structure of a PP2A holoenzyme suggests an important role of the C-subunit carboxy-terminus (further referred as C-tail) in holoenzyme assembly (45). Based on the evidence provided by numerous biochemical and cell biology experiments, it was concluded that post-translational modifications of C-tail are of utmost importance for holoenzyme assembly and B-subunits selection (50). These modifications include phosphorylation of Thr-304 (51,52) and Tyr-307 (51,53,54) and carboxymethylation of Leu-309 (55,56).

Reversible methylation of the PP2A core enzyme is a conserved and essential regulatory mechanism (57-60). Methylation of the carboxy-terminal Leu-309 in a conserved $TPDYFL_{309}$ motif of the PP2A C-subunit has been shown to enhance the affinity of the PP2A core enzyme with a fraction of the B-subunits (59) (Fig. 1.6). Thus, changes in PP2A methylation appear to regulate formation of different PP2A complexes and, consequently, shift the specificity of PP2A phosphatase activity in cells. To support this notion, blocking PP2A methylation in yeast caused a set of phenotypes that are consistent with decreased formation of PP2A holoenzymes (57). It

has also been demonstrated that the methylation levels of PP2A changed during the cell cycle, suggesting a critical role of methylation in cell cycle regulation (60). Changes in this peptide motif also affected interaction of the C-subunit with α4 protein, presumably through alteration of methylation (29). On the other hand, it was determined that overexpession of α4 leads to increased methylation of the PP2A catalytic subunit in COS-1 cells (61).

PP2A methylation is essential for cell function as knockout of LCMT-1 (60) or PME-1 (62) leads to apoptotic cell death, proving that reversible PP2A methylation is indispensable for cell function. Consistent with this notion, the LCMT-1 activity was shown to be essential for the tumor-suppression activity of PP2A (26). Interestingly, it has been suggested that LCMT-1 activity is dependent on the level of homocysteine, which, in turn, is linked to folate and vitamin B_{12} metabolism (63). This interdependence, potentially, may lead to decreased holoenzyme assembly (especially B-subunit containing) in the absence of these vitamins, which is linked to the development of Alzheimer's disease (63-65) and cancer (66).

1.6. Roles of PTPA in the biogenesis of PP2A

The catalytic subunit of PP2A undergoes several molecular events: 1) folding, 2) activation, which includes selective loading of active site metals, 3) formation of core enzyme, and 4) methylation, before assembly into a functional PP2A holoenzyme. As described above, methylation of the C-subunit is important for holoenzyme biogenesis: it promotes assembly of PP2A core enzyme with regulatory B-subunits. However, besides enzymes directly responsible for reversible methylation, LCMT-1 and PME-1, there are other PP2A interacting proteins involved in catalytic subunit maturation: phosphotyrosyl phosphatase activator (PTPA), TIPRL, and α4.

The studies in yeast provided insights into the biological function of PTPA. The yeast genome encodes two PTPA homologs: Rrd1 and Rrd2. They are involved in diverse aspects of cellular function, including cell cycle progression (67,68), stress response (69,70), mitosis (71), and transcription (72-74). Rrd1 and Rrd2 were shown to specifically interact with the yeast homologs of PP2A (Pph21/22) and PP2A-like phosphatases, PP4 (Pph3) and PP6 (Sit4) (75,76), which likely underlies the cellular function of Rrd1 and Rrd2. In mammalian cells, knockdown of PTPA results in a phenotype similar to PP2A-deficiency and leads to transformation (26) or apoptosis (77), depending on the cell type.

Despite a plethora of cell biology experiments that demonstrate the importance of PTPA in cellular function, the exact mechanism and function of PTPA remain to be understood. Three mechanisms of PTPA action have been proposed: 1) *cis/trans* peptidyl-prolyl isomerase activity toward Pro-190 of PP2Ac; 2) altering substrate preferences; and 3) stabilizing an active conformation of the PP2Ac active site. The first theory is supported by the crystal structure of the yeast PTPA analog, Rrd1 (Ypa1), co-crystallized with a PPIase peptide substrate (78). The structure-based mutational analysis showed that Ypa1 residues involved in peptide binding are also important for the biological function of PTPA in yeast. Although possible, so far this mechanism of PTPA action lacks rigorous biochemical characterization or extended examination in mammalian cells.

PTPA was also believed to modulate the substrate specificity of PP2A (79). *In vitro*, PTPA stimulates the basal tyrosyl phosphatase activity of PP2A core enzyme in the presence of Mg^{2+}/ATP, which relies on ATP hydrolysis that occurs only in the presence of both PTPA and PP2A (80). High concentration of PTPA was shown to inhibit the serine/threonine phosphatase

activity of PP2Ac. Recent results from our laboratory indicate that PTPA is involved in folding of the PP2A active site and, as a consequence, facilitates loading of the metal ions (81). This is supported by the structure of human PTPA in complex with PP2A, where PTPA interacts with the active site of PP2A (81). Current experiments suggest that the ATPase activity is required for the selective loading of proper metal ions into the active site of PTPA. Studies in this thesis further support this model: at a molar concentration comparable to PP2Ac, PTPA enhances both the phosphatase activity and methylation of PP2Ac via interactions between the active site and PP2A methyltransferase (LCMT-1).

1.7. α4 was considered a noncanonical PP2A subunit

As described earlier, a majority of PP2A *in vivo* exists as trimeric complexes known as holoenzymes, each containing a catalytic (C), scaffolding (A) and regulatory (B) subunit. In addition to holoenzymes, a small portion of PP2A is found complex with α4, displacing regulatory and scaffolding subunits. Thus, the α4 protein was considered to be a noncanonical PP2A subunit. PP2A also associates with TIPRL (82,83), resulting in trimeric α4:TIPRL:PP2Ac complexes. Remarkably, binding of either of these proteins excludes binding of scaffolding A and regulatory B subunits (82,84,85). Although well-documented by numerous cell-biology experimental reports, the functions of α4 and TIPRL in PP2A biogenesis are not fully understood.

α4 is also known as immunoglobulin-α4-binding protein 1 (IGBP1), and is involved in regulation of T and B cell development. The association of α4 with PP2A can range from 2 to 10% of total PP2A depending on the cell cycle stage, cell condition and type (18,82,84,86,87). In yeast, the binding between α4 (*tap42*) and PP2A can be disrupted by rapamycin, potentially due

to down-regulation of Target of Rapamycin (TOR) signaling (88,89). In mammalian cells, however, the effect of rapamycin on the interaction between α4 and PP2Ac is controversial; it was observed in some studies (18,84,86,90), but not in others (61,85,91-93).

Until recently, the biological consequences of the α4-PP2Ac interaction remained not completely understood. α4 was recognized as a regulator of PP2A activity, but it increases the phosphatase activity toward some substrates and decreases it toward others (84,87,92,94-97). Further studies showed that recombinant PP2A and PP6 co-expressed with α4 in insect cells have decreased activity toward both p-nitrophenyl phosphate (pNPP) and myelin basic protein (97).

In recent years, it has been recognized that α4 may play a role in modulating the population of PP2A complexes, rather than directly controlling their specificity toward certain substrates. This conclusion was supported by the fact that the inactive PP2A mutant, H118N, exhibits higher affinity toward α4 than the PP2A A-subunit (98). At higher temperatures, α4 renders the catalytic subunit of PP2A enzymatically inactive, but protects it from proteasome degradation (87). α4 was long known to interact with MID1, a E3-ubiquitin ligase (96,99), and interaction between PP2A and α4 was shown to prevent PP2A polyubiquitination by MID1 (Fig. 1.8) (100). Lys-41 of PP2A Cα-subunit is likely a potential ubiquitination site, as indicated by a global analysis of lysine ubiquitination (101).

1.8. Figures and tables

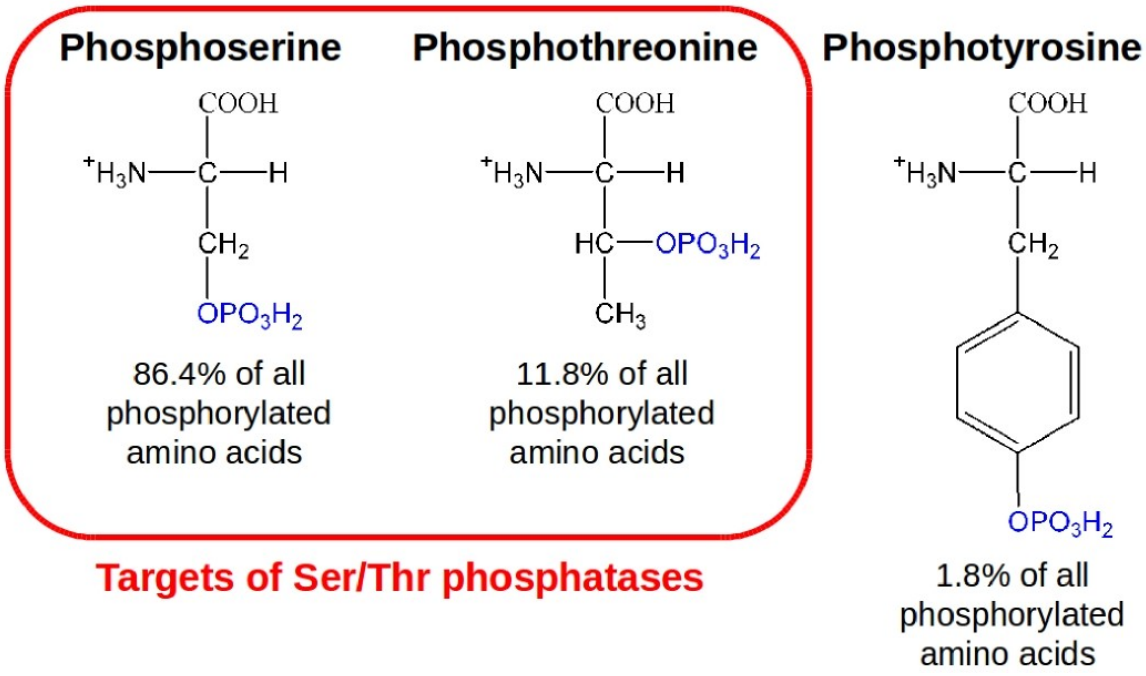

Figure 1.1. Substrates of protein phosphatases. Substrates of Ser/Thr phosphatases are highlighted.

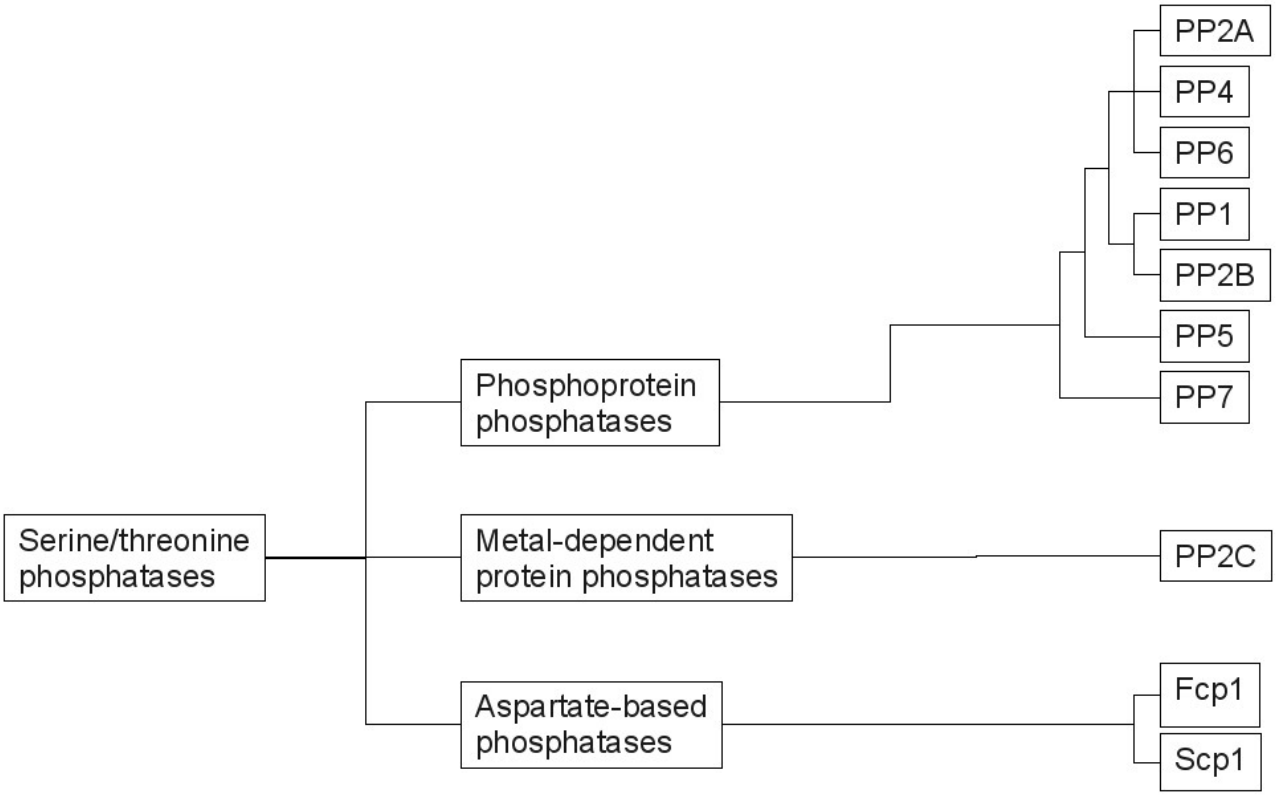

Figure 1.2. Classification of Ser/Thr phosphatases. Based on sequence similarity and catalytic mechanism Ser/Thr phosphatases can be divided into 3 classes, which can be further subdivided into families.

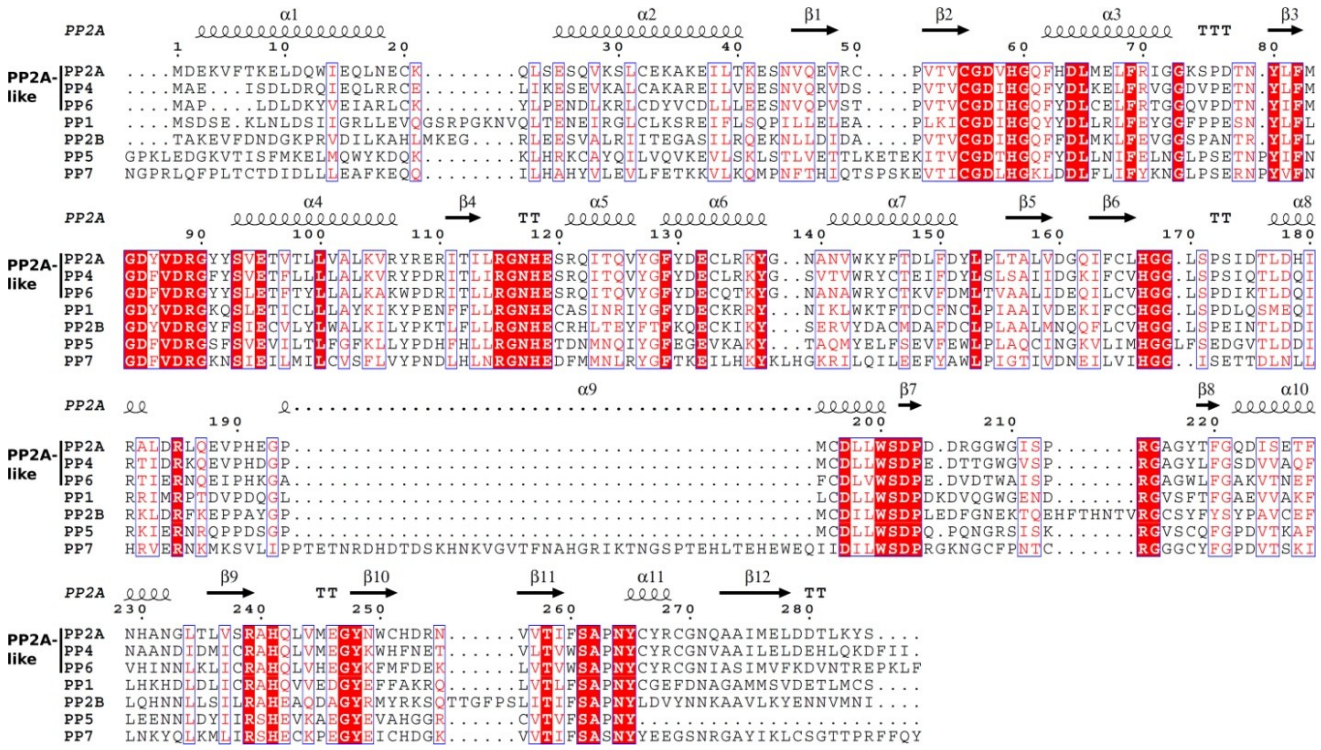

Figure 1.3. Alignment of PPP family of Ser/Thr phosphatases. PP2A, PP4 and PP6 are indicated as PP2A-like phosphatases. Secondary structure of PP2Ac derived from the structure of B' holoenzyme (PDB ID: 2NPP). α-helices are shown as spirals and labeled α1 to α11. β-strands are shown as arrows and numbered β1 to β12. Regions of high similarity are highlighted in pink and identical regions are highlighted in red.

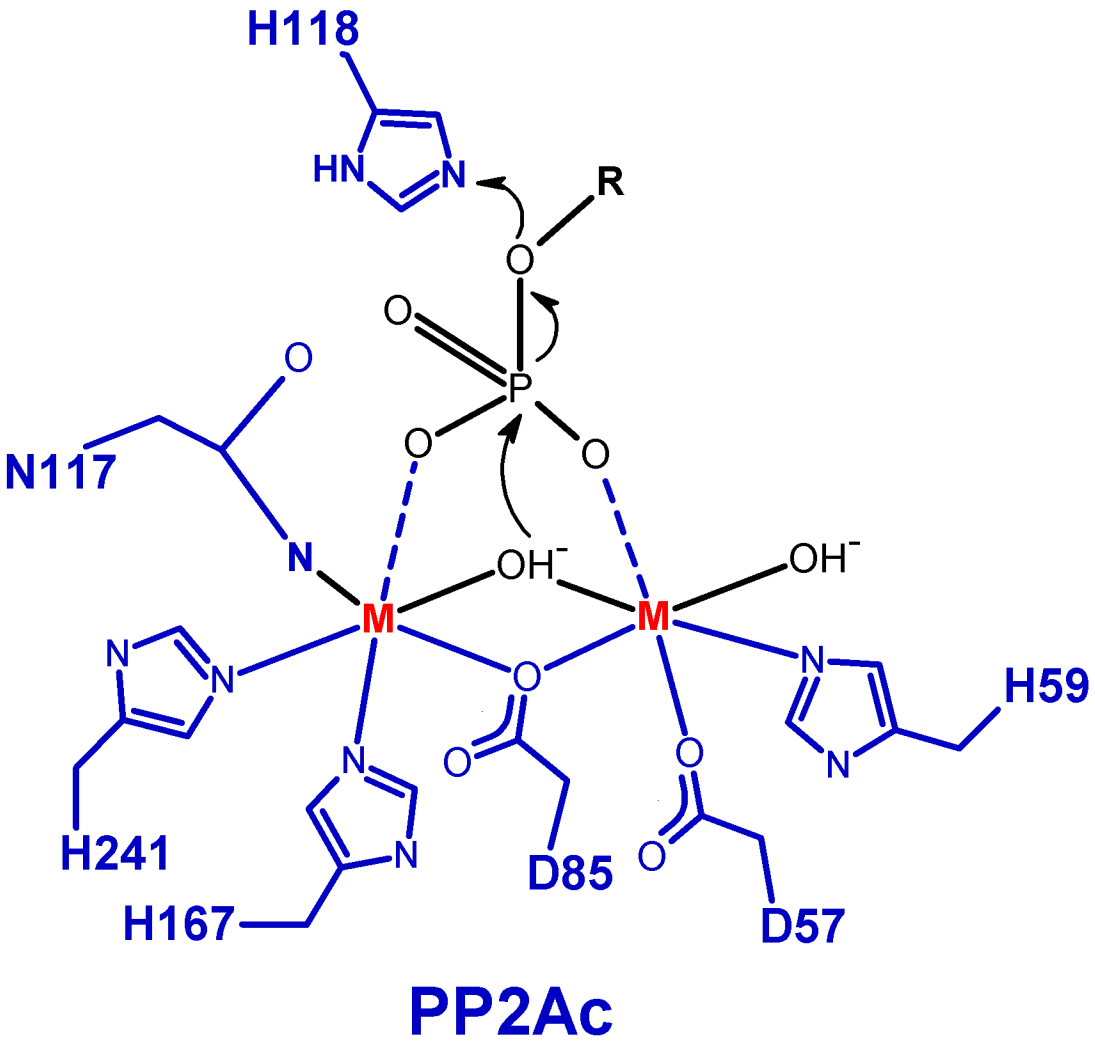

Figure 1.4. Illustration of the catalytic mechanism of dephosphorylation by PP2A.

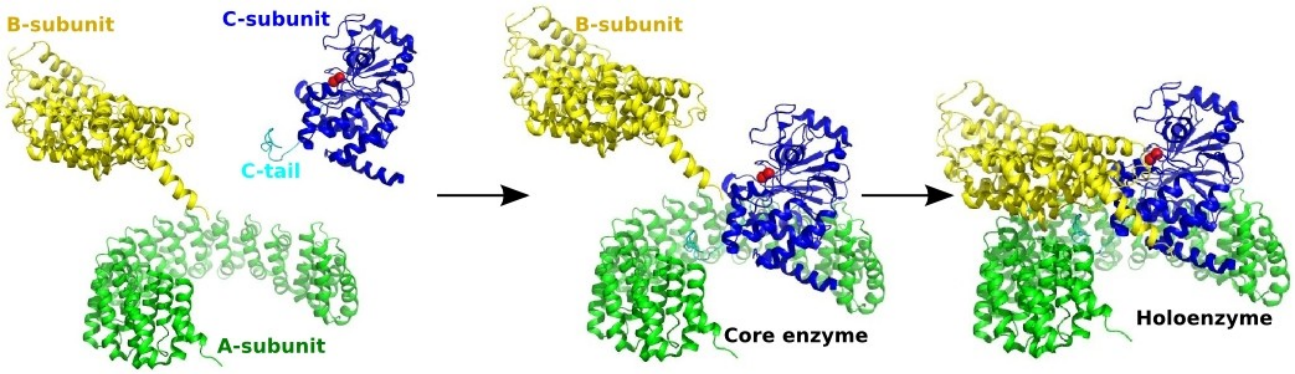

Figure 1.5. PP2A holoenzyme assembly (PDB ID: 2NYL). Left panel: all components of PP2A holoenzyme are in isolation. Middle panel: PP2A A- and C-subunits associate and form PP2A core enzyme. Right panel: PP2A B-subunit binds to core enzyme and forms PP2A holoenzyme.

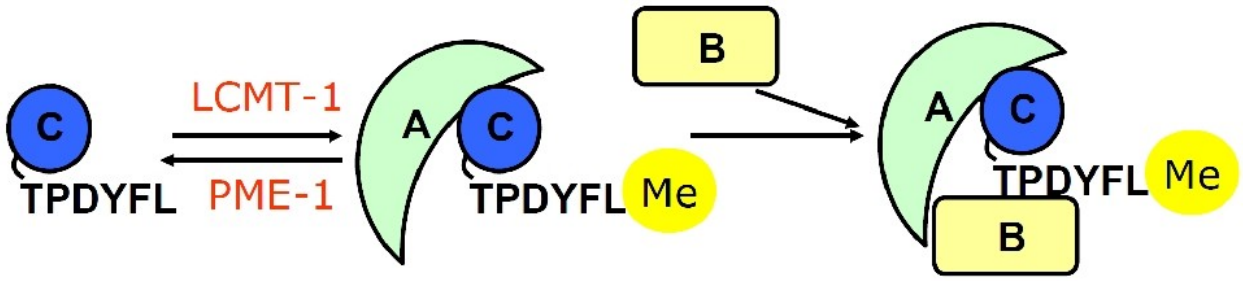

Figure 1.6. Methylation of PP2A by LCMT-1 promotes assembly of PP2A holoenzymes. C-terminal Leu-309 of C-subunit is reversibly carboxymethylated by LCMT-1 and demethylated by PME-1. Methylation increases affinity between PP2A core enzyme and B-subunit and facilitates formation of holoenzymes.

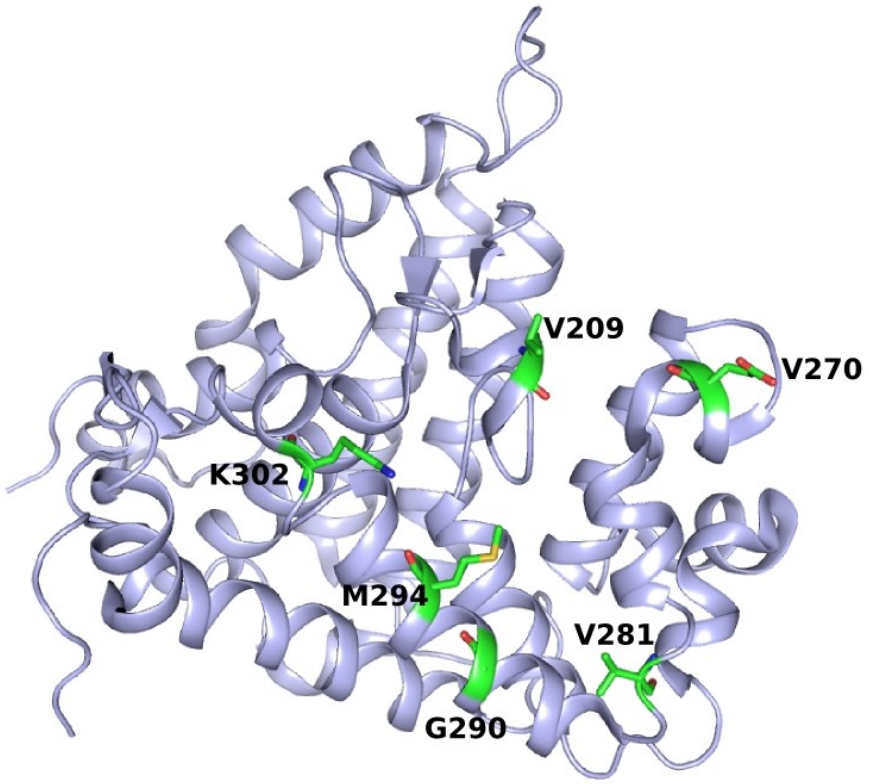

Figure 1.7. Structure of human PTPA (PDB ID: 2HV6). Residues critical for the interaction with PP2Ac (79) are shown as sticks, where carbon, oxygen, nitrogen and sulfur atoms colored green, red, blue and yellow, respectively.

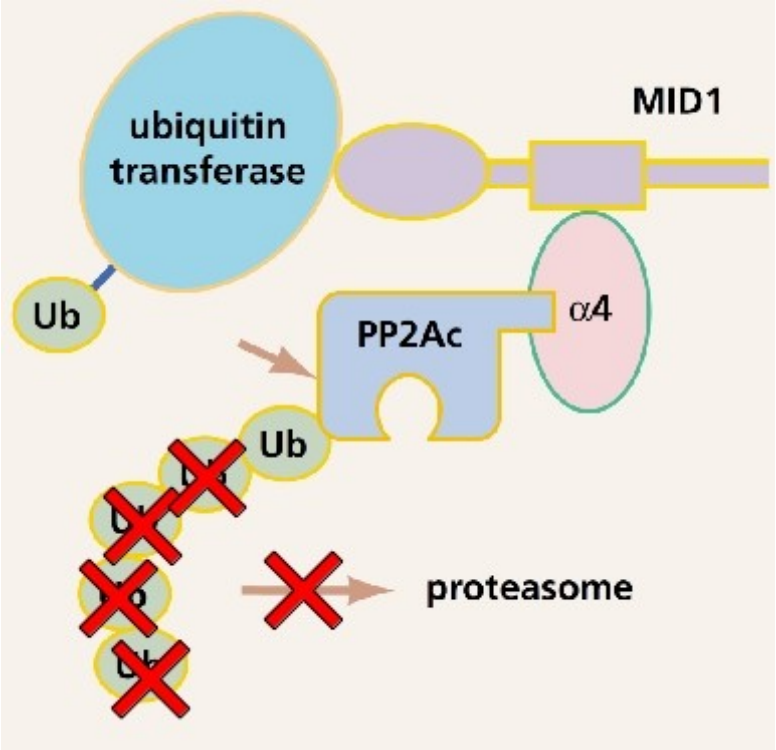

Figure 1.8. Role of α4 in PP2A ubiquitination: mediation of monoubiquitination by MID-1 E3-ligase, which prevents polyubiquitination (99).

Chapter 2
Structural and biochemical characterization of interaction between PP2A and LCMT-1

A version of this chapter has been published as:

Stanevich V*, Jiang L*, Satyshur KA, Li Y, Jeffrey PD, Li Z, Menden P, Semmelhack MF, Xing Y. "The structural basis for tight control of PP2A methylation and function by LCMT-1" Mol Cell. 2011 Feb 4;41(3):331-42.

*These two authors contributed equally to the manuscript.

My contributions included protein purification, crystallization of PP2Ac:LCMT-1 complex (together with Dr. Y. Xing), measuring methyltransferase and phosphatase activities, performing ITC. Dr. L. Jiang performed cell biology experiments. Drs. Y. Li and M. Semmelhack synthesized the chemical mimic of SAM. Dr. Y. Xing collected X-ray diffraction data for the PP2Ac-LCMT-1 complex and built the model, assisted by Dr.K. Satyshur. Dr. Y. Xing designed the project and wrote the manuscript.

2.1. Abstract

Proper assembly of PP2A holoenzymes is required for the normal function of eukaryotic cells. Methylation of the C-subunit carboxyl terminus by leucine carboxyl methyl transferase 1 (LCMT-1) is a pivotal mechanism in regulation of PP2A holoenzymes assembly. LCMT-1 is an essential enzyme conserved from yeast to mammals, and LCMT-1 knockout leads to apoptosis. To understand the molecular basis of the interaction between LCMT-1 and PP2A, we determined the crystal structure of PP2A-LCMT-1 complex trapped in the intermediate step of reaction by usage of a SAM cofactor mimic. The crystal structure shows that LCMT-1 binds to two separate sites on PP2Ac: the PP2Ac carboxyl terminal peptide, and the PP2A active site. The interaction with the PP2A carboxyl terminus buries 1370 $Å^2$ of otherwise exposed surface area and is stabilized by extensive hydrophilic and hydrophobic contacts. The interaction with the PP2A active site is surprising, which ties the regulation of PP2A methylation to the phosphatase activity of PP2A. These studies reveal the molecular basis of PP2A methylation and establish a new role of LCMT-1 in tight control of PP2A function, important for the cell cycle and cell survival.

2.2. Introduction

Reversible methylation of PP2A is catalyzed by two highly conserved enzymes, a 38-kDa PP2A-specific leucine carboxyl methyltransferase (LCMT-1) (55,56,102) and a 42-kDa PP2A-specific methylesterase (PME-1) (55). PME-1 catalyzes removal of the methyl group, opposing the function of LCMT-1 (Fig. 1.6)(55). Overexpression of PME-1 causes phenotypes similar to those associated with loss of the methyltransferase gene (57). The crystal structure of PME-1 in complex with PP2A catalytic subunit (103) indicates that PME-1 has a dual role in PP2A regulation: indirect inactivation by demethylation and direct inactivation by removal of catalytic ions from PP2A active site (103), which provides important insights into PP2A regulation.

The crystal structures of PPM1 – a yeast homolog of LCMT-1, in apo form and in complex with S-adenosyl methionine (SAM) or S-adenosyl homocysteine (SAH) were reported (104). The structure contains a central β-sheet flanked with α-helices on both sides of the molecule. The methyltransferase (MT) motif in the structure is similar to other SAM dependent methyltransferases (105). No significant differences were observed between the apo- and the cofactor-bound forms of PPM1. The structure of PPM1 in the presence of AdoMet led the authors to propose a catalytic mechanism of PP2A carboxymethylation. It was suggested that the unstructured TPDYFL carboxyl-terminal sequence of the PP2A catalytic subunit accesses the SAM factor located at the center of the enzyme through a 14 Å deep cavity roughly perpendicular to the SAM binding site. Further catalysis is carried out by the positioning of the reactants in a conformation that differs from that in solution, which is achieved by the extra charges present in the active site.

The project on crystallization of PP2Ac:LCMT-1 complex was initiated by Dr. Y. Xing. During the initial stages of the project, Dr. Xing et al. were able to solve the structure of human LCMT-1 in complex with S-adenosylhomocysteine (SAH), the enzymatic product of the methyltransferase reaction (106). The structure was solved by molecular replacement with the model of the yeast ortholog, PPM1, described above and refined to 1.9 Å resolution. Human LCMT-1 contains a canonical SAM-dependent methyltransferase domain and a unique lid domain consisting entirely of α-helices (Fig. 2.1). The MT domain comprises a central β sheet (β1–7) lying between two groups of α helices: αZ, αA, and αB on one side and αC, αD, and αE on the other. The lid domain is formed by three of the four unique motifs in LCMT-1 and forms a deep active-site pocket that binds to the carboxyl terminus of PP2A tail. Alignment of the structures of LCMT-1 and PPM1 revealed a key α helix, α1, within the first nonconserved unique motif, which is located next to both the substrate and the cofactor binding pockets.

2.3. Methods

Protein Preparation

All constructs and point mutations were generated via a standard PCR-based cloning strategy. LCMT-1 Δ19 (20–338) and missense mutants were cloned in pET15b (Invitrogen) and overexpressed at 37°C in *E. coli* BL21 (DE3). N-terminal truncation (Δ19) improved LCMT-1 solubility with no loss of enzyme activity (data not shown). For convenience, LCMT-1Δ19 is further referred to as LCMT-1. The soluble fraction of *E.coli* cell lysate was purified over Ni-NTA (QIAGEN) and further fractionated by cation-exchange chromatography (Source15S, GE Healthcare) after removal of His_6-tag. The PP2A core enzyme was assembled by passing PP2Ac through a stoichiometric amount of GST-Aα immobilized on glutathione resin. The AC dimer was released by on-column thrombin cleavage and further purified by ion-exchange chromatography. The stable PP2A-LCMT-1 complexes were assembled by mixing of the PP2A core enzyme or the C subunit with LCMT-1 and SAM analog at 1:2:10 molar ratio, incubated at 30°C for 1 hr, and purified by anion exchange chromatography (Source 15Q, GE Healthcare) and gel filtration chromatography (Superdex200, GE Healthcare). Due to the difficulty of PP2A methylation *in vitro*, an excess amount of LCMT-1 was used to improve the level of covalent crosslink of PP2A to SAM analog.

Crystallization and Data Collection

Crystals of the PP2Ac (Δ294–298)-LCMT-1 complex were grown at 18°C via the sitting-drop vapor-diffusion method by mixing of the complex (5 mg/ml) with an equal volume of reservoir solution containing 100 mM Tris (pH 8.2), 22%–26% PEG4000 (v/v), 200mM sodium acetate, and 5 mM DTT. Diffracting crystals were generated by micro-seeding and obtained

crystals were flash frozen. The native data sets for the PP2Ac-LCMT-1 complex were collected at APS LS-CAT and processed with the software HKL2000 (107).

Structure Determination

The structure of the PP2Ac-LCMT-1 complex was solved by molecular replacement with two models, LCMT-1 and the C subunit (residues 6–293) from the structure of the PP2A core enzyme (PDB ID: 2IE3), and one complex per asymmetric unit was found. The structure was built with Coot (108) and refined with REFMAC restraints with TLS (109) and weights adjusted on the basis of R_{free}. The PP2A tail was built after the electron density map was improved. The SAM analog was built with Sybyl (Tripos), and the topology file was generated with Dundee (110) for REFMAC refinement. Two TLS groups were used: (1) the C subunit (1–293) and (2) LCMT-1 together with the SAM-analog and the last six residues of the PP2A tail. The structure was refined to 2.7 Å.

GST-Mediated Pulldown Assay

LCMT-1 or LCMT-1 mutants (10 mg in 100 ml binding buffer) were mixed with 20 ml glutathione resin with immobilized GST-tagged PP2A A-C dimer (10 mg) in the presence of 1 mg/ml BSA. The protein bound to resin was separated from unbound protein by repeated washing and analyzed by SDS-PAGE gels and Coomassie blue staining.

Methylation Assay

Methylation assays were performed by mixing of LCMT-1 (4–10 nM), PP2A(10–100 nM), and [3H]-SAM (3 mM) in a reaction buffer containing 50 mM MOPS (pH 7.2), 20 mM DTT (omitted for oxidized PP2A), and 50 mM $MnCl_2$ (omitted for PPi-treated PP2A). After

incubation at 37°C for 2–20 min, the reactions were stopped and precipitated by addition of 25% ice-cold trichloroacetic acid. The radioactivity of precipitate was quantified by scintillation counting. The results were used to estimate the rate of methylation. For dot blot, the indicated amount of PP2A core enzyme before and after *in vitro* methylation by LCMT-1 was spotted onto PVDF membrane and blotted by an antibody that specifically recognizes the unmethylated PP2A tail to determine the level of PP2A methylation (Millipore, clone 4b7).

Isothermal Titration Calorimetry

Binding affinities were measured by isothermal titration calorimetry (ITC). In brief, 15 mM PP2A core enzyme was titrated with 300 mM LCMT-1 or LCMT-1 T29V with a VP-ITC microcalorimeter (MicroCal). All proteins were prepared in a buffer containing 20 mM Tris (pH 7.5), 50mMNaCl, and 50 mM $MnCl_2$. The data were fitted with Origin 7.0.

Phosphatase Assays

PP2A phosphatase activity was measured with a Ser/Thr Phosphatase Assay Kit 1 (Upstate Biotechnology) according to manufacturer's instructions. Two microliters of 1 mM phospho-Thr peptide substrate (K-R-pT-I-R-R) were added to 20 ml of PP2A sample (40–100 nM). The reaction was carried out at 30°C for15 min and stopped by the addition of 50 ml malachite green solution. The absorbance at 620 nm was measured after 10 min incubation at room temperature.

Activation, Inhibition, Inactivation, and Oxidation of PP2A

Free C or the core enzyme of PP2A were mixed with PTPA at a 1:1 molar ratio with C_2 ceramide (N-Acetyl-D-sphingosine, Sigma) or synthetic peptide (KRTIRR) at the indicated concentration and incubated at 37°C for 5 min for PP2A activation. Okadaic acid was added to

the core enzyme at a 2:1 molar ratio for PP2A inhibition. The PP2A core enzyme (1 mg/ml) was incubated at 37°C with 1mM PPi for 50 min for inactivation and, after desalting, was diluted 100-fold into buffer containing 25 mM Tris (pH 8.0), 150 mM NaCl, and 20 mM DTT for phosphatase activity and methylation assay. The PP2A core enzyme was changed to DTT-free buffer by gel filtration chromatography to remove DTT (Superdex 200, Amersham); the peak fraction (1.5 mg/ml) was incubated with 20 mM H_2O_2 at 37°C for 30 min and, after desalting, was diluted at least 100-fold into reaction buffer containing 25mM Tris (pH 8.0), 150 mM NaCl, and 50 mM $MnCl_2$ for the phosphatase activity and methylation assay. Phosphatase activity and methylation assay were performed as described above. All assays were performed in duplicates and repeated three times. Average values and standard error were calculated. Where indicated, values were normalized to the positive control.

2.4. Results

2.4.1. Crystallization and overall structure of the PP2A:LCMT-1 complex

Study of PP2A methylation by x-ray crystallography was complicated by the low affinity between PP2A and LCMT-1, and the transient, instable PP2A:LCMT-1 complex. Attempts to directly mix and crystallize the complex were not successful. Utilization of a truncated form of the PP2A A-subunit (mini-A), containing mainly the HEAT repeats required for C-subunit binding, and the fusion proteins of A and LCMT-1 were not successful for crystallization of the PP2A-LCMT-1 complex. As described in detail later, the difficulty of crystallization can be also attributed to the malleable conformation of the PP2A active site and the direct contacts between LCMT-1 and the PP2A active site (described later). Because of this, only 50% of PP2A methylation can be achieved *in vitro*, which hinders formation of homogeneous protein sample required for crystallization.

To overcome this obstacle, we used a SAM-cofactor analog (111) to stably trap the enzymatic intermediate of the PP2A-LCMT-1 complex. In the presence of PP2A and LCMT-1, this compound is covalently cross-linked to the carboxylate group of PP2A Leu-309 (Fig. 2.3). Since the compound binds to a deeply buried SAM-binding pocket of LCMT-1 perpendicular to the binding pocket for the C-tail of PP2A, it could not be released upon crosslink to PP2A. As a consequence, the PP2A:LCMT-1 complex was trapped as a stable enzymatic intermediate. The resulted PP2A:LCMT-1complex, however, did not lead to diffracting crystals. To reduce the structural flexibility, an internal deletion of five residues was introduced to the C-tail (Δ294-298), which did not interfere with LCMT-1-binding, and allowed generation of the stable PP2A (Δ294-298):LCMT-1 complex trapped by the SAM analog.

This led to diffracting crystals for the PP2A:LCMT-1 complex. The X-ray diffraction data was collected using the synchrotron beamlines at APS. The structure was determined by molecular replacement using human LCMT-1 and PP2Ac from a core enzyme (PDB ID: 2IE3) as the search models and final model of PP2Ac:LCMT-1 was refined to 2.7 Å (table 2.1).

The structure of the PP2Ac:LCMT-1 complex shows that the lid domain of LCMT-1 makes extensive contacts with both PP2A C-tail and the PP2A active site (Fig. 2.4 A). The six carboxyl-terminal residues of PP2A C-tail bind to the deep pocket formed by the LCMT-1 lid domain (Fig. 2.4 B). The beginning of the C-tail is located near the LCMT-1 lid domain, which allows the C-tail to readily enter the substrate-binding pocket of LCMT-1. As expected, the carboxylate group of PP2A Leu-309 is covalently bound to the SAM-analog (Fig. 2.5). Interestingly, the top ridge of the lid domain of LCMT-1 makes broad contacts with the active site of PP2A, which underlies an important mechanism for control of PP2A methylation by activation of the phosphatase activity. This mechanism can serve as a checkpoint for holoenzyme formation, which ensures that only the properly folded, active C-subunit is methylated and subsequently assembled into holoenzymes.

2.4.2. Structural basis for recognition and methylation of PP2A C-tail by LCMT-1

The active site pocket of LCMT-1 can be divided into two portions: the upper entry tunnel and the active site pocket (Fig. 2.6 A). Both make extensive contact with PP2A tail, burying 1370 $Å^2$ of otherwise exposed surface area. The upper entry includes helix α4 and the binding loop (BL) of the lid domain (Fig. 2.6 B). Lys-62 in the lid domain makes H-bond interactions to Asp-306 of the C-tail. A hydrophobic patch of LCMT-1, formed by residues Phe-237/Met-241/Leu-245, serves as a platform for the interaction with PP2A Tyr-307, which explains the

previously reported observation that phosphorylation or mutation of Tyr-307 eliminates methylation of PP2A. The deep pocket consists of α7 in the lid domain and αZ with several other β-sheets in the SAM-MT domain (Fig. 2.6 C). Several hydrophobic residues from α7 and αZ form close contacts with Phe-308 of PP2A.

LCMT-1 residue Arg-73 from αZ helix forms double H-bond interactions to the SAM cofactor and Leu-309 of PP2A, crucial for restricting the positions of the cofactor and the C-tail for catalysis. Additionally, the side-chain of Thr-29 in α1 forms H-bond with the sulfur atom of SAH, which further stabilizes cofactor for enzymatic reaction. Consistent with the structural observations, R73A mutation completely eliminated methylation while T29V decreased the activity by 8-fold. Interestingly, the T29V mutant appears to have higher affinity to PP2Ac than the wild-type LCMT-1, as shown by pull-down and ITC experiments. This can be explained by an increased hydrophobic interaction between PP2A Leu-309 and the newly introduced Val-29 in the T29V mutation (Fig. 2.6 C). This makes LCMT-1 T29V a dominant negative mutation that was employed for the cell biology experiments (106).

2.4.3. The contacts between LCMT-1 and the PP2A active site are required for methylation

The rim of LCMT-1 lid domain makes extensive contacts to the PP2A active site, burying 1600 $Å^2$ of otherwise exposed surface area. This interface is around 1.5 times larger than that between LCMT-1 and C-tail (Fig. 2.7 A) and comprises several structural elements of PP2A necessary for phosphatase activity. In particular, several active site loops (CL) of PP2A, including CLs 6, 8, 14, 15, 17 and 19, interact with helix α7 and the loop between α6 and α7 of LCMT-1 (Fig. 2.7 B, Table 2.2). Two conserved acidic residues of LCMT-1, Asp-303 and Glu-

304, form rich H-bond network around catalytic Mn^{2+} ions of PP2A, including contacts to Arg-89 and Arg-214, residues that are essential for binding of the phosphoryl group of PP2A substrates. Besides Arg-89, another residue in CL19 (the longest loop near PP2A active site), Arg-268, makes H-bond interactions with Glu-65 in the BL loop of LCMT-1. The interface between LCMT-1 and the PP2A active site also buries a cysteine pair: Cys-266/Cys-269, which is located near the active site of PP2A and has adverse effects on PP2A activity after oxidation (112-115) (Fig. 2.7 B).

We performed structure-based mutational analysis to determine the role of LCMT-1 interaction with the PP2A active site and the C-tail in PP2A methylation. LCMT-1 mutations E65R and D303R at the interface with the PP2A active site compromise the interaction between LCMT-1 and PP2Ac and, consequently, the methyltransferase activity of LCMT-1 (Fig. 2.8). Their effect is similar to the effect of mutations at the interface with the C-tail: K62E and F237D. Mutations located outside of these two interfaces have much less effect (Fig. 2.8). As was mentioned above, T29V mutation of LCMT-1 enhances interaction with PP2A, but results in a decreased methylation rate, likely due to a reduced rate of release of methylated PP2A (Fig. 2.10).

The crystal structure of LCMT-SAH complex had eight molecules of LCMT-1 in the asymmetric unit, which allowed alignment of these copies together with the structure of the PP2Ac-LCMT-1 complex. This allowed identification of conformational changes in LCMT-1 required for PP2A-binding. LCMT-1 helices α4 and BL undergo significant structural changes upon binding to LCMT-1. Comparison of the structure of the PP2A:LCMT-1 complex with the most similar apo-enzyme structure shows that LCMT-1 lid domain rearranges significantly after

binding to PP2A that allows to accommodate PP2A C-tail into the substrate-binding pocket of LCMT-1 (Fig. 2.9). These changes are triggered by the repulsive contacts between Ile-240 in helix α4 and the hydrophobic surface on the edge of the PP2A active site. This structural analysis suggests how the interaction of LCMT-1 with the PP2A active site triggers rearrangements in LCMT-1, which allows entry of the PP2A C-tail into the substrate-binding pocket of LCMT-1. This explains the long-puzzled observation that LCMT-1 can not methylate the C-tail peptide alone.

2.4.4. The activation-dependent PP2A methylation provides a checkpoint for formation of active PP2A holoenzymes

The extensive contacts of LCMT-1 with the active site of PP2A suggest a mechanism for regulation of LCMT-1-binding and PP2A methylation by the conformation of the PP2A active site. If this is true, PP2A methylation may serve as a checkpoint for the biogenesis of PP2A holoenzymes that allows the active PP2Ac to be preferably methylated and enhanced for assembly into holoenzymes. To test this hypothesis, we measured LCMT-1 methylation activity toward PP2Ac inactivated by pyrophosphate (PPi) treatment. We recently discovered that incubation of the C-subunit with PPi leads to chelation and removal of catalytic metal ions from the PP2A active site (Fig. 4.2), which leads to destabilization of the active site followed by dramatic changes in overall PP2Ac fold (described in more details in chapter 4). As expected, inactivation of PP2Ac by PPi caused complete elimination of LCMT-1 activity toward PP2Ac (Fig. 2.11 A). This finding supports our hypothesis that the properly folded PP2A active site is required for PP2A methylation by LCMT-1. It also explains the previous observation that LCMT-1 could not methylate PP2Ac harboring mutations at the active site (59).

Under physiological conditions in cell, plenty of protein and small-molecule factors regulate phosphatase function of PP2A. We tested several of them to examine whether they have the same effect on the phosphatase activity of PP2A and methyltransferase activity of LCMT-1. First, we tested the effect of PTPA on PP2A methylation. Interestingly, at a molar concentration similar to PP2A, PTPA stimulated both the phosphatase activity of PP2A and its methylation by LCMT-1 (Fig. 2.11 B). This data provided the first *in vitro* evidence that PTPA may function as a chaperone in priming an active conformation of the PP2A active site. As shown later in Chapter 3, the A-subunit of PP2A can also enhance methylation of PP2Ac, presumably by stabilizing the PP2Ac fold, restricting the C-tail mobility by the horseshoe-shaped architecture of the A-subunit, and by weak charge-charge interactions with LCMT-1.

Besides PP2A-interacting proteins, several small molecules were reported to modulate the function of PP2A including polycations (116), ceramide (41), tumor-inducing toxins, and oxidative stress molecules (114). Ceramide, a small molecule released into cytosol during apoptosis, is reported to stimulate PP2A function (42,117). We showed that LCMT-1 also enhanced PP2A methylation by LCMT-1 similar to enhancement of the phosphatase activity (Fig. 2.12 A). Consistent with the fact that the positively charged peptides can increase the phosphatase activity of PP2A (116), a polycationic peptide, KRTIRR, accelerated PP2A methylation by LCMT-1 (Fig. 2.12 B). Furthermore, a highly potent PP2A inhibitor, okadaic acid, binds directly to the PP2A active site (118) and completely blocks PP2A methylation and phosphatase activity (Fig. 2.13). Both the phosphatase and PP2A methylation were simultaneously reduced by incubation of PP2A in a DTT-free buffer or in the presence of 20 μM

H_2O_2, presumably due to oxidation of Cys-266 and Cys-269, the two cysteine residues located in the close proximity of PP2A active site.

2.5. Discussion

PP2A is the most abundant eukaryotic cell phosphatase immensely involved in all cellular processes. Despite its importance for cell survival, regulation of PP2A assembly into the functional holoenzymes remains incompletely understood at the molecular level. Research described in this chapter established the structural and biochemical basis for PP2A methylation by LCMT-1. This was achieved by crystallization of the PP2A:LCMT-1 complex trapped as an intermediate of the reaction by utilization of a SAM-cofactor analog. The key conclusion of this study is that LCMT-1-mediated PP2A methylation relies on a direct binding to and an active conformation of the PP2A active site. It is important to mention that Dr. L. Jiang from our laboratory has extended the structural insights into the mechanistic understanding of LCMT-1 function and PP2A:LCMT-1 interaction in cells (106), which establish an important link between the structural basis of LCMT-1 and its role in cell survival (106).

Previous studies have shown that PME-1 can block methylation of inactive PP2A in yeast (43). It is probable that LCMT-1, PTPA and PME-1 work together in the concerted manner during the biogenesis of PP2A holoenzymes to control activation, methylation and subsequent association of PP2A core enzyme with regulatory subunits to form functional holoenzyme. Despite the complexity of PP2A holoenzyme biogenesis, the concerted action of these regulatory proteins, especially LCMT-1-mediated activation-dependent methylation, provides a mechanism that the activated and properly folded C-subunits are selectively enhanced to assemble into holoenzymes. This ensures formation of active holoenzymes and minimizes the uncontrolled phosphatase activity of free C-subunit prior to assembly into holoenzymes. This likely explains why LCMT-1 knockdown led to apoptosis. LCMT-1 knockdown can attenuate conversion of

activated free C-subunits into substrate-specific holoenzymes and thus lead to cell-detrimental, uncontrolled phosphatase activity. The reduced holoenzyme assembly can also contribute to apoptosis, as loss of PP2A holoenzymes was previously shown to cause cell death (43). Thus, the tight control of PP2A activation and methylation likely provides an important mechanism for cell survival (Fig. 2.14).

The level of PP2A methylation was shown to vary during the cell cycle by variation of the cellular level of PTPA and PME-1 (119). Research from this chapter reveals another mechanism for regulation of PP2A methylation by sensing the conformation and changes of the PP2A active site. Due to the malleable and highly regulated nature of the active site, LCMT-1 may serve as a "hub" sensing signals from varied factors that alter the conformation and activity of the active site. Based on these, modulation of PP2A-LCMT-1 interaction may serve as an important target for pharmacological regulation of cancer cells.

2.6. Figures and tables

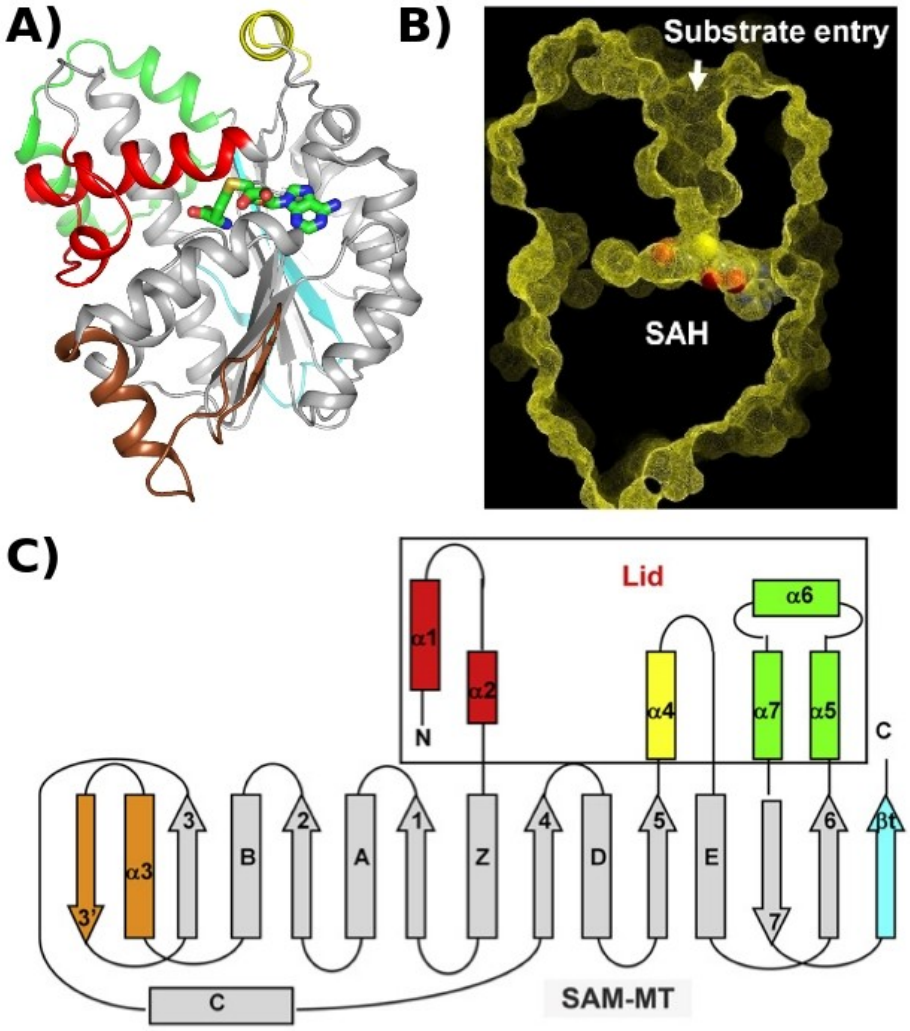

Figure 2.1. Structure of human LCMT-1 in complex with SAH. **(A)** Overall structure of LCMT-1 bound to SAH in ribbon. **(B)** A slice of LCMT-1 surface showing the binding pockets for PP2A tail and the cofactor. SAH is bound and shown in spacefill. **(C)** Schematic showing the topology of the LCMT-1 structure. The canonical SAM-MT domain is shown in gray, and the unique motifs inserted to different locations of the SAM-MT domain are in color, three of which (red, yellow, and green) form the lid domain as indicated. Helices are shown as cylinders and strands as arrows. The N- and C- termini are labeled.

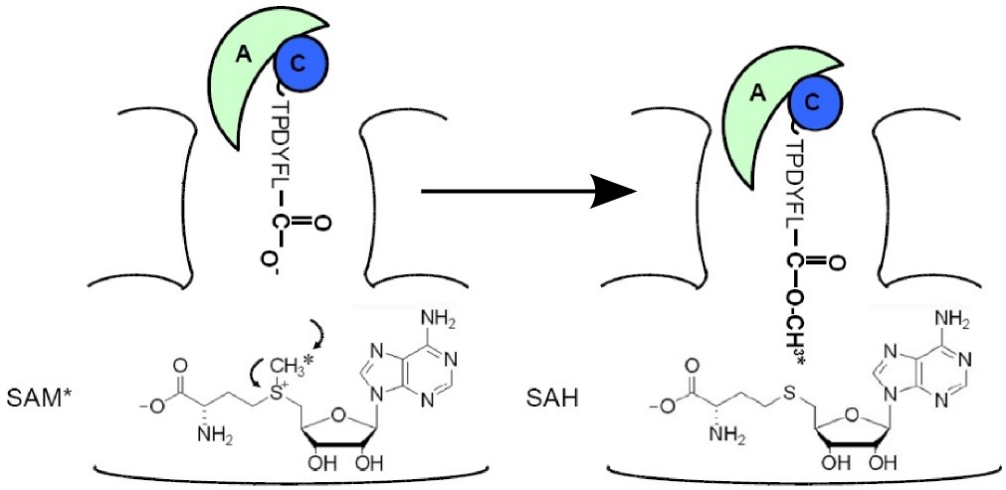

Figure 2.2. Illustration of LCMT-1 catalyzed methylation of PP2A C-tail.

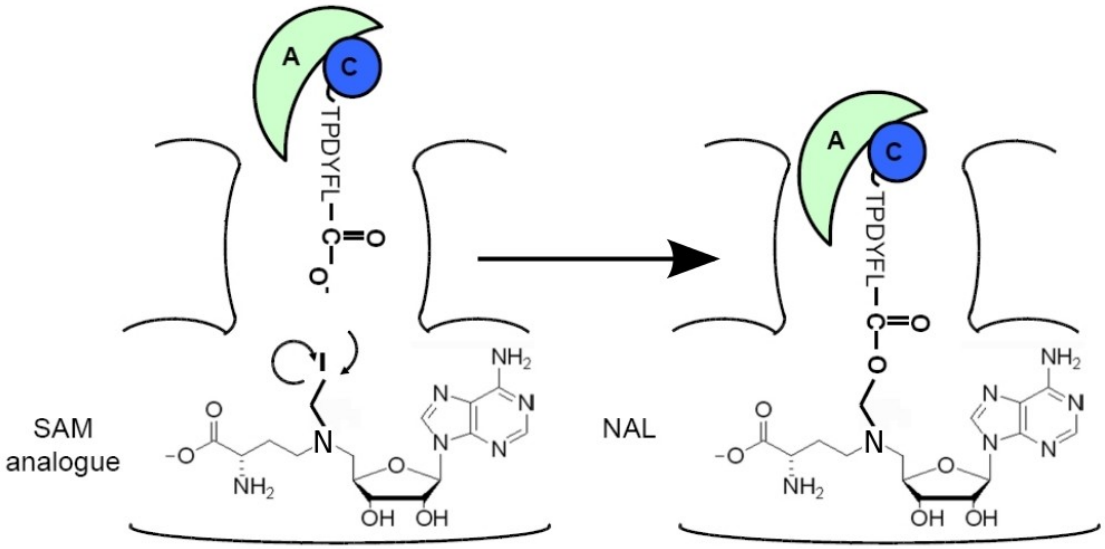

Figure 2.3. Illustration of LCMT-1 catalyzed covalent crosslink of the synthesized SAM mimic to PP2A C-tail.

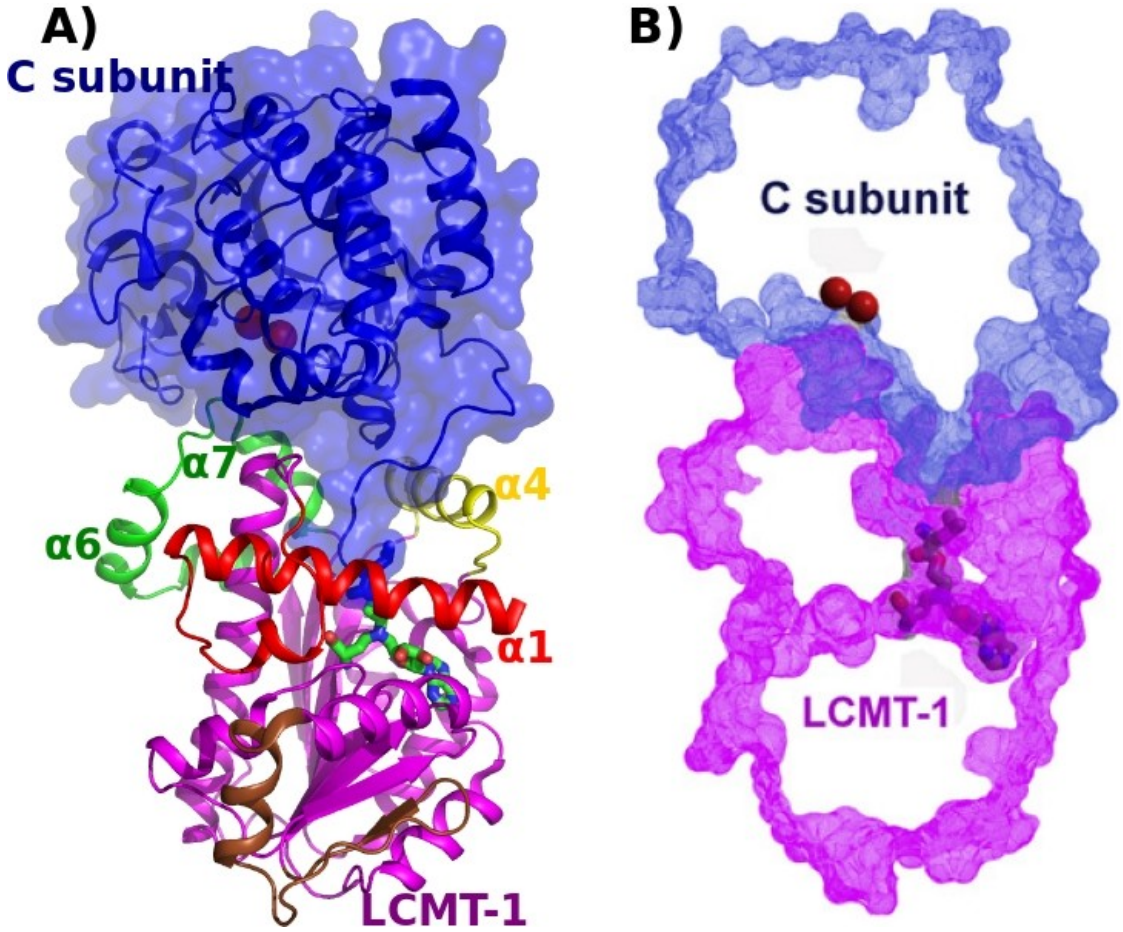

Figure 2.4. Overall structure of the PP2Ac:LCMT-1 complex. **(A)** The MT domain of LCMT-1 is colored magenta, unique motifs are colored as in Fig. 2.1, PP2Ac is in blue, and SAM mimic and Leu-309 are shown as sticks. **(B)** A slice of surface showing that LCMT-1 binds to the PP2A active site. Two catalytic metal ions are shown as red spheres.

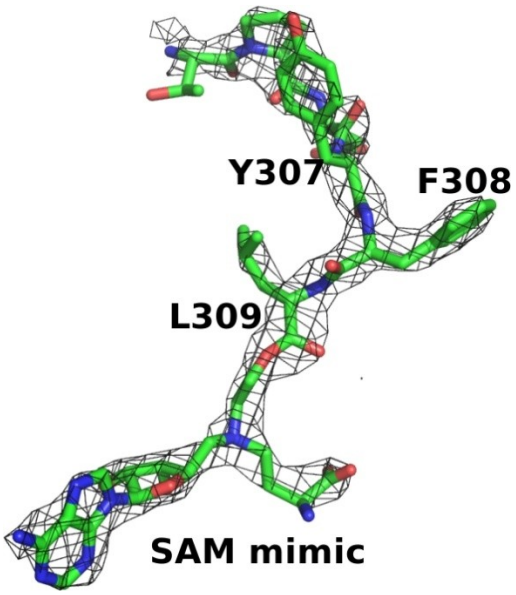

Figure 2.5. The $2F_o$-F_c electron density map at 1.8 σ (gray) for peptide 'TPDYFL'' of PP2A tail and covalently bound SAM mimic (shown as sticks, colored by atom type).

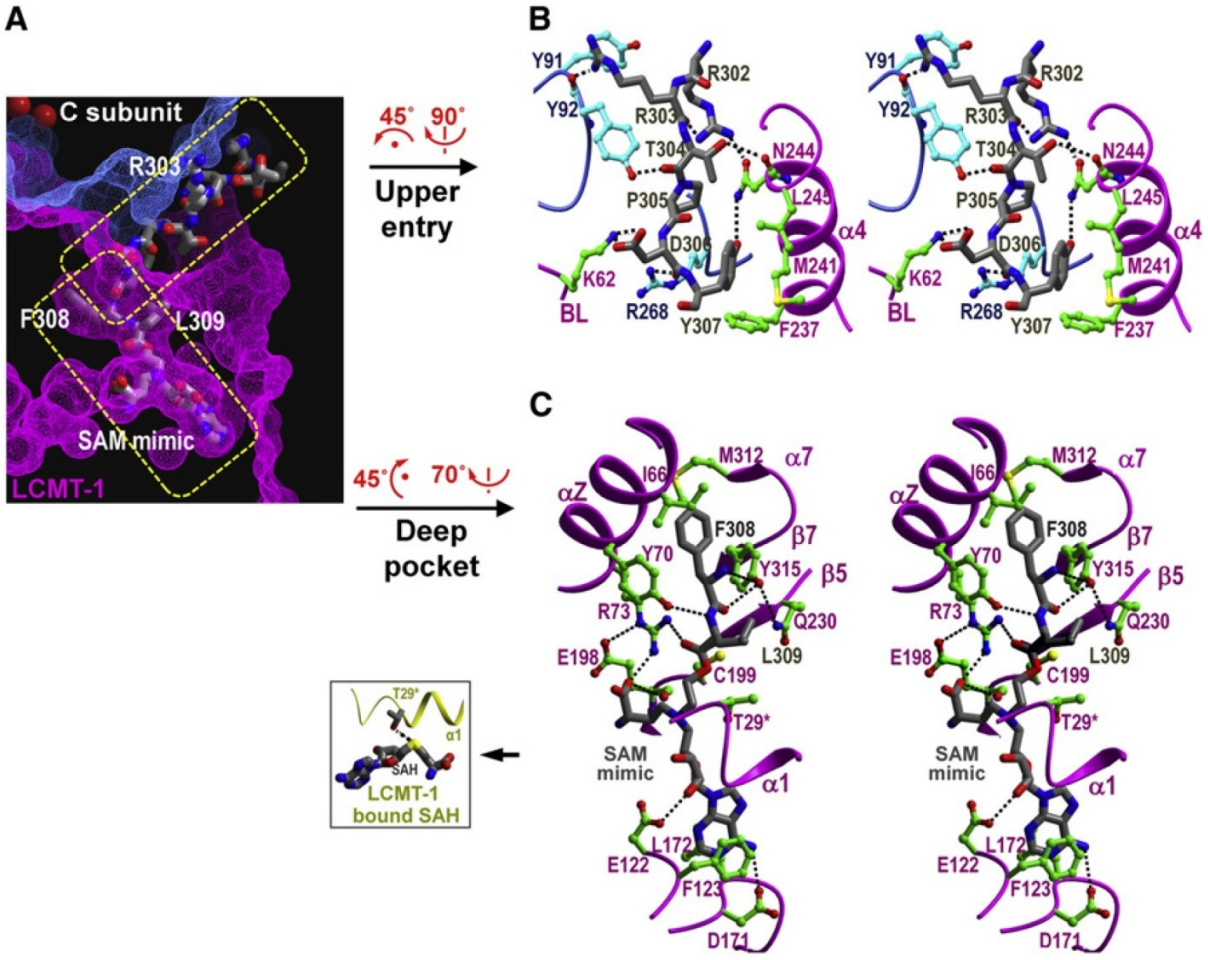

Figure 2.6. Binding and methylation of the PP2A tail by LCMT-1. **(A)** A slice of surface showing the binding pocket for PP2A tail, divided into the upper entry and the deep pocket. Residues Arg-303, Phe-308, Leu-309 and SAM mimic are labeled. **(B)** A stereo view of the upper entry. Residues from LCMT-1, the PP2A tail, and the PP2A core are colored green, gray, and cyan, respectively. **(C)** A stereo view of the deep pocket. The color scheme is the same as in (B). The hydrogen bond between Thr-29 in α1 of LCMT-1 and the sulfur atom of SAH is highlighted (inset).

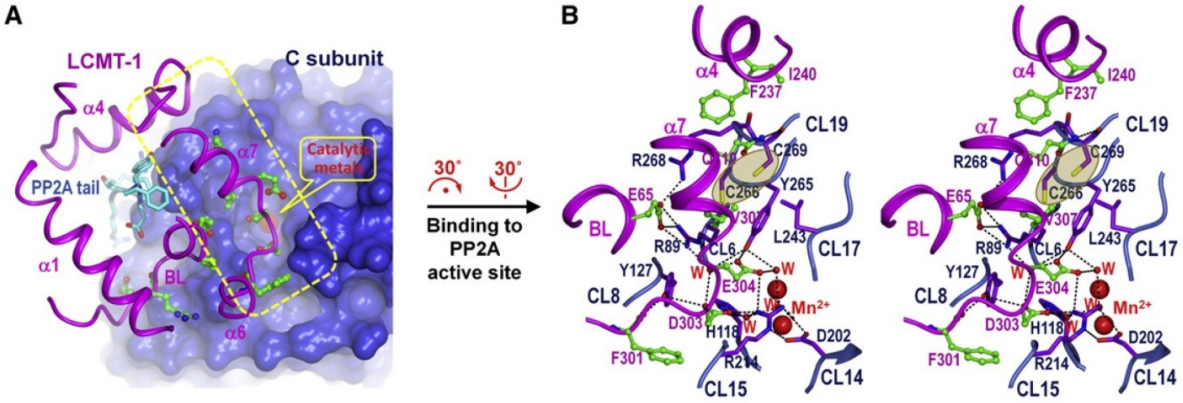

Figure 2.7. Interface of LCMT-1 to the PP2A active site. **(A)** The lid domain of LCMT-1, the protein core, and the tail of the C subunit are shown as ribbon, surface, and cylinder, respectively. **(B)** A close-up stereo view of the interface to the PP2A active site. Residues from LCMT-1 and the C subunit of PP2A are colored green and purple, respectively.

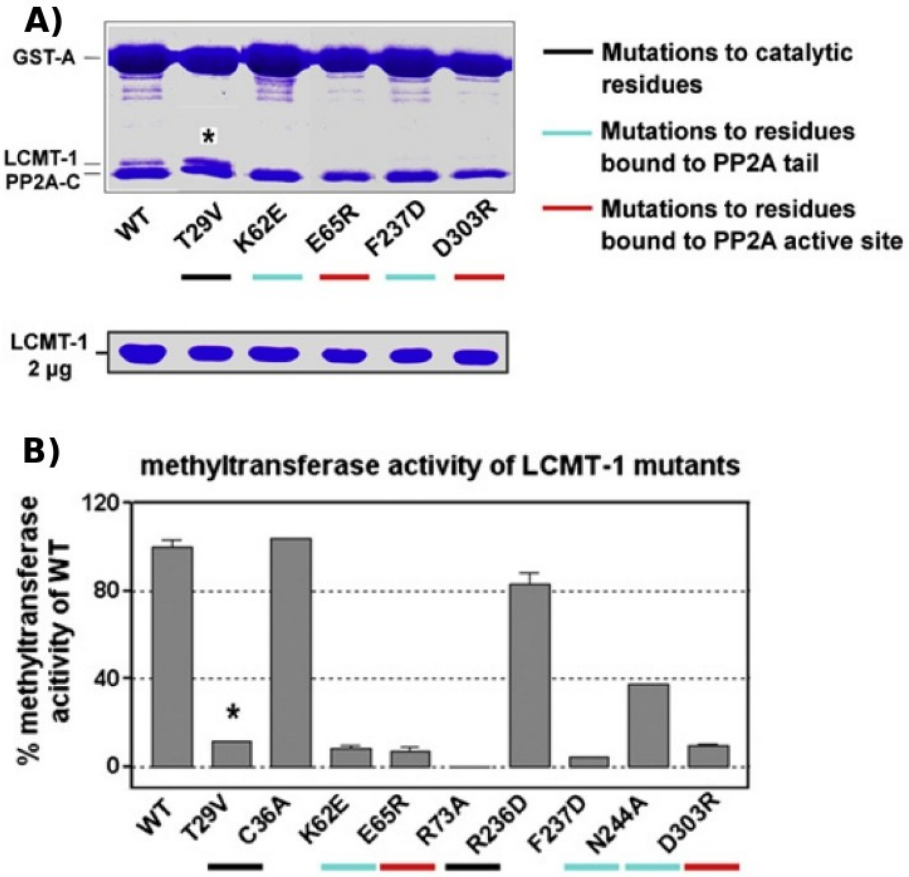

Figure 2.8. Structure-based mutational analysis of the PP2Ac-LCMT-1 interface. **(A)** Pull-down assay with GST-tagged PP2A core enzyme immobilized on GS4B resin and an equal amount of LCMT-1 wild-type (WT) or mutants in the mobile phase. **(B)** Methylation of the PP2A core enzyme by wild-type LCMT-1 and LCMT-1 mutants.

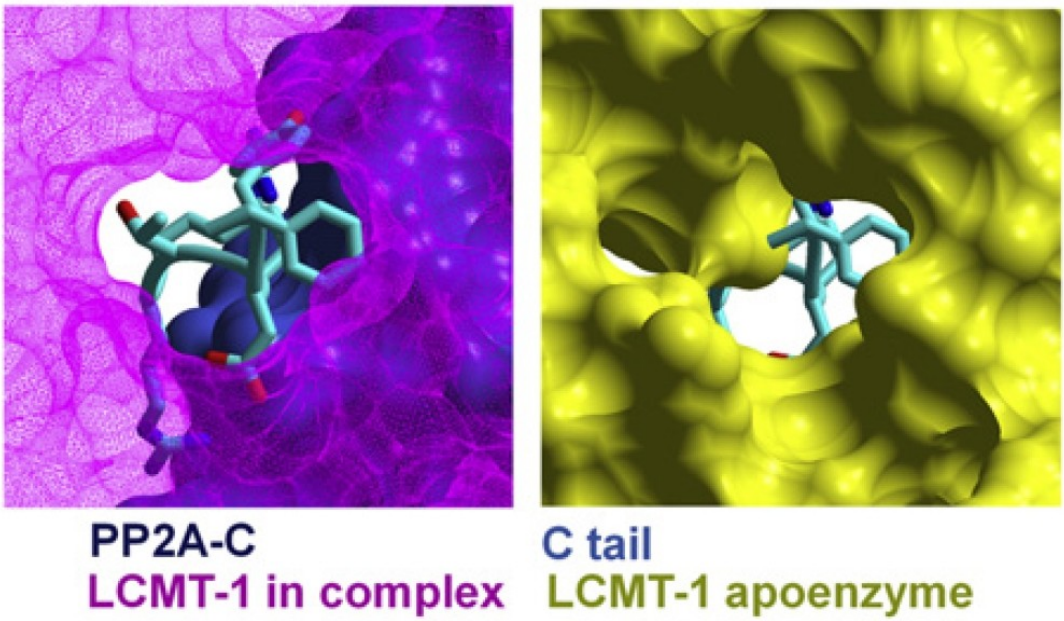

Figure 2.9. Changes in the conformation of the substrate-binding pocket of LCMT-1 allowing binding of the PP2A C-tail. The C-tail is shown as cylinder and the rest of the model as surface.

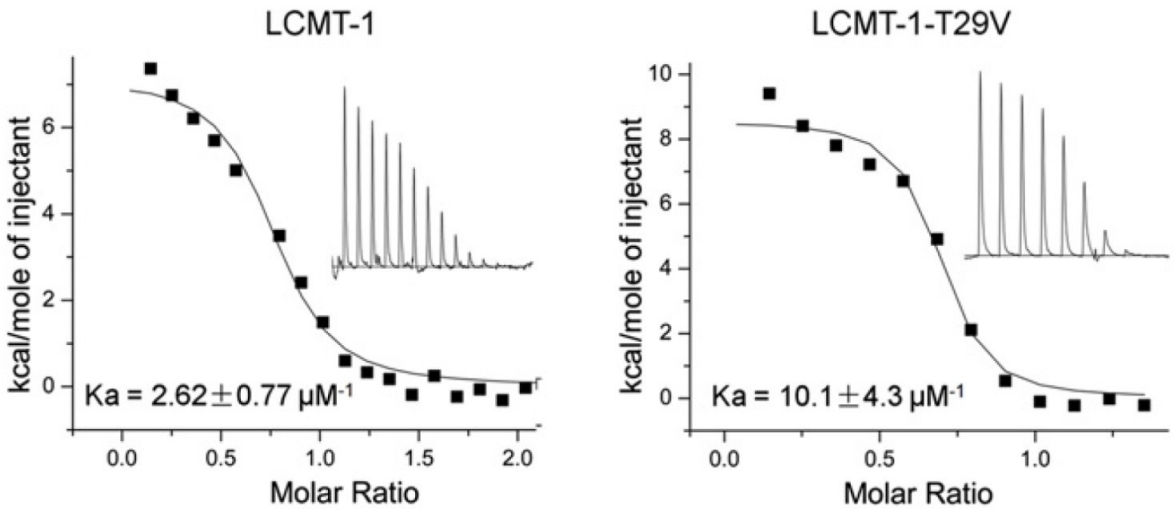

Figure 2.10. ITC measuring the binding affinity of the PP2A core enzyme to LCMT-1 and LCMT-1 T29V.

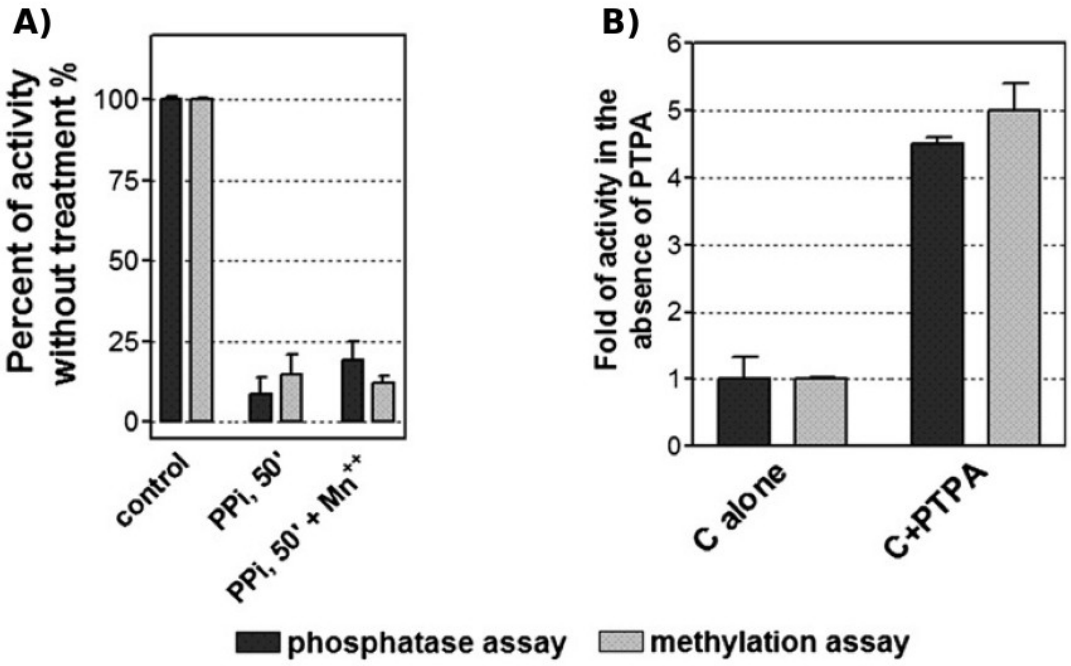

Figure 2.11. (A) Simultaneous loss of LCMT-1 methylation activity and the phosphatase activity of PP2A core enzyme by incubation with pyrophosphate (PPi) for 50 min. **(B)** PTPA stimulates the phosphatase activity and LCMT-1-mediated methylation of the C subunit.

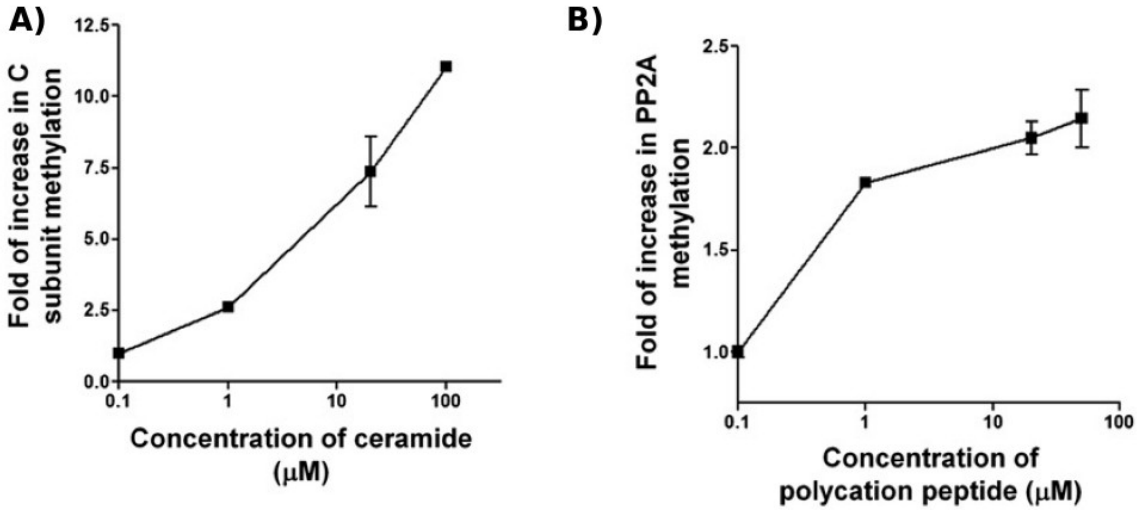

Figure 2.12. Positive effect of ceramide **(A)** and polycationic peptide KRTIRR **(B)** on the LCMT-1 methyltransferase activity.

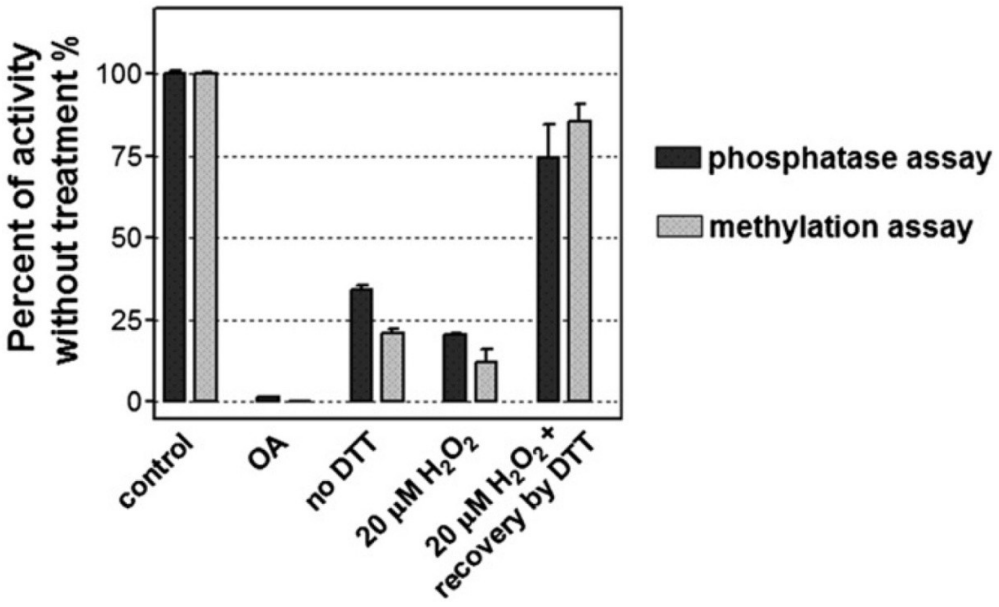

Figure 2.13. Simultaneous loss of LCMT-1 methylation activity and the phosphatase activity of the PP2A core enzyme caused by okadaic acid and mild oxidation upon removal of DTT or in the presence of 20 μM H_2O_2.

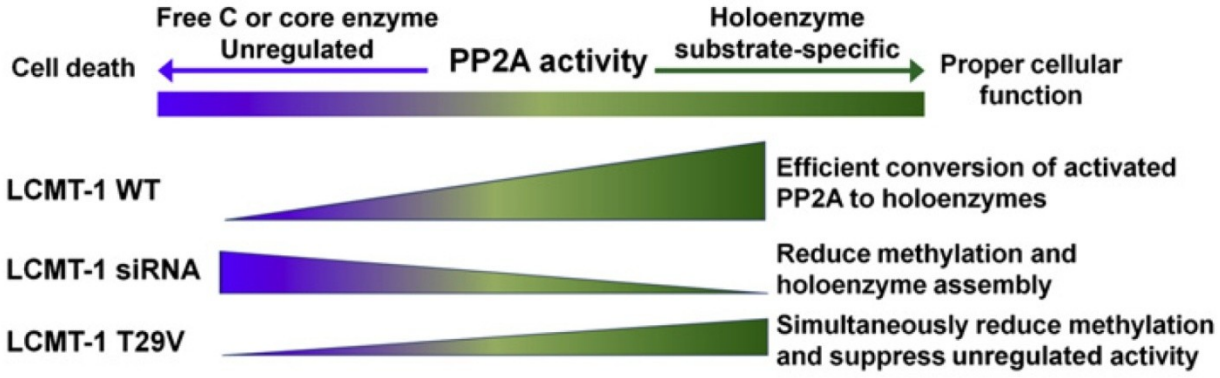

Figure 2.14. The effect of PP2A phosphatase activity on cell fitness. The phosphatase activity of free C or the core enzyme is less controlled and can be detrimental to the cell; substrate-specific phosphatase activity of holoenzymes is essential for proper cellular function. Normal cells expressing WT LCMT-1 facilitate efficient transition of activated PP2A to holoenzymes, thus minimizing uncontrolled phosphatase activity. The effect of LCMT-1 knockdown or expression of LCMT-1 T29V is illustrated.

Table 2.1 Data collection and refinement statistics of PP2Ac:LCMT-1 complex	
Data collection	
Space group	P212121
Resolution (Å)	50-2.7
Unique observations	17,595
Data redundancy	7.5 (5.2)
I/sigma	7.5 (4.4)
Completeness	98.9% (92.9%)
R_{sym}	0.136 (0.349)
Refinement	
Resolution (Å)	48.3-2.7
Number of reflections	16,510
R_{work}/R_{free}	19.9%/25.0%
Number of atoms	
Protein	5,001
Ligand/ion	37
Water	121
Average B factors (plus TLS contribution)	14.7 (43.7)
Rmsds	
Bond lengths (Å)	0.007
Bond angles (°)	1.03
Ramachandran plot	
Preferred regions (%)	94.7
Allowed regions (%)	4.7
Outliers (%)	0.5
X-ray diffraction data were collected on one crystal. Values in parentheses are for the highest-resolution shell.	

Table 2.2 PP2A active site loops that interact with LCMT-1					
Protein loops in C	Residue range	Active site loops	Metal chelating residues	Interface to LCMT-1	Interface to PTPA (81)
CL1	17-25				
CL2	42-45				
CL3	49-54				
CL4	56-61	X	D57, H59		
CL5	73-79				
CL6	83-92	X	D85	X	X
CL7	107-110				
CL8	115-128	X	N117	X	X
CL9	136-141				
CL10	151-155	X			
CL11	159-162				
CL12	166-175	X	H167		
CL13	182-194	X			
CL14	203-207	X		X	X
CL15	212-217	X		X	X
CL16	232-236				
CL17	240-247	X	H241	X	X
CL18	251-256				
CL19	260-272	X		X	X
CL20	279-284				

Chapter 3
Mechanisms of the scaffold subunit in enhancement of PP2A methylation

The studies presented in this chapter is submitted for publication:

Stanevich V, Guo F, Jiang L, Xing Y "Mechanisms of enhancement of Protein Phosphatase 2A methylation by the scaffold subunit" (submitted/under review, Plos One)

My contributions included protein purification, measuring methyltransferase and phosphatase activities, determining kinetics of methyltransferase reaction, performing ITC, writing manuscript (together with Dr. Y. Xing). Dr. F. Guo performed PTPA and A-subunit knockdown experiments. Dr. L. Jiang characterized recombinant PP2A C-subunit purified from insect cells and assisted cell biology experiments. Dr. Y. Xing designed the project and wrote the manuscript.

3.1. Abstract

Protein phosphatase 2A (PP2A) is a major serine/threonine phosphatase in eukaryotic cells with complex composition. PP2A holoenzymes share a common core-enzyme formed by catalytic (C) and scaffold (A) subunits, but have a variable regulatory (B) subunit that controls substrate specificity and subcellular localization of the holoenzyme. Carboxyl methylation of PP2A-tail by leucine-carboxyl methyltransferase 1 (LCMT-1) is an important mechanism regulating holoenzyme assembly. It was recently shown to require activation of PP2A phosphatase activity. Here we showed that LCMT-1 has a higher methylation activity toward the core enzyme than the free C-subunit. The A-subunit enhances PP2A methylation via three combined mechanisms: 1) restriction of the mobility of PP2A-tail for accelerated entry into the LCMT-1 active site pocket; 2) weak charge-charge interactions between the N-terminal HEAT repeats of the A-subunit and the negatively charged residues of LCMT-1; and 3) stabilization of PP2A fold. Consistent with these observations, the A-subunit acts concertedly with PP2A phosphatase activator (PTPA) to maintain the normal methylation level of PP2A in *HeLa* cells. Collectively, our studies revealed novel mechanisms of the scaffold subunit in PP2A methylation important for proper holoenzyme generation.

3.2. Introduction

Protein phosphatase 2A (PP2A) is one of the most abundant serine/threonine phosphatases in eukaryotic cells and functions as heterotrimeric holoenzymes. Each holoenzyme contains catalytic C- and scaffold A-subunits, and a highly diverse regulatory B-subunit (8). The A- and C-subunits form a stable core-enzyme, and each has two closely related isoforms, α and β, with the α isoform being the predominant form. Variable regulatory subunits are divided into 4 families, with a total of approximately 30 members (16). The regulatory subunits define the substrate specificity and cellular localization of PP2A holoenzymes.

PP2A holoenzyme assembly is highly regulated by methylation of the last leucine residue (Leu-309) of the catalytic subunit carboxylterminal peptide (C-tail, residues 294-309) (58,121-123). Observations from yeast and mammalian cells showed that methylation of the C-tail is required for holoenzyme assembly with B, B' and B'' families of regulatory subunits *in vivo* (51,58,122). Methylation is reversibly controlled by leucine carboxyl methyltransferase 1 (LCMT-1) and PP2A methylesterase 1 (PME-1) (55,56,102). Recent structures of PP2A in complex with LCMT-1 and PME-1 revealed that these enzymes also play a role in coupling PP2A phosphatase activity to methylation. PME-1 mediates PP2A inactivation by eviction of catalytic metal ions in addition to catalyzing PP2A demethylation (103). LCMT-1 binds directly to the PP2A active site and requires an active conformation of the PP2A active site for methylation of PP2A-tail, thereby ensuring that the active PP2Ac is selectively enhanced to be methylated and assembled into holoenzymes (106). The ability of LCMT-1 to couple PP2A methylation to activation was demonstrated by the fact that removal of PP2A catalytic metal ions led to simultaneous loss of PP2A phosphatase activity and its ability to be methylated.

Furthermore, PP2A phosphatase activator (PTPA) stimulates both PP2A phosphatase activity and LCMT-1-mediated methylation by approximately 5-fold (106).

The A-subunit is a HEAT (huntingtin-elongation-A subunit-TOR) repeat protein containing 15 HEAT repeats. It mainly functions as a scaffold protein recruiting regulatory and catalytic subunits for formation of trimeric PP2A holoenzymes. In each holoenzyme, the carboxylterminal HEAT repeats (11-15) of the A-subunit interact with the catalytic subunit, and the N-terminal HEAT repeats (1-8) interact mutually exclusively with one of the regulatory subunits. In addition to its role as a scaffold protein, the A-subunit was suggested to play a role in PP2A methylation in yeast. A recent study showed that methylation of the yeast PP2A, Pph21/Pph22, is compromised by deletion of *TPD3*, the yeast homolog of the A-subunit, and Tpd3 is required for maintenance of active Pph21 and proper generation of PP2A holoenzymes (43). Despite the importance of the scaffold subunit in PP2A methylation, the underlying mechanism remains unclear.

Our recent study revealed a highly malleable nature of the PP2A active site and the overall PP2A-fold, and discovered that PTPA functions as a novel activation chaperone that sculpts and stabilizes an active conformation of PP2A (81). In this chapter, we describe an involvement of the A-subunit in PP2A methylation. We show that the A-subunit increases LCMT-1-mediated methylation of the catalytic subunit by combination of restriction of C-tail mobility, weak charge-charge interactions with negatively charged residues of LCMT-1, and stabilization of PP2A fold and the active site conformation. The latter partially mimics the function of PTPA in retaining an active conformation of PP2A that is required for LCMT-1-binding during methylation of PP2Ac. Our studies establish a novel role of the A-subunit in PP2A biogenesis,

which works concertedly with PTPA and LCMT-1 for the strict control of PP2A activation, methylation, and subsequent holoenzyme formation.

3.3. Methods

Protein purification. All protein constructs were generated by standard PCR molecular cloning technology. The Aα-subunit gene was cloned into pQlink vector and expressed in *E. coli* DH5α as GST-tagged protein by overnight induction at 23°C. Human LCMT-1 was cloned into pET15b vector (Invitrogen) and overexpressed at 37°C in *E. coli* BL21 (DE3) as the His_6-tagged protein. The PP2A Cα-subunit was expressed in insect cells as His_8-tagged fusion protein using Bac-to-Bac baculovirus expression system (Invitrogen). After affinity purification, all tags were cleaved by TEV protease, and proteins were further purified by ion exchange chromatography (Source 15Q/S, GE Healthcare). Stable PP2A core enzyme was assembled as described previously (120). Briefly, the Cα-subunit after Ni-NTA affinity purification was passed through GS4B resin immobilized with GST-Aα, followed by three washes. After elution and TEV protease cleavage, the core enzyme was further purified by anion exchange chromatography (Source 15Q, GE Healthcare).

Inactivation and reactivation of PP2A. PP2A core-enzyme or free catalytic subunit (10 μM) was inactivated by treatment with 1 mM pyrophosphate (PPi) in 25 mM Tris pH 8.0, 150 mM NaCl, 5 mM DTT for the specified amount of time at 37°C. The protein was diluted 50-fold with assay buffer with or without $MnCl_2$ (100 μM final concentration) for reactivation. Samples were normalized by amount of the C-subunit using SDS-PAGE prior to assays measuring the phosphatase activity or methylation by LCMT-1. All experiments were performed in triplicates and repeated at least twice. Mean±SEM were calculated and shown. Where indicated, results were normalized to positive control.

Methylation assay. Methylation was performed by mixing 14 nM LCMT-1 with indicated concentrations of PP2A and ^{3}H-SAM (50 μM) in a reaction buffer containing 25 mM Tris pH 8.0, 150 mM NaCl, 5 mM DTT, 1 mg/ml BSA, 50 μM $MnCl_2$ (omitted for PP2A inactivated by pyrophosphate treatment). The reaction was carried out at 37°C for 12 min and stopped by addition of 25% (w/v) TCA. After incubation on ice for 10 minutes, the precipitate was washed twice with 5% TCA, redissolved in 70% EtOH, and the radioactive signal was measured using liquid scintillation counting. The enzyme kinetics was analyzed with GraphPad Prism 5.0 and Sigma Plot 7.0 (Enzyme Kinetics Module) software, and K_m and K_{cat} were calculated.

Phosphatase activity. Two microliters of 1 mM phosphopeptide substrate (K-R-pT-I-R-R) were added to 50 μl of 20 nM PP2A. The reaction was carried out at room temperature for 15 min, stopped by addition of 100 μl of malachite green solution. The amount of the released phosphate was quantified by absorption at 620 nm after 10 min incubation.

Isothermal titration calorimetry (ITC). The binding affinities between PP2A and LCMT-1 were determined by titrating 300 μM LCMT-1 to 15 μM PP2A in 20 mM Tris, pH 7.5, 150 mM NaCl, 50 μM $MnCl_2$ using a VP-ITC microcalorimeter (MicroCal). The data were fitted with Origin 7.0 to calculate the equilibrium dissociation constant.

3.4. Results

3.4.1. The A-subunit increases methylation of PP2Ac

The purified recombinant C-subunit over-expressed in insect cells is barely methylated, as shown by western blotting using an antibody that specifically recognizes the unmethylated PP2A-tail (4b7) (Fig. 3.1). NaOH treatment converts all PP2A C-subunits into the unmethylated form (124). The recombinant C-subunit gave similar signals for the unmethylated PP2A-tail prior to and after NaOH treatment, indicating that the level of methylation for the recombinant PP2Ac is negligible. After incubation with LCMT-1/SAM, the signal for the unmethylated PP2A-tail was significantly reduced, and could be reversed by NaOH treatment.

To determine the role of the A-subunit in methylation of PP2Ac by LCMT-1, we compared the rate of methylation in the presence and absence of the A-subunit (Fig. 3.2 A), and determined the influence of the A-subunit on the binding affinity between PP2A and LCMT-1 (Fig 3.2 B). The A-subunit increased the binding affinity by 2-fold, and significantly increased the methylation rate. Study of the enzyme kinetics for methylation showed that the presence of the A-subunit decreased K_m for more than 6-fold (Fig 3.3).

3.4.2. The A-subunit helps to stabilize the PP2A fold

One of our hypotheses on the effect of the A-subunit on methylation is that the A-subunit plays a role in stabilization of the PP2Ac fold, similar to PTPA. To test this hypothesis, we designed a mini-A construct of the A-subunit with an internal deletion of HEAT repeats 2-10, retaining the C-terminal HEAT repeats required for the C-subunit binding. Since mini-A and LCMT-1 bind to the opposite surface of PP2Ac, utilization of mini-A allowed us to determine

the effect of the A-subunit binding with PP2Ac that might indirectly affect PP2A methylation, independent of potential interactions between the N-terminal HEAT repeats and LCMT-1. The enzyme kinetics of PP2Ac methylation showed that the presence of mini-A reduced the K_m by about 2-fold, which is similar to the effect of PTPA on PP2A methylation (Fig. 3.3). This result suggests that the A-subunit can enhance PP2A methylation in part by stabilization of PP2A fold similar to PTPA (125).

Recent studies in our group suggest a dynamic nature of free PP2Ac. Chelation and eviction of catalytic metal ions by pyrophosphate (PPi) led to partial unfolding and rapid aggregation of PP2Ac (125). To further demonstrate whether the A-subunit binding could help stabilize the protein fold of PP2Ac, we determined whether the presence of mini-A could prevent aggregation of PP2Ac upon eviction of catalytic metal ions. The catalytic metal ions were removed by PPi, and protein aggregation was monitored by measuring absorption at 320 nm in the presence of mini-A and α4 (Fig. 3.4). We recently showed that α4 could stabilize the inactive PP2Ac in a partially folded soluble form (Chapter 4) (125) . The presence of mini-A significantly reduced aggregation of PP2Ac upon eviction of catalytic metal ions. This is likely due to the ability of the A-subunit binding to reduce the relay of allosteric conformational changes caused by perturbation of the active site (chapter 4). Consistent with this result, the presence of the A-subunit reduced the rate of PPi-mediated PP2A inactivation, and the phosphatase activity could be recovered completely or partially by addition of Mn^{2+} ions depending on the duration of incubation with PPi. These results suggest that, after removal of catalytic metal ions in the presence of the A-subunit for the limited period of time, the protein fold of PP2Ac was partially stabilized and allowed re-loading of Mn^{2+} for reactivation. Due to sensitivity of LCMT-1-

mediated PP2A methylation on the active site and the protein fold of PP2Ac, this function of the A-subunit likely contributes to its ability to enhance methylation of PP2Ac.

3.4.3. The N-terminal HEAT repeats of the A-subunit likely contributes to enhanced PP2A methylation by restriction of PP2A-tail.

The role of the A-subunit-binding on stabilization of PP2A fold accounts for only a fraction of the total effect of the A-subunit on PP2A methylation. The K_m for methylation of PP2Ac associated with mini-A is more than 2-fold higher than the K_m for PP2Ac associated with the full-length A-subunit. Alignment of structures of PP2A core enzyme and holoenzymes (PDB codes: 2IE4, 2NPP, 3DW8) and the structure of the LCMT-1:PP2Ac complex via residues 1-293 of the C-subunit shows that the top ridge of the N-terminal HEAT repeats of the A-subunit is oriented for potential interactions with LCMT-1. Furthermore, the N-terminal HEAT repeats and LCMT-1 define a confined space that may restrict the movement of PP2A C-tail, and thus facilitate substrate entry into the substrate-binding pocket and the active site of LCMT-1 (Fig. 3.5 B).

To test the contribution of the N-terminal HEAT repeats and localize the region of the A-subunit important for enhancement of PP2A methylation, we designed the A-subunit constructs with a series of internal deletion of HEAT repeats Δ2-4, Δ2-6, Δ2-8, Δ2-10 (mini-A), resulting in different lengths of N-terminal HEAT repeats of the A subunit (Fig. 3.5 C). The first HEAT repeat (residues 9-54) was retained in all constructs to facilitate expression of soluble, well-folded proteins. These A-subunit constructs were expressed as soluble proteins and were used to assemble PP2A core enzyme with PP2Ac as previously described (118). Kinetic measurements showed that sequential deletion of N-terminal HEAT repeats led to gradual increase of K_m, but

had little effect on the maximum velocity (Fig. 3.6). These data are in agreement with our hypothesis that the A-subunit plays a role in restraining the C-tail movement to facilitate its interaction with LCMT-1. The length of internal truncation correlated with reduction of C-tail restriction and decrease of methylation rate.

To further support this hypothesis, we expressed a C-subunit mutant with a shortened C-tail (Δ294-298) with intact methylation site (Fig 3.7 A). The five residues deleted are located at the beginning of the C-tail outside the LCMT-1-binding site and do not interfere with LCMT-1 interaction. This deletion significantly decreases the length of C-tail and is expected to reduce the C-tail mobility. If our hypothesis is correct, methylation of PP2Ac by LCMT-1 would be enhanced by this deletion. Indeed, similar to the methylation in the presence of A-subunit, the K_m for methylation of PP2Ac Δ294-298 mutant was reduced by 2.5-fold (Fig 3.7 B).

3.4.4. Residues in the A-subunit that affect interaction with LCMT-1 and methylation of PP2A

An alternative mechanism underlying the effect of the A-subunit N-terminal HEAT repeats on PP2A methylation is that residues from these HEAT repeats directly participate in interaction with LCMT-1. Surface electrostatic potential shows that a significant portion of the N-terminal A-subunit is negatively charged. At the same time, the surface of LCMT-1 outside the interface with the C-subunit has substantial amount of positively charged residues (Fig. 3.8). To test whether these charged surfaces contribute to LCMT-1-A-subunit interaction and methylation of PP2A core enzyme, we mutated the negatively charged residues on the N-terminal surface of A-subunit, including Asp-61,Glu-62, Glu-100, and/or Glu-101. PP2A-A_D61A/E62K and PP2A-A_E100A/ E101K mutations barely altered the K_m values for methylation of PP2A core enzyme,

but reduced V_{max} by 20% (Fig. 3.9 A). PP2A-A_D61A/E62K/E100A/E101K and PP2A-A_D61R/E62R/E100R/E101R quadruple mutations exhibited no effect on K_m, but further reduced V_{max}. The reduced V_{max} can be attributed to aggregation of the A-subunit bearing these mutations as indicated by gel-filtration chromatography (Fig. 3.9 B). As a consequence, a fraction of PP2A core enzyme bearing these mutations would be inaccessible for methylation and thus decrease V_{max} of the reaction. The unaltered K_m indicates that these mutations most likely have no effect on the interaction between LCMT-1 and the mono-dispersed PP2A core enzyme.

Due to the dynamic nature of the scaffold subunit, we examined different models of PP2A core enzyme associated with LCMT-1. In one of the models, Arg183 and Arg258 may interact with a patch of negatively charged residues in LCMT-1: Asp-20, Asp-D171, Glu-177, and Glu-180 (Fig. 3.10). Mutations to these two arginine residues, PP2A-A R183E and PP2A-A R258E, did not affect V_{max}, but increased K_m for methylation of PP2A core enzyme (Fig. 3.11). The changes of K_m caused by these mutations are likely due to decrease in the binding affinity between LCMT-1 and the PP2A core enzyme. This notion was supported by pull-down of LCMT-1 in titrated concentrations by PP2A core enzymes containing wild type or mutant A-subunit (Fig. 3.12). The estimated K_d for PP2A core enzymes bearing these mutations is higher than that containing wild-type A-subunit.

3.5. Discussion

Due to the pivotal role of PP2A in cell function and the fact that PP2A function relies on the assembly of numerous trimeric holoenzymes, intensive efforts were dedicated to the characterization of PP2A holoenzyme formation and factors that regulate this process. In particular, methylation of the C-tail, reversibly controlled by LCMT-1 and PME-1, is critical for holoenzyme assembly. Recent studies from our and other groups revealed hierarchical controls of PP2A holoenzyme biogenesis, a process that involves PP2A activation, methylation and holoenzyme assembly. This work extended an emerging theme of the tight control of PP2A holoenzyme biogenesis and revealed the novel mechanism of the A-subunit in PP2A methylation.

It is important to mention that there are other results obtained in our laboratory in regard of the effect of the A-subunit on methylation that were not described in this chapter. Dr. F. Guo in our laboratory tested the effect of the A-subunit and PTPA knockdown in *HeLa* cells on PP2A methylation. Knockdown of the A-subunit or PTPA alone led to a slight decrease of methylation. Knockdown of both genes increased the level of the unmethylated PP2A by more than 50%. This strongly supports our notion that PTPA and the A-subunit work concertedly to facilitate proper PP2A methylation in mammalian cells.

The A-subunit possesses intrinsic structural flexibility, important for bridging the interaction of the regulatory and catalytic subunits and formation of diverse PP2A holoenzymes from different families and for regulating the substrate access to the PP2A active site (45,47). The A-subunit was considered an important tumor-suppressor (126), and several mutations in it have been linked to tumorigenic transformation (127). The mechanism of the A-subunit in PP2A

methylation is coherent with its role in holoenzyme assembly, which provides insight into the function of this important PP2A-interacting protein. Favorable orientation of interacting proteins is the most common mechanism by which the scaffold subunit increases the rate of reaction. The mechanism of the A-subunit in PP2A methylation is unique in that it relies to a small extent on interaction with LCMT-1. Instead, the ability of the A-subunit to enhance methylation is the result of cumulative contributions from three different mechanisms.

First, the A-subunit serves as a steric barrier to decrease the mobility of the C-tail and facilitate its entry into the LCMT-1 active site. To support this mechanism, we showed that sequential deletion of an increasing number of the A-subunit N-terminal repeats leads to the gradual increase in the K_m for methylation (Fig. 3.5 C, 3.6). Furthermore, shortening the C-tail by internal deletion Δ294-298 enhances PP2A methylation, presumably by reducing the C-tail mobility (Fig. 3.7 A, B). The mini-A constructs missing the N-terminal HEAT repeats also exhibited enhanced PP2A methylation, most likely due to that binding of the A-subunit stabilizes the native PP2A fold, which in turn helps to maintain an active conformation of PP2A that is required for PP2A methylation (Fig. 3.4 A, B). The ability of the A-subunit to stabilize the native PP2A fold is less robust than PTPA, presumably because PTPA is a dedicated chaperone that binds directly to the active site (81). Finally, we identified two arginine residues at HEAT repeats 5 and 7 of the A-subunit that contribute to LCMT-1 binding and methylation of PP2A-tail (Fig. 3.11, 3.12).

Based on our *in vitro* and *in vivo* studies, we propose a working model for the role of the A-subunit in PP2A methylation (Fig. 3.13). As shown in our previous studies (106) and confirmed in this work, PP2A with an inactive conformation is not a substrate for LCMT-1.

Upon activation, the free C-subunit remains a less favorable substrate for methylation. Formation of the core enzyme upon activation makes PP2A the most favorable substrate for LCMT-1, which leads to rapid methylation and recruitment of the regulatory subunits cooperatively by the methylated C-tail and the A-subunit. The role of the A-subunit in this process is three fold: 1) it works concertedly with PTPA to stabilize the active conformation of PP2A and to prevent partial unfolding of the C-subunit (Chapter 4), which is required for methylation; 2) it increases the methylation rate by both restriction of the C-tail and weak charge-charge interactions with LCMT-1; and 3) it recruits the regulatory subunit together with the methylated C-tail. Thus, together with previous studies, the results presented in this chapter reinforce the unifying theme of tight control of PP2A holoenzyme biogenesis and illuminate the coherent mechanism of the A-subunit and its synergy with PTPA in orchestrating PP2A activation, methylation, and holoenzyme assembly.

3.6. Figures and tables

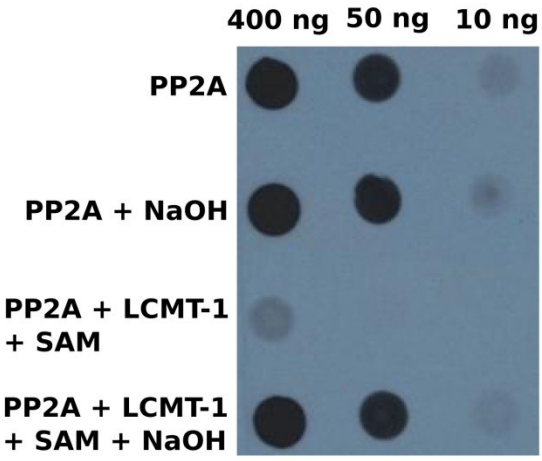

Figure 3.1. Analysis of methylation status of PP2A used in the assays. After purification, PP2A was probed with 4b7 antibody, which recognizes specifically the unmethylated PP2A C-tail. Treatment with NaOH removes the methyl group from the C-tail (124). The same intensity of signal with (PP2A+NaOH) and without (PP2A) NaOH treatment indicates that the recombinant PP2Ac purified from insect cells was unmethylated. The signal for the unmethylated PP2A was decreased upon methylation by LCMT-1 (PP2A+LCMT-1+SAM) and reappeared after NaOH treatment (PP2A+LCMT-1+SAM+NaOH).

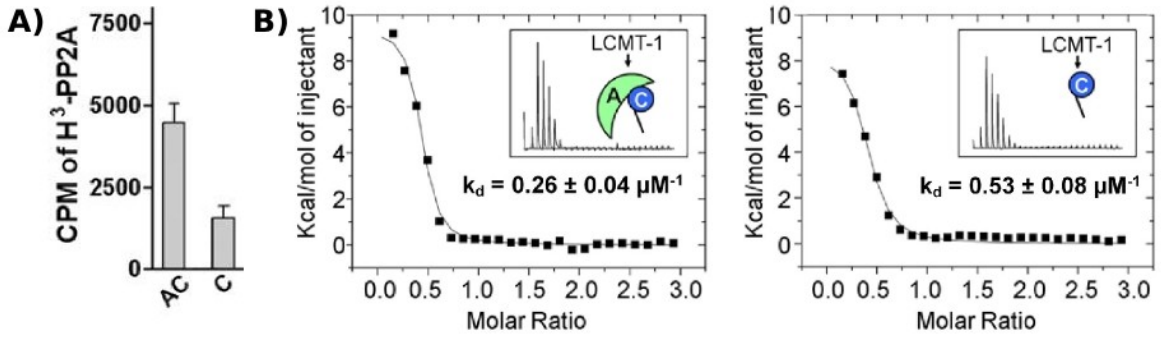

Figure 3.2. The A-subunit enhances methylation of PP2A by LCMT-1. **(A)** LCMT-1 has a higher methylation rate toward PP2A core enzyme (AC) than free PP2Ac (C). **(B)** ITC indicates that LCMT-1 has a higher binding affinity toward PP2A core enzyme than free PP2Ac.

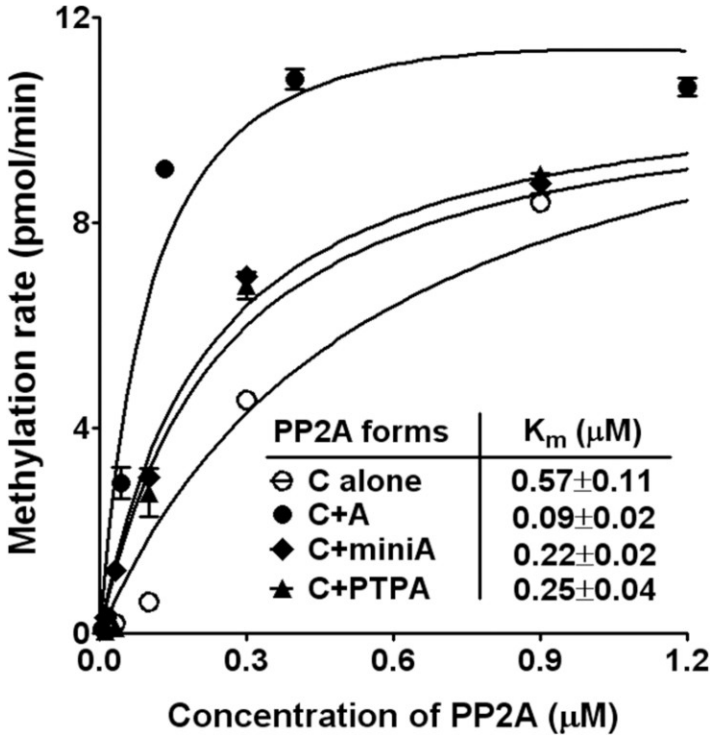

Figure 3.3. Influence of the A-subunit, mini-A, and PTPA on PP2A methylation, tested by addition of these proteins in a stoichiometric amount to PP2Ac, prior to measurement of the kinetics of PP2A methylation.

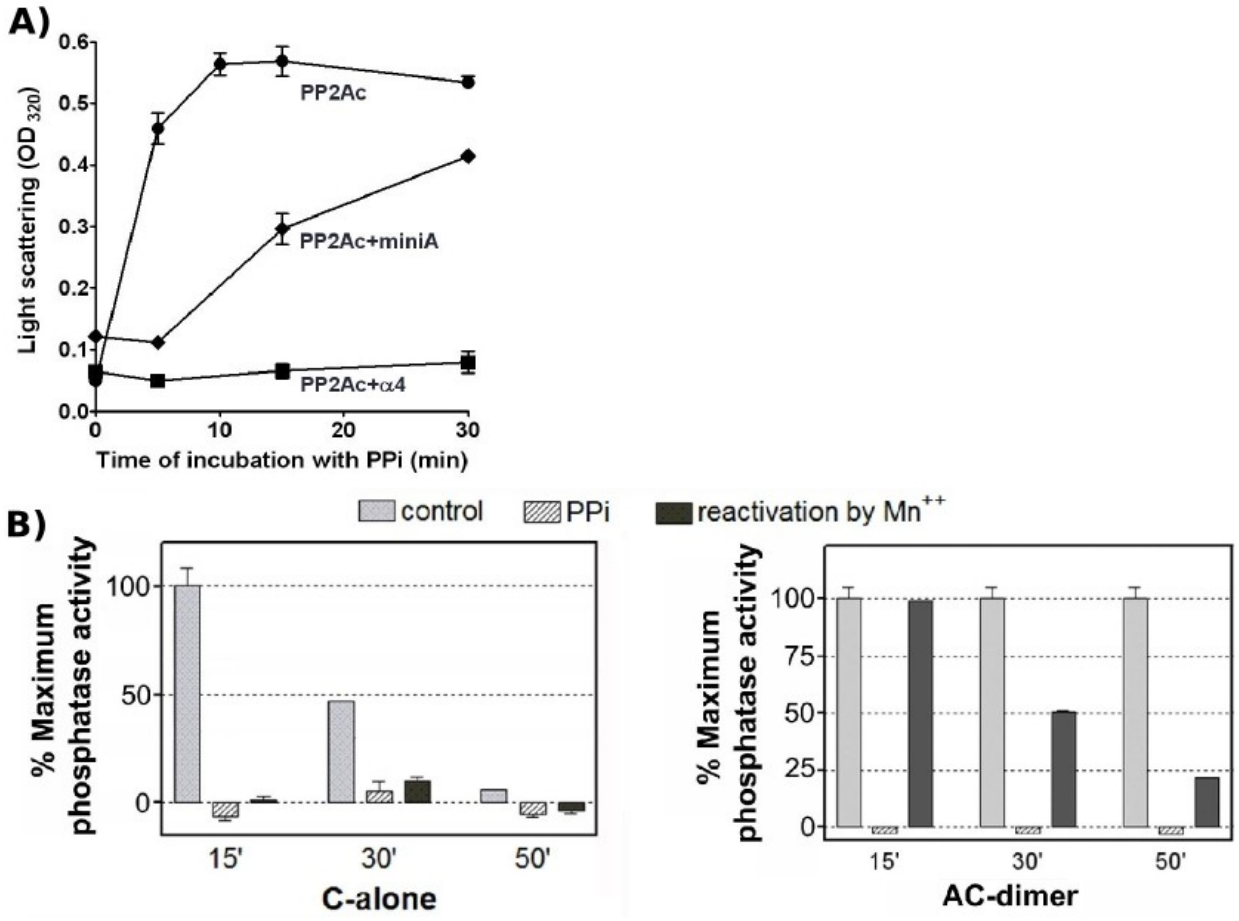

Figure 3.4. Stabilization of PP2Ac fold by the A-subunit. **(A)** PP2Ac was incubated with 2mM PPi at 37°C in the presence or absence of mini-A (the A-subunit missing HEAT-repeats 2-10 (Δ2-10)) and α4. Protein aggregation was monitored by absorption at 320 nm; **(B)** Free PP2Ac and AC-dimer were incubated at 37°C in the presence or absence of 2 mM PPi. The phosphatase activity was measured at the indicated time using pThr peptide as substrate. The samples treated with PPi were reactivated by the addition of 50 μM $MnCl_2$.

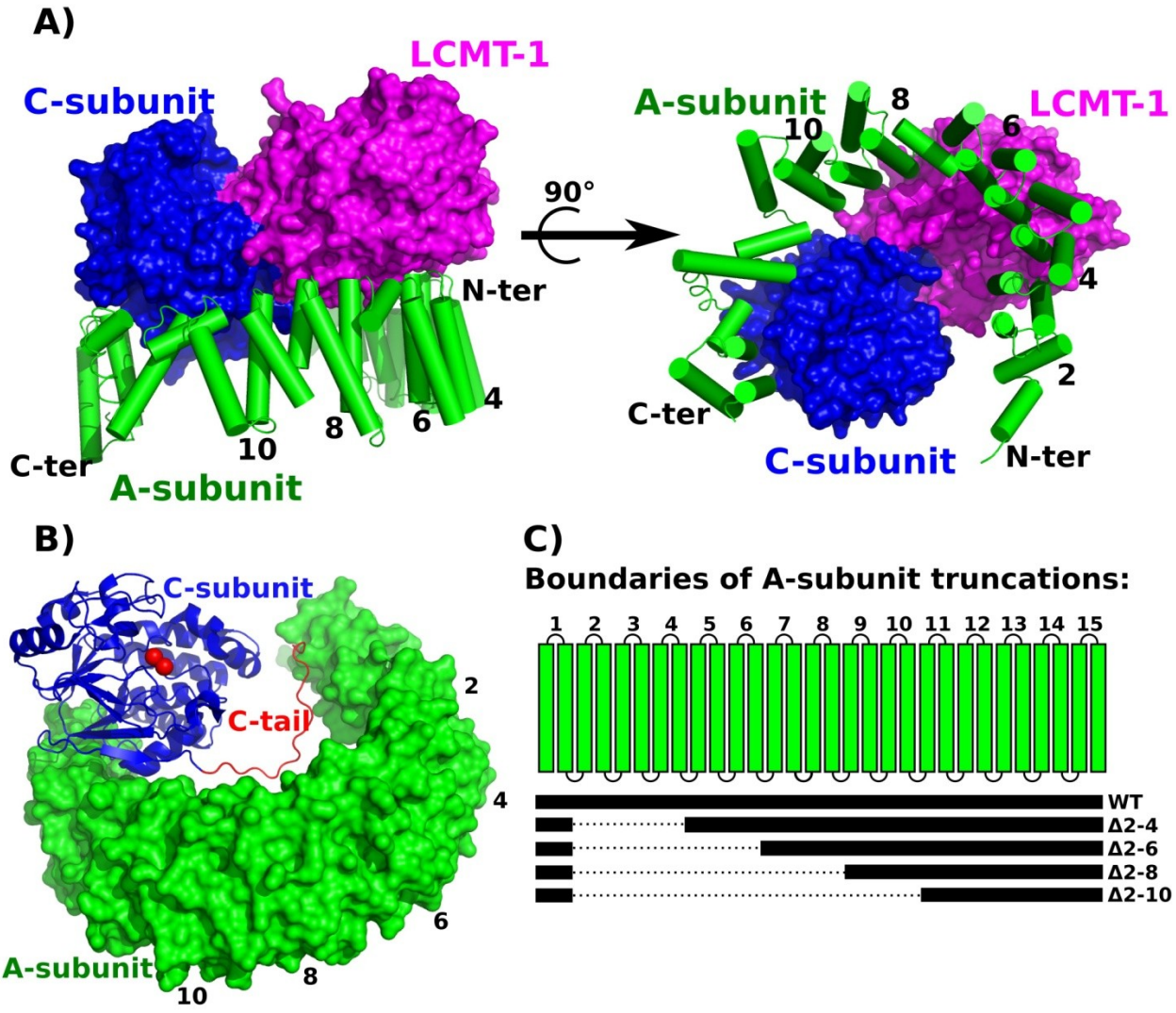

Figure 3.5. Analysis of PP2A structure shows that the A-subunit may serve as a steric barrier for PP2A C-tail movement. **(A)** The structure of the PP2Ac-LCMT-1 complex (PDB ID: 3P71) aligned to the PP2A holoenzyme (PDB ID: 2NPP) via PP2Ac (RMSD < 0.4Å). The C-subunit and LCMT-1 are derived from PP2Ac-LCMT-1 model and shown as blue and magenta surfaces, respectively. The A-subunit is shown as green cylinders and derived from the structure of the PP2A holoenzyme. Positions of HEAT-repeats where truncations were made are indicated by the numbers. **(B)** Structure of PP2Ac holoenzyme (PDB ID: 2NPP) with B-subunit not shown. The color scheme is the same as in (A). **(C)** Schematic representation of truncations introduced to the A-subunit to test the effect of the PP2A C-tail mobility on methylation rate.

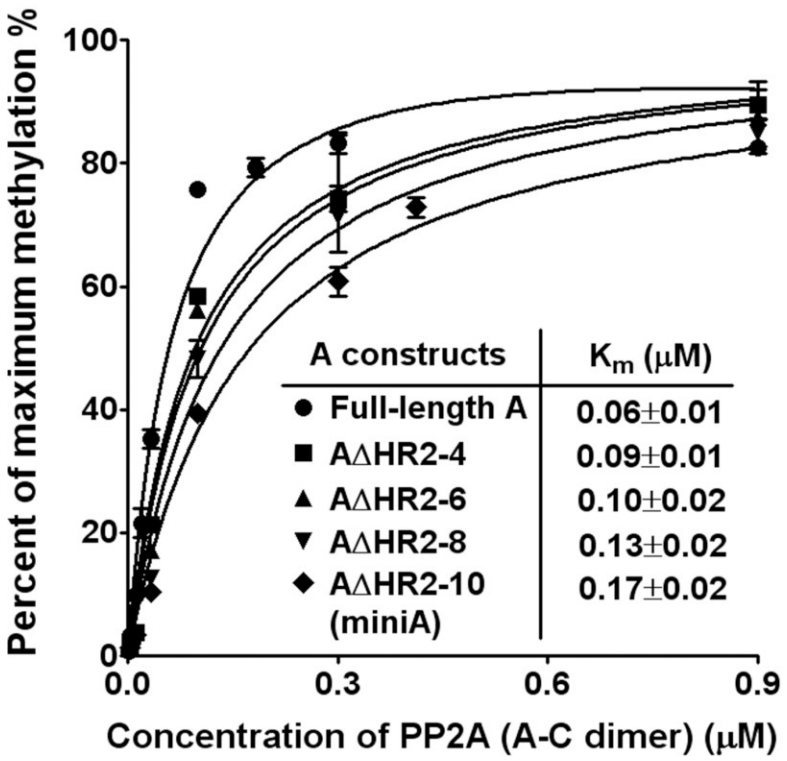

Figure 3.6. The effect of the A-subunit truncation on the kinetics of PP2A methylation. Full-length or truncated A-subunits were assembled with PP2Ac to create core enzymes, and kinetics of methylation was measured to compare the effect of the A-subunit truncations.

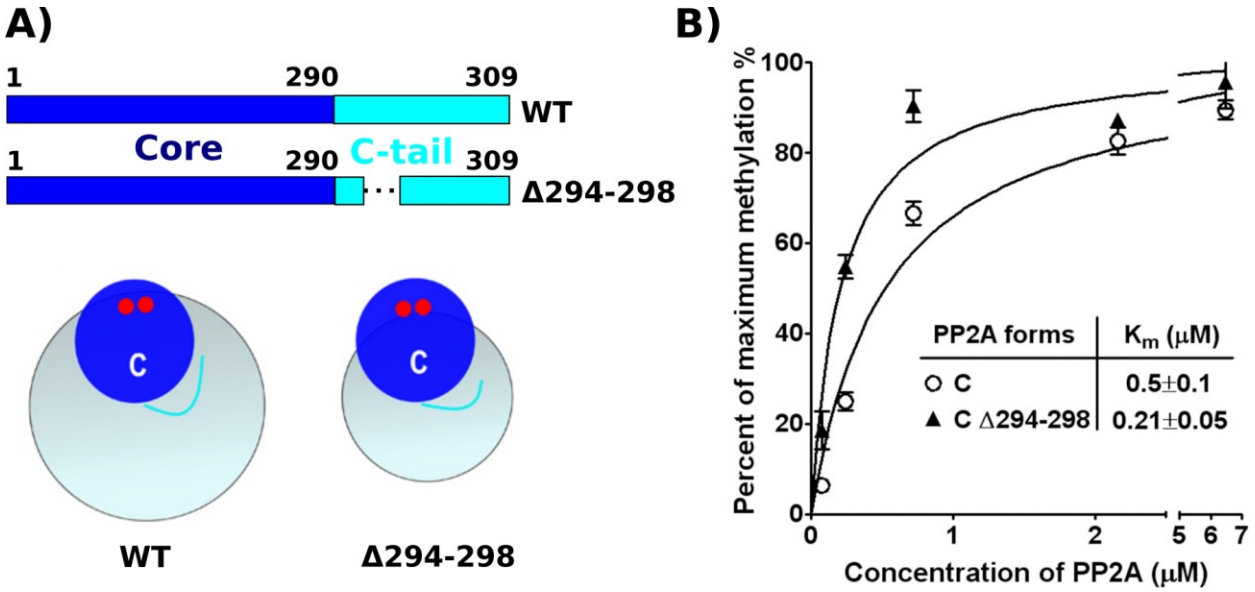

Figure 3.7. The effect of shortening PP2A C-tail on the kinetics of PP2A methylation. **(A)** Schematic representation of Δ294-298 truncation of PP2Ac. PP2Ac is shown as blue sphere with two red circles representing Mn^{2+}. The C-tail is shown in cyan. The circle filled with pale blue color around PP2Ac indicates the space of movement of PP2Ac C-tail. Note that the Δ294-298 truncation reduces the space for the C-tail movement than wild-type PP2Ac. **(B)** Kinetics of methylation were measured using wild-type PP2Ac or PP2Ac Δ294-298.

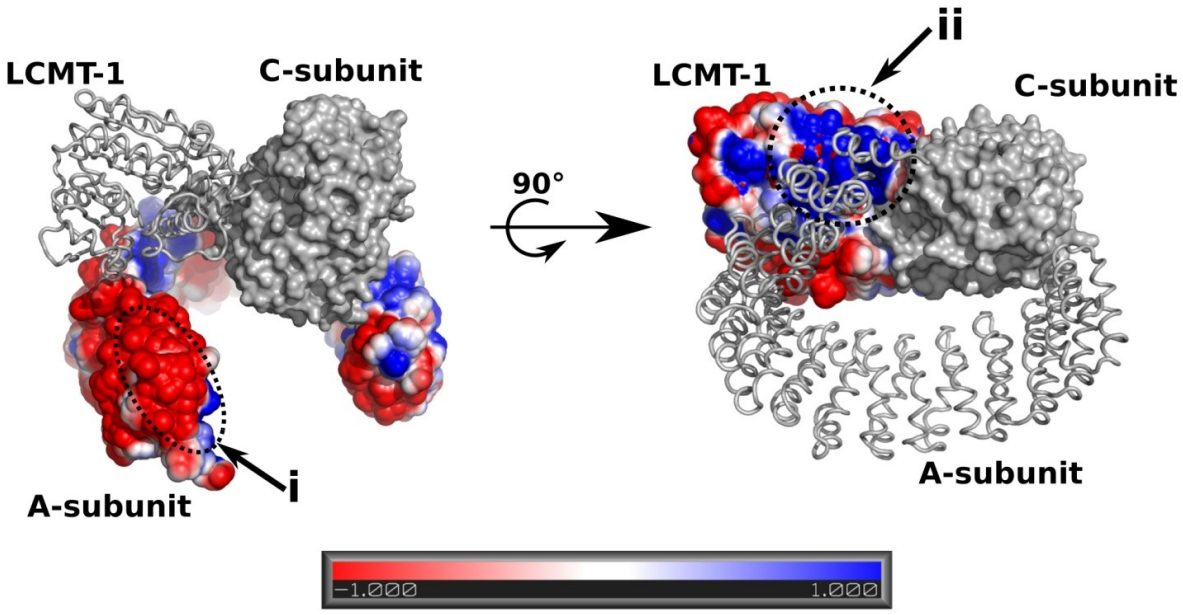

Figure 3.8. Potential charge-charge interactions between the A-subunit and LCMT-1. **(A)** The structure of PP2Ac-LCMT-1 (PDB ID: 3P71) aligned to the structure of PP2A holoenzyme (PDB ID: 2NPP) via PP2Ac (RMSD < 0.4 Å). The C-subunit and LCMT-1 are derived from the PP2Ac-LCMT-1 structure and shown as gray ribbon and surface, respectively. The A-subunit is derived from the structure of the PP2A holoenzyme and the electrostatic potential of A is shown. Region (i) indicates a negatively charged patch on the surface of A-subunit consisting of Asp-61, Glu-62, Glu-100 and Glu-101. **(B)** A perpendicular view of (A). The A- and C-subunits are represented in gray ribbon and surface, respectively. The electrostatic potential of LCMT-1 is shown. Region (ii) indicates a positively charged patch on the surface of LCMT-1.

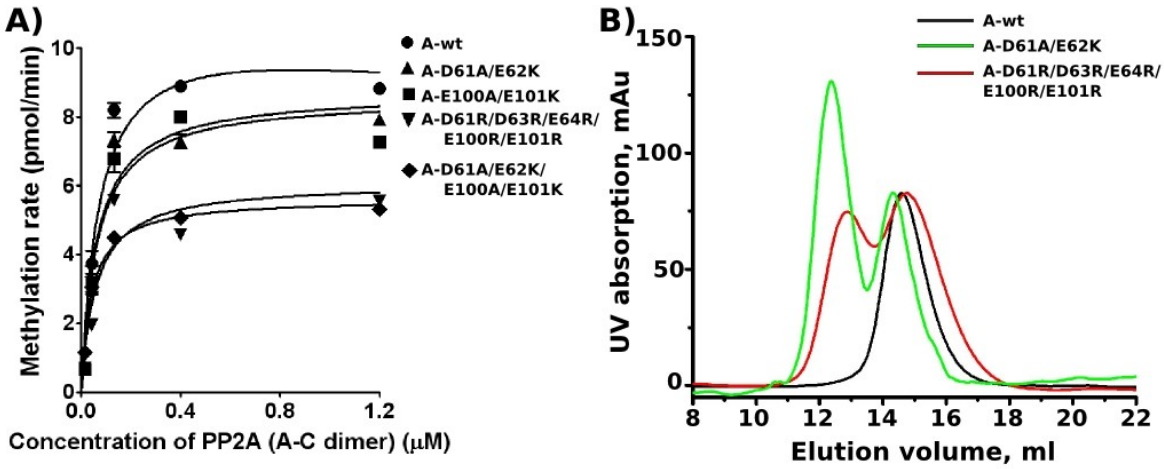

Figure 3.9. The role of the negatively charged N-terminal residues in the kinetics of PP2A methylation. **(A)** Kinetics of PP2Ac methylation was measured in the presence of wild-type or the indicated mutant A-subunits. **(B)** Gel-filtration spectra of wild-type or mutant A-subunits.

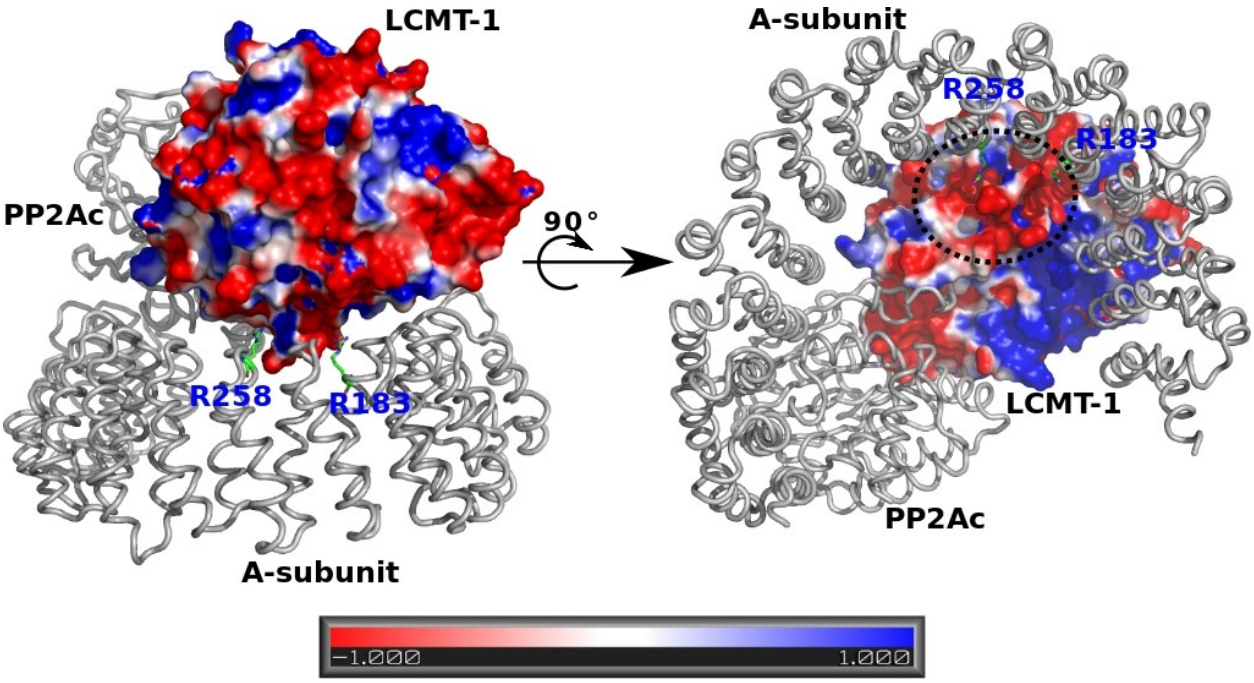

Figure 3.10. Potential interactions between Arg-183/Arg-258 of the A-subunit with LCMT-1. The PP2A A- and C-subunits are shown as gray ribbon. LCMT-1 is shown in surface with electrostatic potential. The position of A-subunit was modeled as one of the intermediate states between the available structures for PP2A core enzyme and holoenzymes (PDB IDs: 2IE4, 2NPP, 3DW8) morphed using Chimera software (128). Arg-183 and Arg-258 are shown as green sticks. A negatively charged surface of LCMT-1 potentially involved in interaction with Arg-183/Arg-258 is circled with dotted line in the right panel.

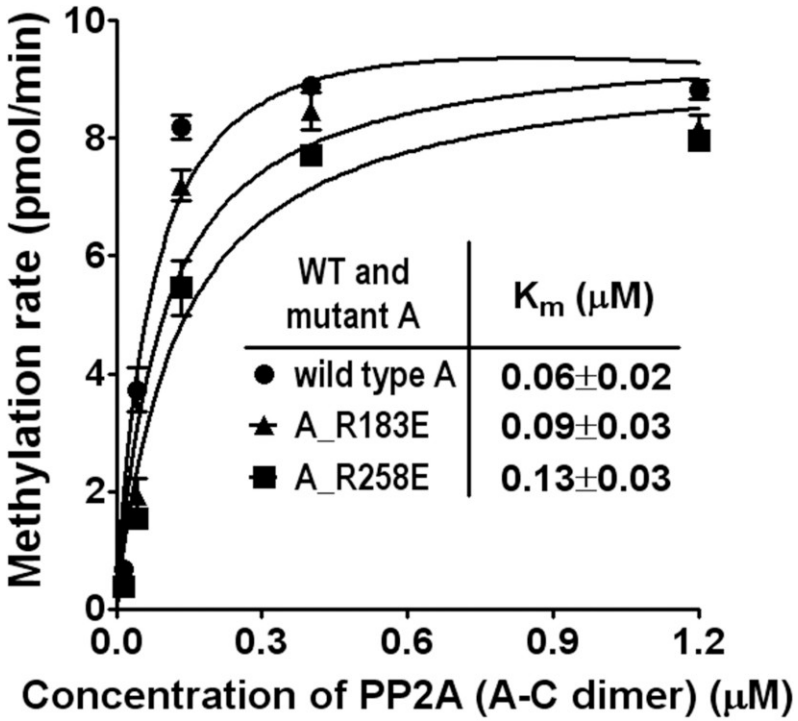

Figure 3.11. The effect of mutations to Arg183 and Arg258 on the kinetics of PP2A methylation by LCMT-1. Methylation of PP2Ac was measured in the presence wild-type or mutant A-subunits.

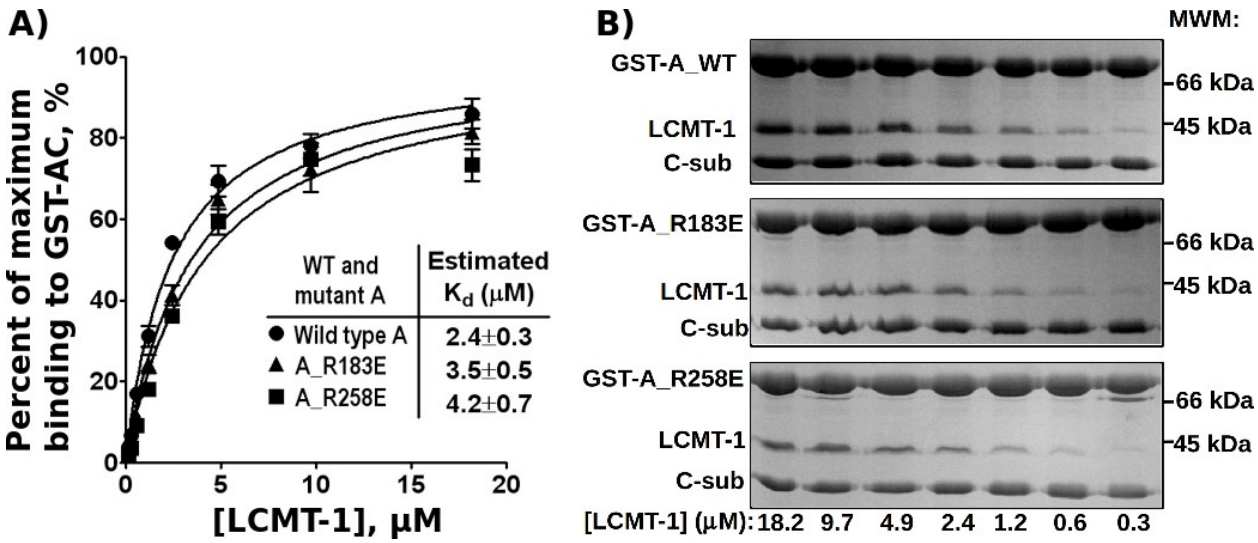

Figure 3.12. The effect of mutations to Arg183 and Arg258 on the binding affinity between PP2A core enzyme and LCMT-1.**(A)** K_d for interactions between LCMT-1 and wild-type or mutant A-subunits determined by pull-down of LCMT-1 in titrated concentrations as shown in **(B)**. **(B)** Wild-type or mutant PP2A core enzymes were immobilized on GS4B-resin by the GST-tag fused to the N-terminus of the A-subunit. Equal aliquots of resin with immobilized GST-AC were mixed with various concentrations of LCMT-1, followed by two washes with the assay buffer and examination of the bound proteins on SDS-PAGE. The signal was quantified using ImageJ software (129).

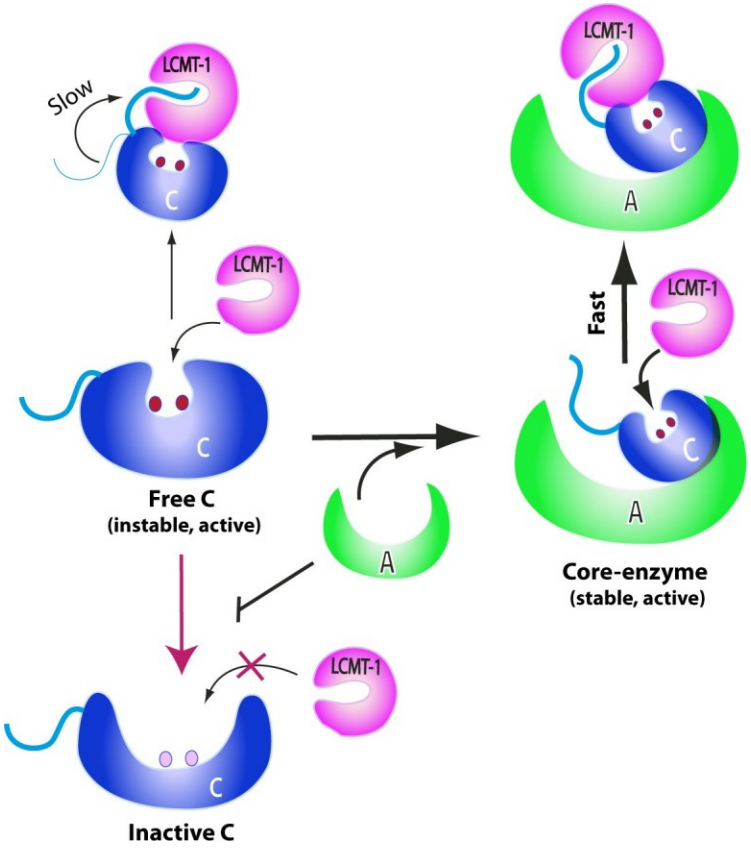

Figure 3.13. A working model illustrating the role of the A-subunit in facilitating PP2A methylation. Methylation of the free C-subunit is prohibited prior to activation and inefficient prior to formation of the core enzyme. The presence of the A-subunit stabilizes the protein fold of the activated C-subunit, and restricts the mobility of the C-tail. These effects of the A-subunit, together with its weak interaction between LCMT-1 via Arg183/258, facilitate methylation of PP2Ac and assembly of holoenzymes.

Chapter 4

Mechanisms of α4 in PP2A stability and latency

A version of this chapter has been published as:

Jiang L*, Stanevich V*, Satyshur KA, Kong M, Watkins GR, Wadzinski B, Sengupta R, Xing Y "Structural basis of protein phosphatase 2A stable latency" Nat Commun. 2013 Apr 16;4:1699.

*These two authors contributed equally to the manuscript.

My contributions included protein purification, protein crystallization, model building (together with Drs. K.Satyshur and Y. Xing), measuring phosphatase activities, performing ITC. Dr. L. Jiang collected X-ray diffraction data (together with Dr. K. Satyshur), performed pull-down assays and biology experiments. R. Sengupta performed PP2A inactivation experiments. Dr. Y. Xing designed the project and wrote the manuscript.

4.1. Abstract

α4 is a PP2A binding protein essential for the stabilization and latency of PP2A catalytic subunit (PP2Ac) during cell cycle and under stress conditions. We identified an N-terminal sub-domain of PP2Ac (nPP2Ac) required for α4 binding and obtained crystal structure of the nPP2Ac-α4 complex. Our model shows that the stable interaction between α4 and PP2Ac involves both surface and internal residues of PP2Ac, which become available only after partial unfolding of PP2Ac near the active site. These changes lead to allosteric conformational changes of the central β-sheets that disrupt the A-subunit binding site at the opposite surface. This provides a plausible mechanism for conversion of PP2A holoenzymes to the α4-PP2Ac complex previously observed under stress conditions. Hydrogen-deuterium exchange mass spectroscopy (HDX-MS) analysis provided further structural insights into the dynamics of PP2Ac and its partially folded nature in complex with α4. HDX-MS data shows that a helix switch (120-127) near the active site is already flexible in the active PP2Ac, and the inner structures buried by the helix switch, and a loop switch (183-195), become exposed after α4 binding. The mode of α4 binding leads to several important biological consequences. First, it stabilizes PP2Ac in a latent, inactive form, which minimizes the uncontrolled phosphatase activity of free PP2Ac. Second, the α4-PP2Ac interaction protects the inactive C-subunit from polyubiquitination and degradation, and provides a stable pool of latent PP2Ac for the biogenesis of diverse PP2A complexes. Altogether, the work in this chapter establishes the structural and biochemical basis for stable PP2A latency mediated by α4.

4.2. Introduction

The α4-protein is the mammalian homologue of yeast Tap42, an essential component of the target-of-rapamycin (TOR) kinase pathway that controls translation initiation and cell survival (82) and plays a role in control of the activity of the type 2A phosphatases, Sit4 and Pph21/22 and their interaction with α4 (130,131). Besides in yeast, the physical interaction of α4 with PP2Ac is also well documented in human, murine, and rat cell lines (84,86,92,94).

The secondary and tertiary structure of human α4 was characterized by a variety of biophysical methods (132,133). Based on circular dichroism (CD) spectra, partial trypsin digestion, and thermal unfolding kinetics of the full length and truncated forms of the α4 protein, human α4 comprises two domains: an N-terminal helix domain consisting primarily of α-helices and a C-terminal unstructured domain (132). Based on small angle X-ray scattering (SAXS), the calculated radius of gyration for full-length α4 was calculated to be 41.2 ± 0.8 Å with maximum dimension of 142 Å, while the α4Δ222 and α4Δ236 mutants gave sufficiently decreased radius of gyration of 21.6 ± 0.3 Å and 25.7 ± 0.2 Å, respectively. The structural models derived from the SAXS data suggest that α4Δ222 and α4Δ236 have globular conformation, whereas the full length α4 exhibits elongated shape (132). This observation correlates with the fact that α4 contains an N-terminal folded helix domain and a C-terminal unstructured domain.

These physico-chemical data were later supplemented by crystal structures of the yeast homolog of α4, TAP42 (133). The model is in general accordance with SAXS data of α4 and shows that Tap42Δ234 adopts an all-α-helical conformation with a total of seven helices organized in an antiparallel arrangement (Fig. 4.1). The overall structure of TAP42 is similar to 14-3-3 and tetratricopeptide repeat proteins, which led the authors to propose that α4 can

function as a scaffolding protein for mediating interaction with PP2Ac (134,135). Moreover, structure-based mutational analysis identified positively charged residues in α4 (residues 162-167) critical for binding to PP2Ac and PP6c (Fig. 4.1) (133).

The α4 protein was initially discovered as immunoglobulin binding protein (IGBP1) (136). Later, α4 was recognized as an inhibitor of PP2A. Currently, α4 is believed to play a role in protecting PP2Ac from polyubiquitination and degradation (87,100) and stabilizing PP2Ac in an inactive form (87). Despite detailed biochemical and cell biology characterization, the exact mechanism of α4 function remains elusive, due to the lack of its structure in complex with PP2Ac. In this chapter, we identified a PP2Ac sub-domain sufficient for interaction with α4 and elucidated its crystal structure in complex with α4. We extended crystallographic characterization by utilization of structure-guided mutational analysis and biochemical characterization, in particular HDX-MS, to obtain additional insights into the structural dynamics of full-length PP2Ac in solution after inactivation and binding to α4.

4.3. Methods

Protein preparation.

All constructs and point mutations were generated using a standard PCR-based cloning strategy. The nPP2Ac (1–153), α4 (3–233) and TAP42 (3–233), and their internal deletion constructs and missense mutants were cloned in pQlink vector (Addgene) harboring a GST- or His_8-tag and a TEV-cleavage site between the tag and the recombinant protein. The proteins were overexpressed at 23°C in *E. coli* strain DH5α. The soluble fraction of the E. coli cell lysate was purified over GS4B resin (GE Healthcare) or Ni-NTA resin (Qiagen), and further fractionated by anion exchange chromatography (Source 15Q, GE Healthcare) and gel filtration chromatography (Superdex 200, GE Healthcare), with or without removal of the affinity tag. Expression and assembly of PP2A core enzyme and holoenzyme follow procedures as described in chapter 2. The nPP2Ac–α4 complex was assembled over GS4B resin with immobilized GST-tagged nPP2Ac bound to α4, followed by cleavage of the GST-tag. The complex was further fractionated by anion exchange and gel filtration chromatography to remove the excess amount of nPP2Ac.

Crystallization and data collection.

Crystals of the nPP2Ac–α4 complex were grown at 18 °C by the sitting-drop vapor-diffusion method by mixing 8 mg/ml of the protein complex with an equal volume of reservoir solution containing 12–15% PEG3350 (v/v), 0.3 M Na/K tartrate. Initial crystals appeared after 1 week and grew poorly. The crystal was improved by seeding and by addition of 10 mM praseodymium acetate (additive), and grew to full within 2 weeks. Crystals were equilibrated in a cryoprotectant buffer containing reservoir buffer with 20% glycerol (v/v), and flash frozen in a

cold nitrogen stream at -170°C.The data sets with anomalous signal of selenium-labeled complex were collected at APS LS-CAT and processed using HKL2000 (107).

Structure determination.

The structure was determined by SAD (single-wavelength anomalous dispersion) phasing using CRANK (137) in CCP4 (138). Eight of nine selenium atoms were located by program AFRO/CRUNCH2 and refined using BP3 (139). Following phase improvement and density modification, a large fraction of α4 and PP2A helix motif was automatically built using Buccaneer (140). Model errors were corrected manually based on the electron density map followed by manual building of the rest of the model. The structure was built using Coot (108) and refined using REFMAC restraints with TLS (138). Two TLS groups were used, nPP2Ac and the PP2Ac-binding domain of α4 (3–233). The structure was refined to 2.8 Å, and the free and working R-factors are 22.2% and 17.9%, respectively.

GST-mediated pull-down assay.

To examine the interaction between α4 and PP2Ac or conversion of PP2A core enzyme and holoenzyme to the α4 complex,10 mg of GST-α4 was mixed with a near stoichiometric amount of free PP2Ac, core enzyme or B'γ1 holoenzyme. The mixture was incubated at 37 °C in the presence or absence of 2 mM PPi or 50 mM Mn^{2+} for the indicated period of time in 200 ml of assay buffer containing 25 mM Tris (pH 8.0), 150 mM NaCl, 2 mM dithiothreitol and 1 mg/ml BSA to block non-specific binding. The sample was then bound to10 ml of GS4B resin via GST-tag. After three washes with the assay buffer, the proteins bound to the resin were examined by SDS–PAGE, and visualized by Coomassie blue staining. Alternatively, 10 mg of GST-nPP2Ac was bound to 10 ml of GS4B resin followed by three washes to remove unbound

protein. Ten micrograms of wild-type or mutant α4 was bound to the resin as described above. All experiments were repeated three times; representative results are shown.

Phosphatase assay. PP2A phosphatase activity was measured using a phospho-Thr peptide. Briefly, 2 ml of 1 mM phosphopeptide substrate (K-R-pT-I-R-R) was added to 20 ml of PP2A sample (20–100 nM). The reaction was performed at 30°C for 15 min and stopped by addition of 50 ml of malachite green solution. The absorbance at 620 nm was measured after 10 min incubation at room temperature. All experiments were performed in triplicate and repeated three times. Mean±SEM were calculated.

Isothermal titration calorimetry. To obtain a direct binding affinity between α4 and nPP2Ac, 400 mM of α4 was titrated with 20 mM of nPP2Ac using a VP-ITC microcalorimeter (MicroCal). All proteins were prepared in a buffer containing 20 mM HEPES (pH 8.0) and 100 mM NaCl. The data were fitted by Origin 7.0.

Determination of metal ion content of PP2Ac. The mixtures of active PP2Ac(0.3 mg) and α4 (0.3 mg) were incubated with 50 mM Mn^{2+} or 3 mM PPi at 37°C for 10 min, followed by removal of PPi and unbound Mn^{2+} ions by gel filtration chromatography. Metal contents of both PP2A samples were then determined by ICP-MS. Re-activation of the inactive PP2Ac–α4 complex induced by PPi was performed by co-incubation with 50 mM Mn^{2+} ions, followed by determination of the phosphatase activity and metal content as described above.

H–D exchange mass spectrometry. H–D exchange was performed following a similar procedure as described (141). Briefly, 40 µl PP2Ac (2 mg/ml) bound to Mn^{2+} or with α4 in D_2O containing 10 mM HEPES, pD 8.0, 50 mM NaCl, and 1 mM dithiothreitol was incubated at 37°C for 10 min to allow deuterium intake into residues with exposed backbone amide. PP2Ac

bound with α4 was induced by co-incubation with 1 mM PPi. The samples were incubated for another 30 min at room temperature, followed by addition of 5 µl 0.5 M sodium citrate (pH 2.4) on ice to quench H–D exchange and pepsin digestion for 5 min. Pepsin cleavage was stopped by addition of 1 ml of pepstatinA (2 mM) and immediate freezing in liquid nitrogen. PP2Ac without H–D exchange was used as control. Control sample was characterized both by liquid chromatography-MS to obtain the control spectra and by tandem MS (TOF/TOF) to confirm the peptide sequences of pepsin-cleaved PP2A fragments. PP2A samples that underwent H–D exchange were analyzed by liquid chromatography-MS, and spectra were compared with control to determine the level of backbone amine deuterium intake intoPP2Ac. The spectra of PP2Ac fragments were analyzed using software Mass Hunter (Agilent Technologies), and the level of deuterium intake was calculated using Excel-based software HX Express (142). Ratio of deuterium intake by PP2Ac bound to α4 versusPP2Ac bound to Mn^{2+} for each peptide was used to evaluate increased dynamics in α4-bound PP2Ac.

4.4. Results

4.4.1. Characterization of PP2Ac sub-domain and its co-crystallization with α4

As mentioned above, α4 consists of two domains: an α-helical N-terminal domain (residues 1-234) and an unstructured C-terminal motif (residues 235-340). Several studies have demonstrated that the N-terminal domain of α4 is essential and sufficient for binding to PP2Ac, while the C-terminal unstructured region binds to the B-box domains of MID1 ubiquitin ligase (143,144). To facilitate crystallization of the PP2Ac-α4 complex, we used human α4 construct consisting only of the N-terminal helix domain: residues 1-234. For simplicity, this construct is hereafter referred to as α4.

Initial attempts to assemble *in vitro* complex between α4 and the full-length active PP2Ac failed due to the lack of interaction between these proteins. Based on the earlier reports that α4-PP2Ac interaction was enhanced after heat shock (87) and on our own observation on the flexibility and instability of PP2A active site (106), we hypothesized that α4 interacts preferentially with the inactive PP2Ac.We inactivated PP2Ac by removal of catalytic metals from the active site during incubation with pyrophosphate (PPi) at 37°C (Fig. 4.2 A). The eviction of metal ions after pyrophosphate treatment was confirmed by inductively coupled plasma mass spectrometry (ICP-MS) (Fig. 4.2 B). As expected, removal of catalytic metal ions resulted in PP2Ac inactivation and stable association of α4 with PP2Ac as measured by pull-down assay (125).

I further investigated the biophysical properties of the inactive PP2Ac associated with α4. The PP2Ac- α4 mixture was incubated at 37°C in the presence and absence of PPi and the changes in secondary structure were monitored by circular dichroism (CD) spectrometry.

Obvious changes in CD spectra were detected upon PPi treatment. As shown by a parallel study in the lab, PP2Ac forms aggregate when incubated with PPi alone; aggregation was blocked when PP2Ac was co-incubated with PPi in the presence of α4 (125). Collectively, these results indicate that PP2Ac might undergo partial unfolding upon eviction of catalytic metal ions, which leads to aggregation of PP2Ac; α4 binds selectively to the partially folded PP2Ac and blocks aggregation. This property of α4 is unique among PP2A binding proteins and may underlie its mechanism in PP2A regulation and cellular function.

Despite stable interaction, the α4-PP2Ac complex assembled by co-incubation with PPi did not crystallize even after considerable effort. To improve crystallization of the complex, we explored PP2Ac subdomain that can expose the α4-binding site and form a stable complex with α4 without inactivation reaction. Based on the available structures of PP2A core enzyme and holoenzymes, after extensive testing, we identified that an N-terminal subdomain of PP2Ac (residues 1-153, subsequently called nPP2Ac) is soluble after overexpression in bacteria and able to form a stable complex with α4 without PPi treatment. In the structure of active PP2Ac, this fragment encompasses the N-terminal helix motif and the closely packed β-strands from one of the two central β-sheets (Fig. 4.3). The binding between nPP2Ac and α4 has a dissociation constant of 0.3 μM, as measured by isothermal titration calorimetry (ITC), while the interaction between α4 and the full-length active PP2Ac was barely detectable by ITC (Fig. 4.4). Interaction between nPP2Ac and α4 is evolutionarily conserved, as yeast α4 homolog TAP42 can form a stable complex with human nPP2Ac.

Co-crystallization nPP2Ac with α4 (1-234) yielded diffracting crystals. Initial crystals were further improved by microseeding and additive screen and finally diffracted to 2.8 Å. Initial

attempts to solve the phases by molecular replacement with models of yeast α4 (PDB ID: 2V0P) and the N-terminal part of PP2Ac derived from the core enzyme structure (PDB ID: 2EI3) have failed, most likely due to significant structural changes in the α4-bound nPP2Ac. We then generated Se-Met derivative crystals and determined the structure by SAD phasing. Resulting model was refined to 2.8 Å resolution with R and R_{free} equal to 17.9% and 22.2%, respectively (Table 4.1).

4.4.2. Overall structure of α4-nPP2Ac complex

After we solved the structure of human α4 in complex with nPP2Ac, the structure of murine α4 was reported (145). It enabled us to compare structural changes in mammalian α4 in the free form and after binding to nPP2Ac. As expected, both α4 and nPP2Ac show significant structural rearrangements compared to the structures reported before (Fig. 4.5 B, C). Similar to the structures of murine and yeast α4, human α4 in complex with nPP2Ac adopts open-cone conformation with the first four helices arranged in antiparallel fashion (Fig. 4.5 A). Although overall orientation of helices remains the same, helices 5 and 6 of α4 form a pair of long "tweezers", 45 Å and 55 Å, respectively, which clamp on the ends of the helix motif of PP2Ac. Such arrangement of helices 5 and 6 is not observed in the structure of free murine or yeast α4, and is induced by the binding of PP2Ac (Fig. 4.5 B).

Despite significant structural rearrangements observed in PP2Ac, the structure of the helix motif remains largely unchanged. Unlike the helix motif, the β-strands and the three active site loops in the α4-bound nPP2Ac are shifted and significantly dislodged from their positions in active PP2Ac. One of the helices (C63-69) is transformed into β-strand stabilized by the interaction with another nPP2Ac molecule at the crystal packing interface (Fig. 4.5 A). The

single-layer β-sheet self associates in the nPP2Ac structure and partially resembles bilayer architecture in the full-length active PP2Ac.

4.4.3. Structural basis for α4-nPP2Ac binding

Structural alignment between the nPP2Ac-α4 complex and the active PP2Ac via the unaltered helices in the helix motif (PDB ID: 3IE3) highlights the changes in PP2Ac required for binding of α4. Two structural elements of PP2Ac near the active site need to be unfolded to make binding to α4 possible: a small helix C120-127 ("helix switch") and an extended loop in the C-terminal half of the PP2Ac molecule, C183-195 or "loop switch" (Fig. 4.6).

The helix switch in active PP2Ac clearly interferes with binding of helix 5 in α4 (Fig. 4.6). The helix switch is unfolded in the α4-nPP2Ac complex, by which Ile-123 is shifted from a surface position to an internal hydrophobic pocket, resulting in alternative hydrophobic contacts among PP2A residues Ile-123, Thr-124, and Phe-150. The internal rearrangement of PP2A packing suggests that this process may occur naturally and requires elimination of H-bond interactions in the active PP2A between the sidechains of Thr-124 and Trp-143 and between the sidechains of Arg-121 and Asp-151. The shift of the helix switch is propagated further into the internal packing of PP2Ac and displaces neighboring active site loops, C83-92 and C56-61, and their connected β-strands, presumably by repulsive contacts such as between Val-126 and Asp-88. These changes may also be driven by the intrinsic instability of the active site loops which are largely disordered in the α4-nPP2Ac structure. As result of these changes, the active site conformation required for binding of catalytic ions is completely abolished. Another important structural alteration of PP2Ac required for binding of α4 is the shift of the loop switch (Fig. 4.6). The position of this loop switch in the fully-folded PP2Ac would interfere with binding α4

helices 5 and 6. During inactivation, the loop switch is likely displaced from its normal position, which exposes the inner structure of PP2Ac required for α4 binding.

As a result of the above described changes, the α4-bound PP2Ac is expected to be stabilized in a latent inactive form. We tested this hypothesis by inactivation of PP2Ac with PPi in the presence of α4, with subsequent removal of excess reagents by gel-filtration and reactivation by Mn^{2+}. As expected, PP2Ac inactivated in the presence of α4 could not be reactivated with Mn^{2+}, which confirms that α4 stabilizes the inactive conformation of PP2Ac.

Comparison with previously published structures of PP2A complexes indicates that α4 binding site does not overlap with the A-subunit binding site. Unlike previously suggested (146), the mutually exclusive binding of α4 and the A-subunit with PP2Ac is due to changes in the binding preferences of PP2Ac upon changes in conformation, but not by competition of overlapping binding sites. Indeed, the first central β-sheet of PP2Ac is connected to the active site loops and the helix switch at one end and to the scaffolding subunit binding site at the other. Unfolding of the helix switch and other structural elements near the active site may initiate an allosteric relay via the central β-sheet and compromise the A-subunit binding site at the opposite surface (Fig. 4.7).

4.4.4. Characterization of the α4-PP2Ac interface

α4-PP2Ac interface is unique among the other PP2A interacting proteins because of its requirement for the partial unfolding of PP2Ac. As a result, the α4 binding site includes both surface and inner packing residues of PP2Ac exposed after inactivation and unfolding. Several lysine residues in PP2A: Lys-29, Lys-34, Lys-41 and Lys-144 are located at or near the α4 interface among which Lys-41 was identified as a PP2A ubiquitination site (Fig. 4.8) (101). This

explains how α4 binding may prevent post-translational modifications of these lysine residues, especially the reported polyubiquitination of Lys-41.

α4-PP2Ac interface is primarily formed by the interaction of above mentioned "α4-tweezers", formed by two last helices of α4: 45 Å long helix 5 and 55 Å long helix 6. The interaction surface can be divided into two regions: cluster (I) formed by helix 5 of α4 and PP2Ac helix motif; cluster (II) formed by interactions of the C-terminus of helix 6 and inter-helix loops near the N-terminus of α4 with the helix motif of PP2Ac (Fig. 4.9).The interface in cluster (I) consists primarily of H-bond interactions made by the sidechain of Tyr-162 in α4 to the sidechains of both Glu-33 and Glu-37 in PP2A, and by the sidechains of Lys-158 and Lys-155 in α4 to the sidechains of Asp-148 and Asp-151 and the backbone of Tyr-152 in PP2A. Interactions in cluster (II) include H-bond, charge-charge, van der Waal's and hydrophobic interactions: H-bonds are formed by the sidechains of Glu-214 and Ser-210 in α4 with the sidechains of Tyr-130 and Lys-144 in PP2Ac; salt bridge is between Asp-207 in α4 and Lys-144 in PP2A; van der Waals interactions between Arg-221 in α4 and Tyr-127 in PP2A and between Arg-98, Gln-213, and Glu-214 in α4 and Ala-140 and Trp-143 in PP2A; and hydrophobic contacts between Ile-217 and Leu-218 in α4 and Gln-125 and Tyr-130 in PP2A.

The nPP2Ac-α4 interface explains previous observations on the function of α4 on all PP2A-like phosphatases: PP2A, PP4, and PP6 (94,97,147). Alignment shows that a majority of PP2Ac residues at the interface with α4 are conserved among PP2A-like phosphatases. Double mutation of TAP42 (R163E/K166D) or human α4 (R155E/K158D) completely abolished the interaction with PP2A and PP6 and compromised the function of α4 in protecting PP2A from

degradation (100,133). These observations can be explained by the structure of the α4-nPP2Ac complex since both of these residues are located at the interface with PP2A.

We performed structure-guided mutational analysis to extend the structural insights derived from the α4-PP2Ac structural model. As shown by the pull-down assay using α4-GST construct, α4 mutations R155E, K158D, or Y162D in the helix 5 and E214R in the helix 6 completely eliminated the interaction between α4 and nPP2Ac. E27K mutation of α4 located at the N-terminal inter-helix loops significantly reduced α4-nPP2Ac interaction. On the other hand, α4 mutations located outside the interface: E107K and E206R, had no effect on the binding (125). In agreement with pull-down data, ITC experiments did not detect interaction between α4 mutants R155E or E214R and PP2Ac, while α4 E27K had a dissociation constant K_d around 33 μM, which is 10-fold higher than that of wild-type α4.

4.4.5. Structural changes of PP2Ac in solution after inactivation

The dynamic nature of α4-bound PP2Ac had been reflected by CD spectrometry. To further characterize structural changes in PP2Ac upon inactivation and association of α4, we utilized hydrogen-deuterium exchange mass-spectrometry (HDX-MS). PP2A was treated by PPi in the presence of α4. PP2Ac in the presence of 50 μM $MnCl_2$ (to maintain the active site conformation) was used as control. All peptides identified after pepsin digestion of the PP2Ac treated by PPi (covering 128 of total 309 residues in PP2Ac), exhibited increased deuterium intake, except two peptides in the N-terminal helix motif: 6-13 and 134-149 (Fig. 4.10 B, D). The increase in deuterium intake suggests that there was unfolding of the secondary structure element or exposure of the region to the solvent. The absolute level of deuterium intake was the highest in the peptides encompassing helix switch and the active site loop next to it (Fig. 4.10 A,

C). When compared to the control sample, the difference in deuterium intake with and without PPi treatment is marginal for the helix switch peptide. This means that the helix switch is already flexible in the native PP2A fold.

The biggest difference in deuterium intake before and after PPi treatment is observed in the peptides located internally in the PP2Ac molecule: C150-158 and C256-265, both of which are the part of the central β-sheets. This indicates that PP2Ac central structures become dynamic and exposed in the α4-bound form. Moreover, in the structure of PP2Ac, one of the internal peptides (C150-158) is buried under the loop switch. Therefore, to make this peptide accessible, the loop switch has to be displaced from its normal position, which correlates with our hypothesis that the loop switch is a flexible region of PP2Ac which is altered during inactivation to allow α4 binding.

4.5. Discussion

Despite the critical role of α4 in cell survival, the precise function and mechanism of this protein remain not completely understood. The first crystal structure of the α4-PP2A complex presented here provides a molecular basis for the previous observations on the ability of α4 to bind the inactive form of PP2Ac, to replace the A-subunit binding, and to prevent polyubiquitination of PP2Ac. Our studies provide novel mechanisms of α4 function. It blocks aggregation of metal-free PP2Ac by shielding the inner structures exposed in the partially folded inactive PP2Ac. Binding of α4 requires local unfolding of two structural elements near the PP2A active site: helix switch (C120-126) and loop switch (C183–195). While the helix switch has to undergo helix-loop transformation to allow binding of α4 helix 5, loop switch region has to change its position to expose the binding site for α4 helix 6.

Several important experiments were performed by my colleagues, primarily Dr. L. Jiang, and left beyond the description of the results section in this chapter. Mutually exclusive binding of α4 and PP2Ac was demonstrated *in vitro* by gradual inactivation of PP2Ac, which correlated with transition of PP2Ac from holoenzyme complexes to α4-bound heterodimers (125). Validity of the interface provided by the crystallographic model was confirmed *in vivo*. α4 mutations at the interface with surface residues (Y162D and E214R) or internal residues (R155E and K158D) led to complete elimination or weakened binding to PP2Ac. Besides, these mutants could not reverse effects of wild-type α4 knockout and led to cell death during conditional knockout in MEF cells with *a4-floxed* gene (125). Moreover, cell lines with overexpressed α4 mutants had

higher turnover rate, which confirms importance of α4 binding for the protection of PP2Ac from polyubiquitination.

We provide several lines of evidence showing that our α4-nPP2Ac model reflects α4-PP2Ac interaction. First, α4 cannot bind active PP2Ac, which suggests that PP2Ac has to be altered to make the interaction with α4 possible. Second, α4 binding prevents aggregation of PP2Ac, which is in agreement with our crystallographic model showing that α4 shields the internal surface of PP2A exposed during inactivation and partial unfolding. Third, results from HDX-MS are consistent with the structural observation in that the helix switch is highly flexible even in the active PP2Ac, which makes its helix-loop transformation energetically feasible during inactivation. Besides, peptide buried under the loop switch becomes more dynamic and solvent accessible after inactivation, which also correlates with our α4-nPP2Ac model.

The structure of α4-nPP2Ac provides novel explanation for the mutually exclusive binding of α4 and the A-subunit to PP2Ac. Our studies strongly suggest that the mutually exclusive binding of α4 and the A-subunit is not due to overlapping binding sites on the surface of PP2Ac, but due to allosteric relay through the central β-sheets induced by α4 through the altering of helix switch conformation. Finally, the mode of α4 contacts with both surface and internal residues of PP2Ac explains the role of α4 in stabilization of the inactive form of PP2Ac and protection of PP2Ac from polyubiquitination and degradation.

It is important to note that binding of α4 to the partially folded PP2Ac is unique and somewhat counterintuitive. All the crystal structures of PPP phosphatases reported so far have the same active state conformation of PP2Ac. It became apparent only recently that, in fact, the C-subunit is highly flexible and unstable. The flexibility of the C-subunit was suggested in the

recent study (106), where recombinant PP2Ac could not be fully methylated without preceding priming by PTPA for transition to the fully-active conformation.

We believe that the α4-PP2Ac interaction is important for establishing stable PP2A latency in the cell. The α4 binding site near the active site of PP2Ac prevents non-specific activity of PP2Ac released from the holoenzyme complex during the normal turnover process and, especially, during stress. Besides that, α4 protects PP2Ac from the cellular degradation by dual mechanism. First, α4 binds to the internal residues of PP2Ac, which blocks formation of insoluble aggregation of partially folded PP2Ac. Second, the α4-PP2Ac binding surface shields several critical lysine residues from polyubuqitination, among which, Lys-41 is previously reported to be the target of MID1 mediated ubiquitination (101). Stable PP2Ac latency mediated by α4 as described here is important for cell survival by maintaining a pool of inactive PP2Ac available for activation and subsequent assembly into active substrate-specific PP2A holoenzymes.

4.6. Figures and tables

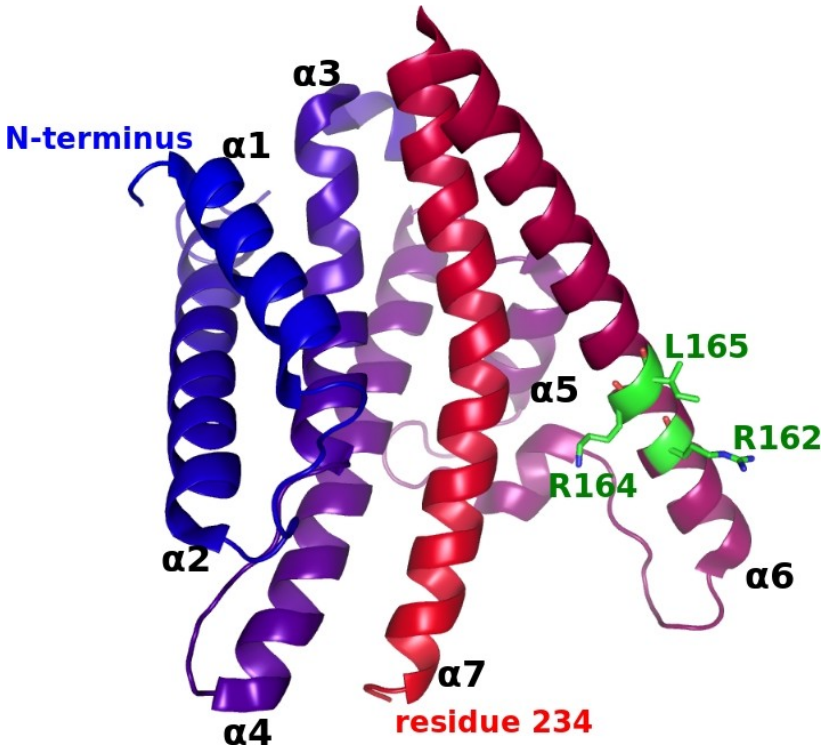

Figure 4.1. Model of yeast α4 homolog TAP42 (PDB ID: 2V0P). Model consists of residues 1-234 and colored in blue-red gradient from N- to C-terminus. Individual helices are labeled as α1-α7. Residues critical for binding to PP2Ac and PP6c (133) are shown as sticks, colored in green and individually labeled.

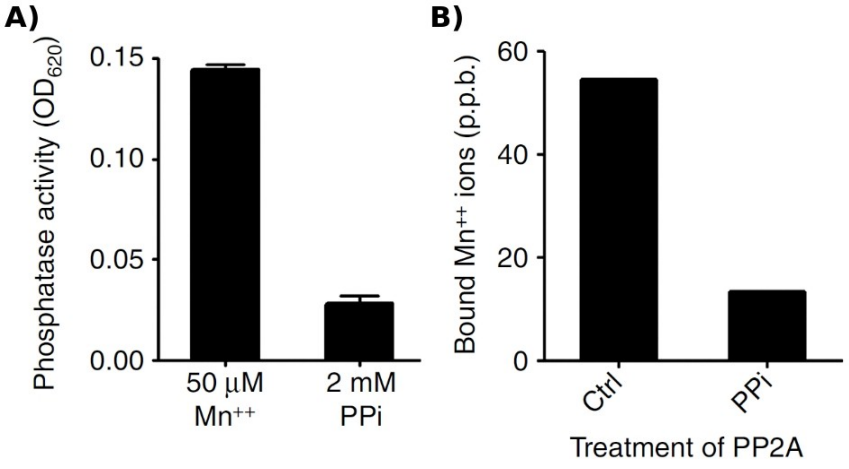

Figure 4.2. Inactivation of PP2A by pyrophosphate. **(A)** The level of phosphatase activity measured after incubation at 37°C with 50 µM $MnCl_2$ or 2 mM pyrophosphate (PPi). **(B)** Changes in the level of Mn^{2+} ions stably bound to PP2Ac before and after PPi treatment.

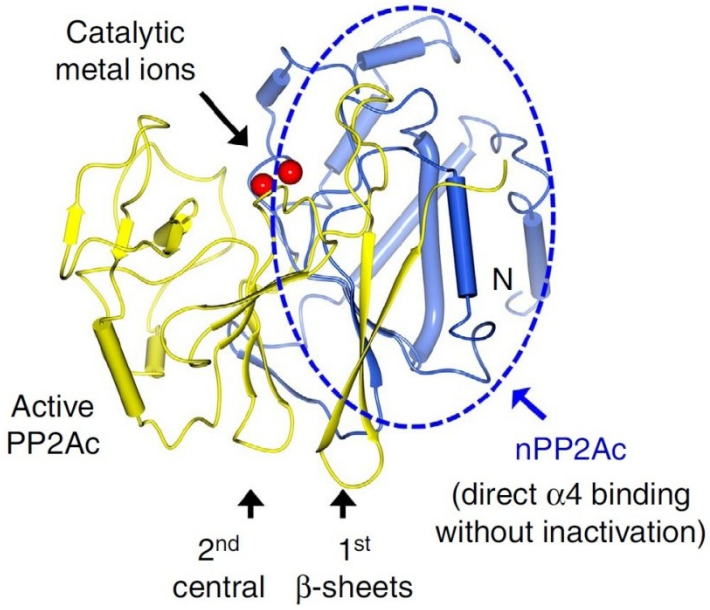

Figure 4.3. α4 interacting domain of PP2Ac.nPP2Ac (blue) is represented using the structure of active PP2Ac (PDB ID: 2NPP).

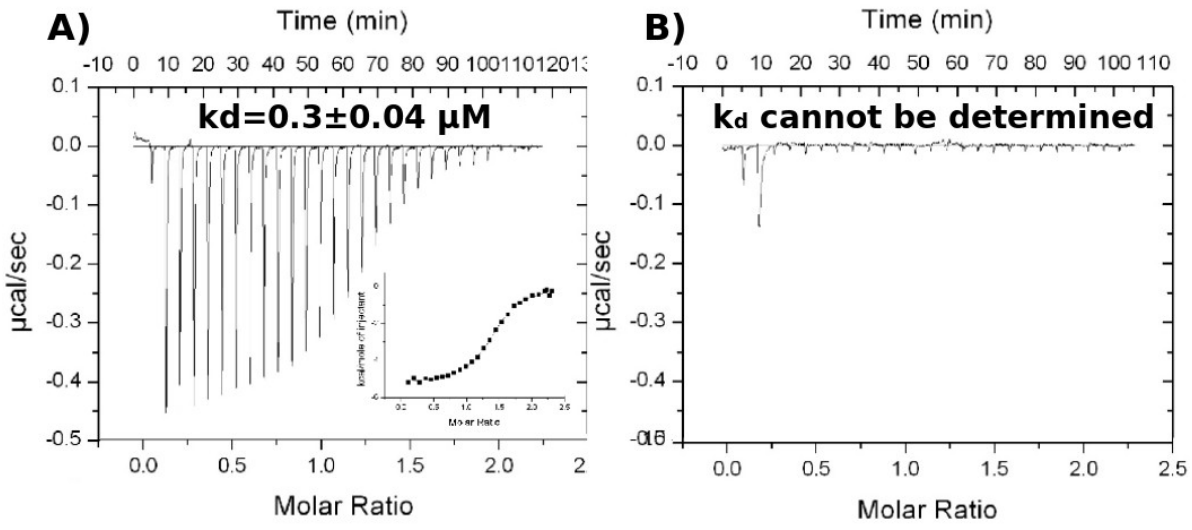

Figure 4.4. ITC determined the binding affinity between α4 and different forms of PP2Ac. **(A)** Interaction of α4 with nPP2Ac. **(B)** Interaction of α4 with active full-length PP2Ac.

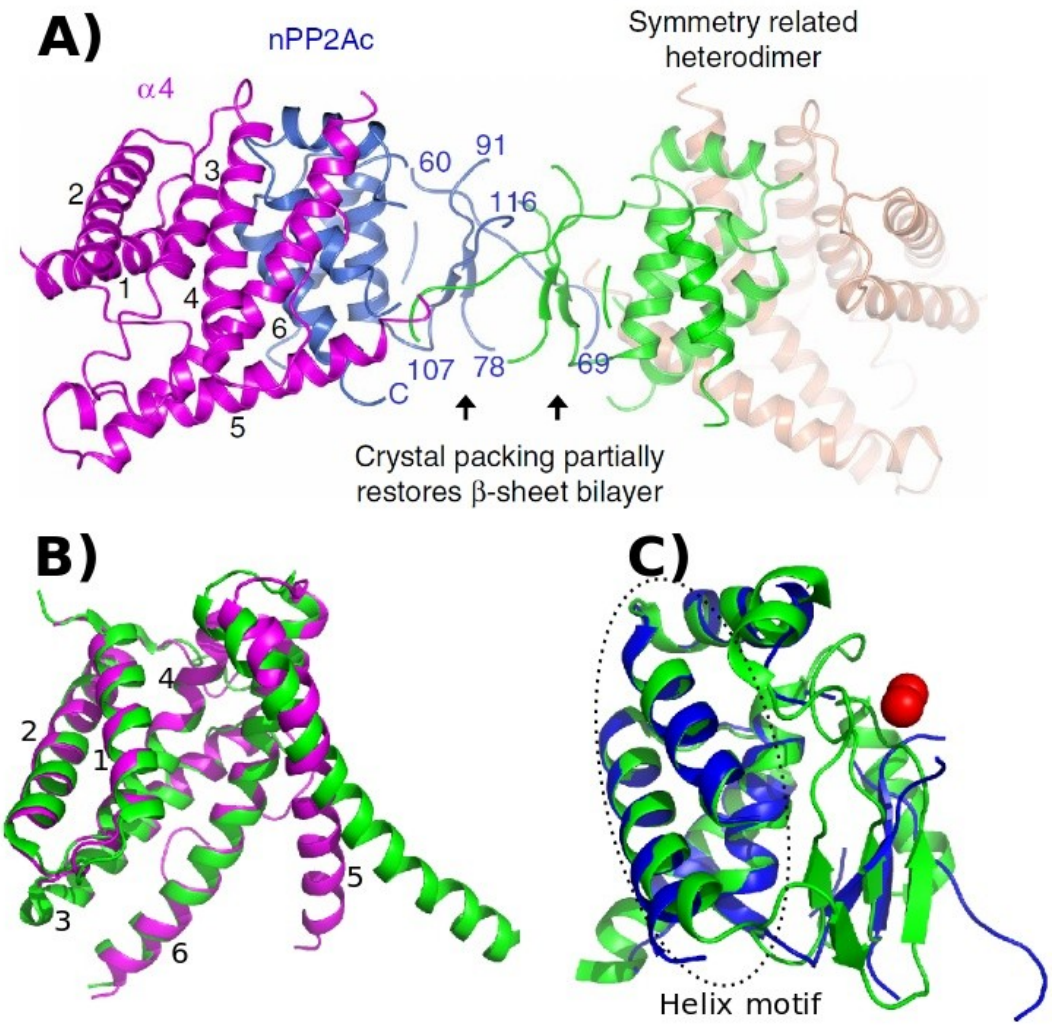

Figure 4.5. Overall structure of α4-nPP2Ac complex. **(A)** Overall structure of the nPP2Ac–α4 complex and the symmetry-related heterodimer in ribbon (PDB ID: 4IYP). nPP2Ac, α4 and their symmetry-related counterparts are colored blue, magenta, green, and orange, respectively. **(B)** Alignment of murine α4 (colored green, PDB ID: 3QC1) and α4 from α4-nPP2Ac complex (colored magenta, PDB ID: 4IYP). Individual helices are labeled 1-6. **(C)** Alignment of PP2Ac residues 1-153, a portion of PP2Ac corresponding nPP2Ac (colored green, PDB ID: 2NPP) and nPP2Ac from α4-nPP2Ac complex (colored blue, PDB ID: 4IYP). Mn^{2+} ions from the structure of active PP2Ac are shown as red spheres.

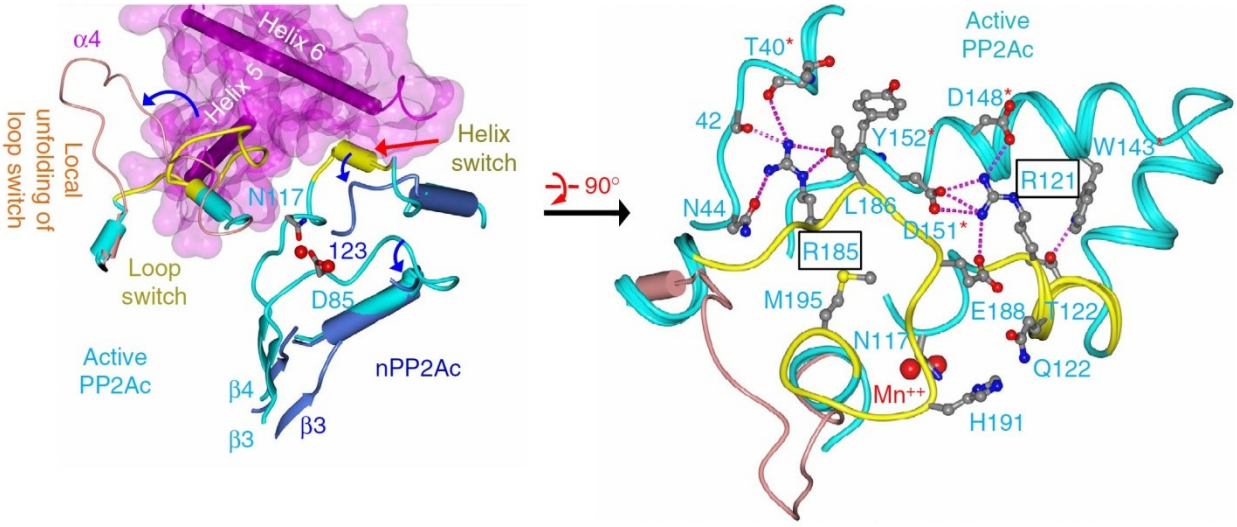

Figure 4.6. Structural changes of PP2Ac associated with α4 binding. **(A)** Illustration of the displacement of the loop switch and helix switch between active PP2Ac and the α4 complex. nPP2Ac and α4 are colored blue and magenta respectively. Active PP2Ac is colored cyan and the helix and loop switches are colored yellow. The loop switch in the partially folded PP2Ac is colored coral. Red spheres represent catalytic metal ions in active PP2Ac. **(B)** A close-up view of PP2A internal packing displaced by α4 binding clustered at two arginine centers. Structure representations and the color scheme are the same as in (A), except that active PP2Ac is shown as ribbon. Residues from active PP2Ac are in ball-and-stick and colored grey.

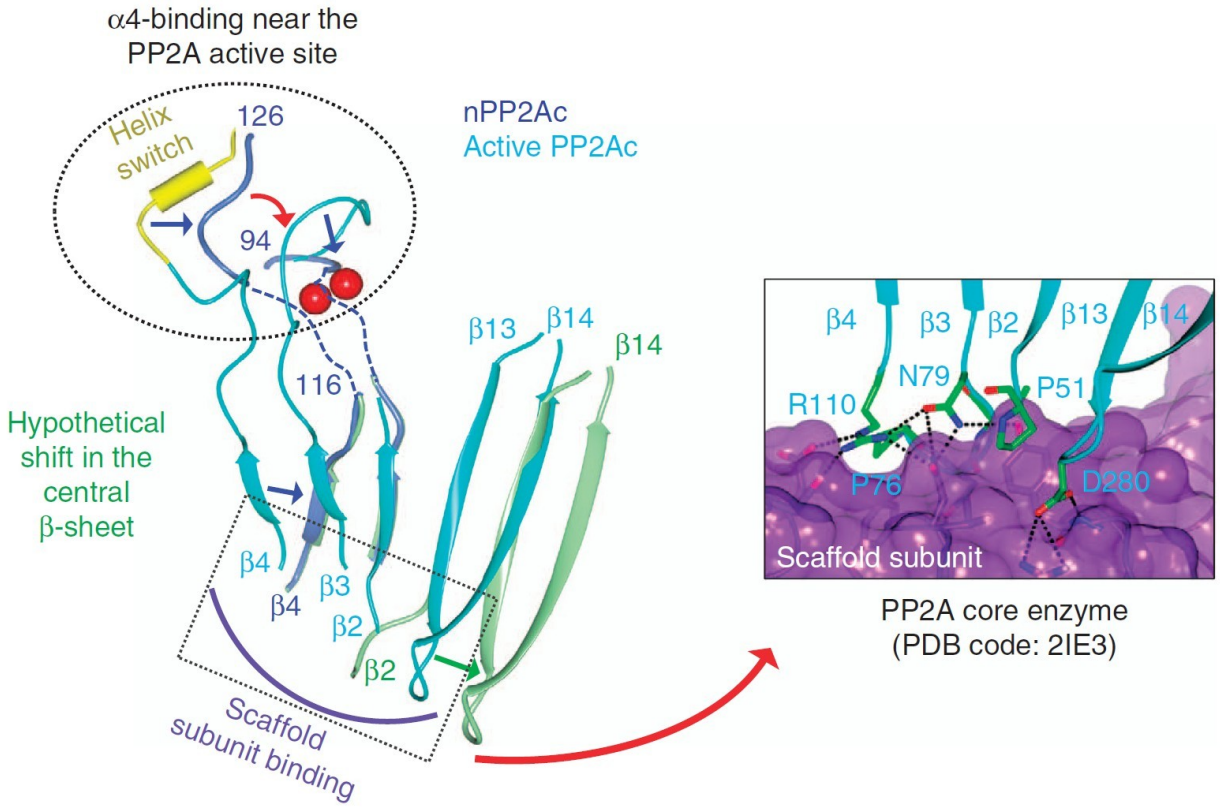

Figure 4.7. Structural basis of mutually exclusive binding of α4 and A-subunit. Illustration of allosteric relay from the α4-binding site, the helix switch, the active site loops and the first central β-sheet, to the scaffold subunit-binding sites at the opposite end of the β-sheet. Hypothetical shift of the central β-sheet is shown in green. A portion of the interface between PP2A scaffold and catalytic subunits is shown (right). Structural presentations and color scheme are similar to Fig. 4.6. The scaffold subunit is shown in surface and colored purple. Residues of the catalytic subunit are in cylinder and colored green.

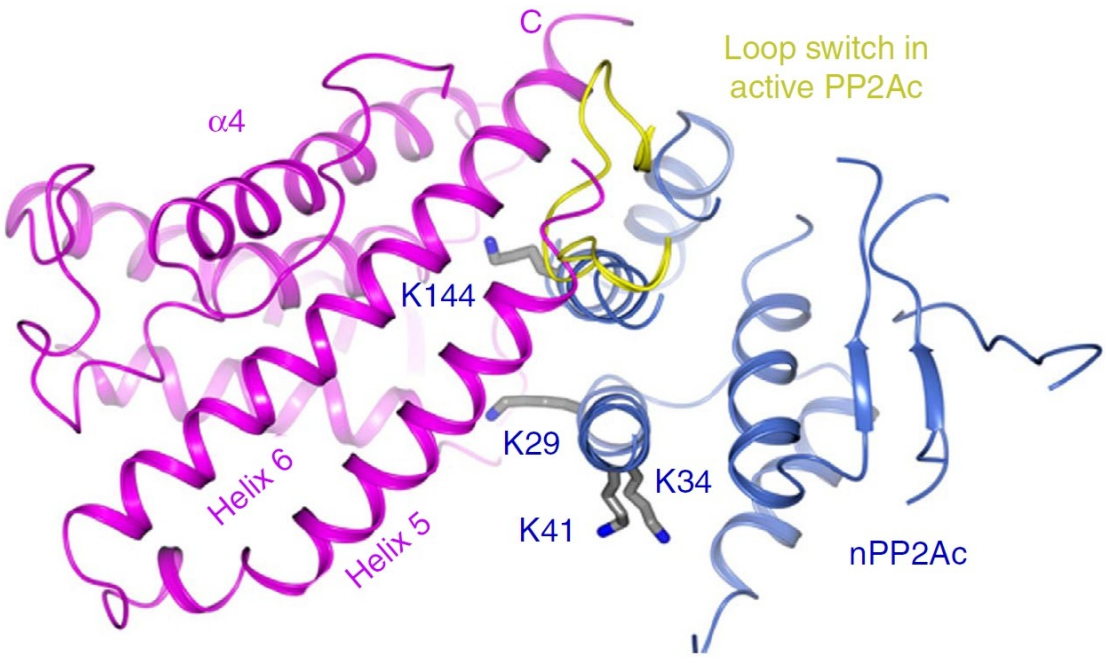

Figure 4.8. Binding of α4 covers several lysine residues on the surface of PP2Ac. Structure of the nPP2Ac– α4 complex highlights PP2A lysine residues (grey) at or near the interface to α4. The loop switch in active PP2Ac is shown (yellow). α4 and nPP2Ac are shown in ribbon and colored magenta and blue, respectively.

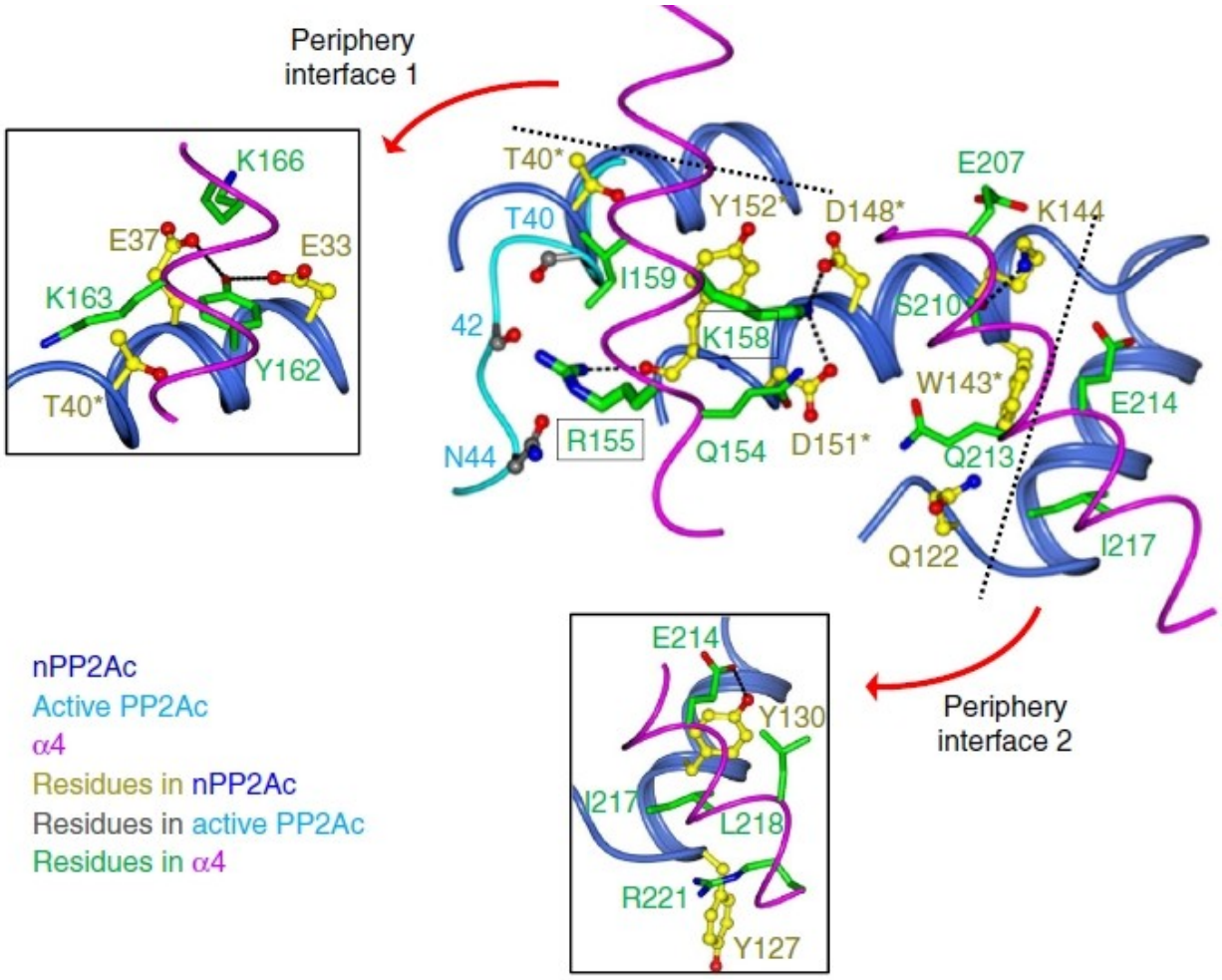

Figure 4.9. Interface of interaction between α4 and PP2Ac. A close-up view of the PP2Ac– α4 interface involving regions of PP2A internal packing and direct contacts with PP2A surface residues at two periphery interfaces (inlets). The nPP2Ac and α4 are in ribbon and worm, respectively. Residues of α4 and nPP2Ac are in ball-and-stick and cylinder and colored green and yellow, respectively.

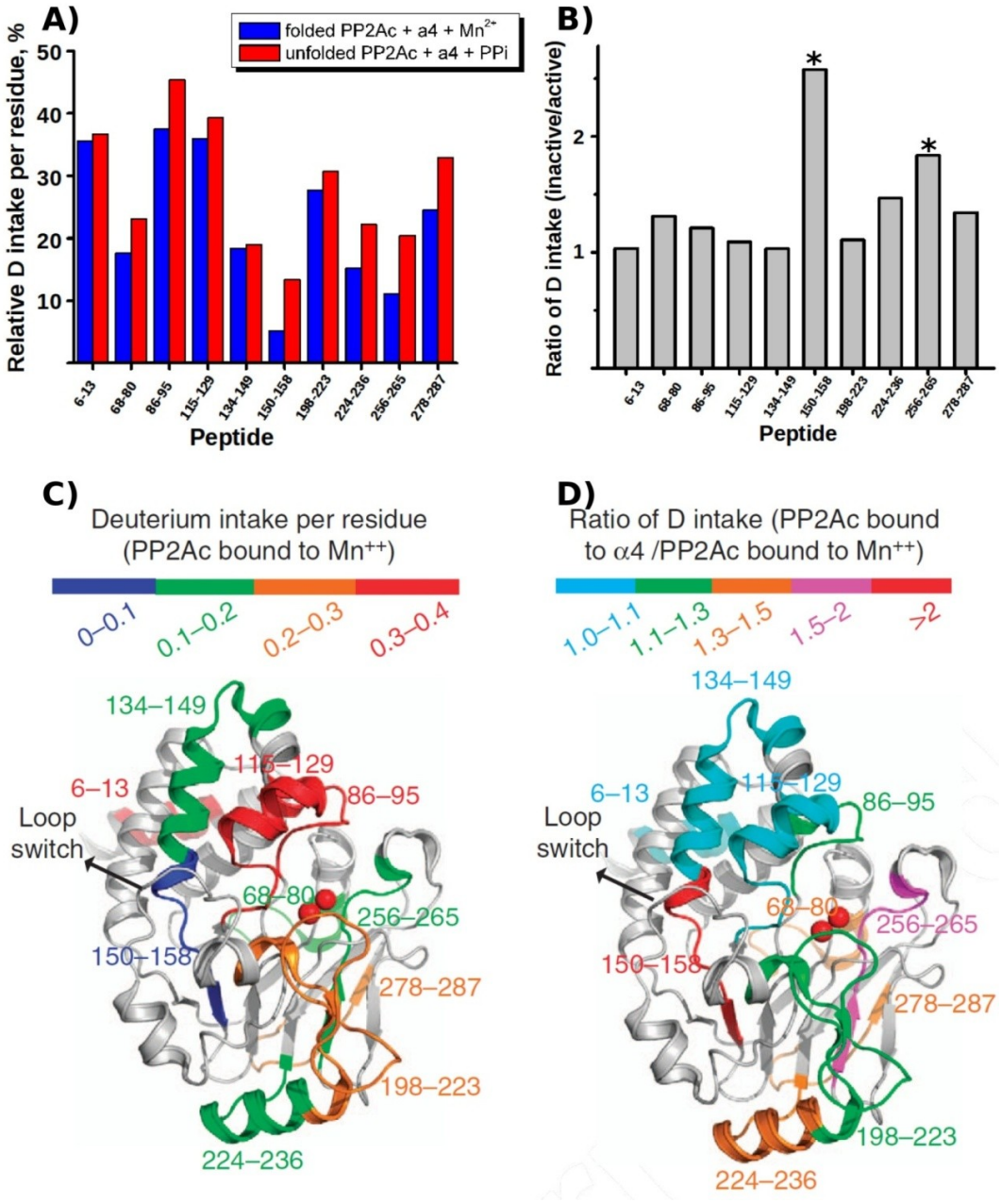

Figure 4.10. HDX-MS of PP2Ac in active and inactive form. **(A)** Absolute deuterium intake into the active PP2Ac (blue) or PP2Ac inactivated by PPi treatment and bound to α4 (red). **(B)** Ratio of deuterium intake of α4-PP2Ac to the active PP2Ac (blue). **(C)** The structure of PP2Ac with color code indicating the level of backbone amide deuterium intake into active PP2Ac peptides. **(D)** Ratio of backbone amide deuterium intake of PP2Ac bound to α4 versus active PP2Ac (bound to Mn^{2+}).

Chapter 5: Literature cited

1. Fischer, E. H., and Krebs, E. G. (1955) Conversion of phosphorylase b to phosphorylase a in muscle extracts. *The Journal of biological chemistry* **216**, 121-132
2. Krebs, E. G., and Fischer, E. H. (1955) Phosphorylase activity of skeletal muscle extracts. *The Journal of biological chemistry* **216**, 113-120
3. Johnson, L. N., and Barford, D. (1993) The effects of phosphorylation on the structure and function of proteins. *Annu Rev Biophys Biomol Struct* **22**, 199-232
4. Johnson, L. N., and O'Reilly, M. (1996) Control by phosphorylation. in *Curr Opin Struct Biol*, England. pp 762-769
5. Barford, D., Das, A. K., and Egloff, M. P. (1998) The structure and mechanism of protein phosphatases: insights into catalysis and regulation. *Annu Rev Biophys Biomol Struct* **27**, 133-164
6. Hunter, T. (1995) Protein kinases and phosphatases: the yin and yang of protein phosphorylation and signaling. in *Cell*, United States. pp 225-236
7. Alonso, A., Sasin, J., Bottini, N., Friedberg, I., Osterman, A., Godzik, A., Hunter, T., Dixon, J., and Mustelin, T. (2004) Protein tyrosine phosphatases in the human genome. *Cell* **117**, 699-711
8. Shi, Y. (2009) Serine/threonine phosphatases: mechanism through structure. *Cell* **139**, 468-484
9. Kamenski, T., Heilmeier, S., Meinhart, A., and Cramer, P. (2004) Structure and mechanism of RNA polymerase II CTD phosphatases. in *Mol Cell*, United States. pp 399-407
10. Ghosh, A., Shuman, S., and Lima, C. D. (2008) The structure of Fcp1, an essential RNA polymerase II CTD phosphatase. in *Mol Cell*, United States. pp 478-490
11. Yeo, M., Lin, P. S., Dahmus, M. E., and Gill, G. N. (2003) A novel RNA polymerase II C-terminal domain phosphatase that preferentially dephosphorylates serine 5. in *J Biol Chem*, United States. pp 26078-26085
12. Yu, X., Chini, C. C., He, M., Mer, G., and Chen, J. (2003) The BRCT domain is a phospho-protein binding domain. in *Science*, United States. pp 639-642
13. Barford, D. (1996) Molecular mechanisms of the protein serine/threonine phosphatases. *Trends in biochemical sciences* **21**, 407-412
14. Zhang, L., Zhang, Z., Long, F., and Lee, E. Y. (1996) Tyrosine-272 is involved in the inhibition of protein phosphatase-1 by multiple toxins. in *Biochemistry*, United States. pp 1606-1611
15. Zhuo, S., Clemens, J. C., Stone, R. L., and Dixon, J. E. (1994) Mutational analysis of a Ser/Thr phosphatase. Identification of residues important in phosphoesterase substrate binding and catalysis. *J Biol Chem* **269**, 26234-26238
16. Eichhorn, P. J., Creyghton, M. P., and Bernards, R. (2009) Protein phosphatase 2A regulatory subunits and cancer. *Biochimica et biophysica acta* **1795**, 1-15
17. Sontag, J. M., Nunbhakdi-Craig, V., Mitterhuber, M., Ogris, E., and Sontag, E. (2010) Regulation of protein phosphatase 2A methylation by LCMT1 and PME-1 plays a critical role in differentiation of neuroblastoma cells. *Journal of neurochemistry* **115**, 1455-1465
18. Kong, M., Fox, C. J., Mu, J., Solt, L., Xu, A., Cinalli, R. M., Birnbaum, M. J., Lindsten, T., and Thompson, C. B. (2004) The PP2A-associated protein alpha4 is an essential inhibitor of apoptosis. *Science (New York, N.Y.)* **306**, 695-698
19. Mochida, S., Maslen, S. L., Skehel, M., and Hunt, T. (2010) Greatwall phosphorylates an inhibitor of protein phosphatase 2A that is essential for mitosis. *Science (New York, N.Y.)* **330**, 1670-1673
20. Gharbi-Ayachi, A., Labbe, J. C., Burgess, A., Vigneron, S., Strub, J. M., Brioudes, E., Van-Dorsselaer, A., Castro, A., and Lorca, T. (2010) The substrate of Greatwall kinase, Arpp19, controls mitosis by inhibiting protein phosphatase 2A. *Science (New York, N.Y.)* **330**, 1673-1677

21. Kong, M., Bui, T. V., Ditsworth, D., Gruber, J. J., Goncharov, D., Krymskaya, V. P., Lindsten, T., and Thompson, C. B. (2007) The PP2A-associated protein alpha4 plays a critical role in the regulation of cell spreading and migration. *The Journal of biological chemistry* **282**, 29712-29720
22. Lee, D. H., Pan, Y., Kanner, S., Sung, P., Borowiec, J. A., and Chowdhury, D. (2010) A PP4 phosphatase complex dephosphorylates RPA2 to facilitate DNA repair via homologous recombination. *Nature structural & molecular biology* **17**, 365-372
23. Nunbhakdi-Craig, V., Schuechner, S., Sontag, J. M., Montgomery, L., Pallas, D. C., Juno, C., Mudrak, I., Ogris, E., and Sontag, E. (2007) Expression of protein phosphatase 2A mutants and silencing of the regulatory B alpha subunit induce a selective loss of acetylated and detyrosinated microtubules. *Journal of neurochemistry* **101**, 959-971
24. Kranias, G., Watt, L. F., Carpenter, H., Holst, J., Ludowyke, R., Strack, S., Sim, A. T., and Verrills, N. M. (2010) Protein phosphatase 2A carboxymethylation and regulatory B subunits differentially regulate mast cell degranulation. *Cellular signalling* **22**, 1882-1890
25. Munz, T., Litterst, C. M., and Pfitzner, E. (2010) Interaction of STAT6 with its co-activator SRC-1/NCoA-1 is regulated by dephosphorylation of the latter via PP2A. *Nucleic acids research*
26. Sablina, A. A., Hector, M., Colpaert, N., and Hahn, W. C. (2010) Identification of PP2A complexes and pathways involved in cell transformation. *Cancer research* **70**, 10474-10484
27. Goudreault, M., D'Ambrosio, L. M., Kean, M. J., Mullin, M. J., Larsen, B. G., Sanchez, A., Chaudhry, S., Chen, G. I., Sicheri, F., Nesvizhskii, A. I., Aebersold, R., Raught, B., and Gingras, A. C. (2009) A PP2A phosphatase high density interaction network identifies a novel striatin-interacting phosphatase and kinase complex linked to the cerebral cavernous malformation 3 (CCM3) protein. *Molecular & cellular proteomics : MCP* **8**, 157-171
28. Westermarck, J., and Hahn, W. C. (2008) Multiple pathways regulated by the tumor suppressor PP2A in transformation. *Trends in molecular medicine* **14**, 152-160
29. Chung, H., Nairn, A. C., Murata, K., and Brautigan, D. L. (1999) Mutation of Tyr307 and Leu309 in the protein phosphatase 2A catalytic subunit favors association with the alpha 4 subunit which promotes dephosphorylation of elongation factor-2. *Biochemistry* **38**, 10371-10376
30. Seshacharyulu, P., Pandey, P., Datta, K., and Batra, S. K. (2013) Phosphatase: PP2A structural importance, regulation and its aberrant expression in cancer. *Cancer Lett*
31. Sablina, A. A., and Hahn, W. C. (2007) The role of PP2A A subunits in tumor suppression. *Cell adhesion & migration* **1**, 140-141
32. Mourtada-Maarabouni, M., and Williams, G. T. (2008) Protein phosphatase 4 regulates apoptosis, proliferation and mutation rate of human cells. *Biochimica et biophysica acta* **1783**, 1490-1502
33. Stefansson, B., and Brautigan, D. L. (2007) Protein phosphatase PP6 N terminal domain restricts G1 to S phase progression in human cancer cells. *Cell cycle (Georgetown, Tex.)* **6**, 1386-1392
34. De Munter, S., Kohn, M., and Bollen, M. (2013) Challenges and opportunities in the development of protein phosphatase-directed therapeutics. *ACS Chem Biol* **8**, 36-45
35. McConnell, J. L., and Wadzinski, B. E. (2009) Targeting protein serine/threonine phosphatases for drug development. *Molecular pharmacology* **75**, 1249-1261
36. Lewy, D. S., Gauss, C. M., Soenen, D. R., and Boger, D. L. (2002) Fostriecin: chemistry and biology. *Curr Med Chem* **9**, 2005-2032
37. Roberge, M., Tudan, C., Hung, S. M., Harder, K. W., Jirik, F. R., and Anderson, H. (1994) Antitumor drug fostriecin inhibits the mitotic entry checkpoint and protein phosphatases 1 and 2A. *Cancer Res* **54**, 6115-6121
38. Wang, G. S. (1989) Medical uses of mylabris in ancient China and recent studies. in *J Ethnopharmacol*, Switzerland. pp 147-162
39. Swingle, M., Ni, L., and Honkanen, R. E. (2007) Small-molecule inhibitors of ser/thr protein phosphatases: specificity, use and common forms of abuse. in *Methods Mol Biol*, United States. pp 23-38

40. Matsuoka, Y., Nagahara, Y., Ikekita, M., and Shinomiya, T. (2003) A novel immunosuppressive agent FTY720 induced Akt dephosphorylation in leukemia cells. *Br J Pharmacol* **138**, 1303-1312
41. Dobrowsky, R. T., Kamibayashi, C., Mumby, M. C., and Hannun, Y. A. (1993) Ceramide activates heterotrimeric protein phosphatase 2A. *J Biol Chem* **268**, 15523-15530
42. Chalfant, C. E., Szulc, Z., Roddy, P., Bielawska, A., and Hannun, Y. A. (2004) The structural requirements for ceramide activation of serine-threonine protein phosphatases. in *J Lipid Res*, United States. pp 496-506
43. Hombauer, H., Weismann, D., Mudrak, I., Stanzel, C., Fellner, T., Lackner, D. H., and Ogris, E. (2007) Generation of active protein phosphatase 2A is coupled to holoenzyme assembly. *PLoS biology* **5**, e155
44. Shi, Y. (2009) Assembly and structure of protein phosphatase 2A. *Science in China.Series C, Life sciences / Chinese Academy of Sciences* **52**, 135-146
45. Xu, Y., Xing, Y., Chen, Y., Chao, Y., Lin, Z., Fan, E., Yu, J. W., Strack, S., Jeffrey, P. D., and Shi, Y. (2006) Structure of the protein phosphatase 2A holoenzyme. *Cell* **127**, 1239-1251
46. Cho, U. S., and Xu, W. (2007) Crystal structure of a protein phosphatase 2A heterotrimeric holoenzyme. *Nature* **445**, 53-57
47. Grinthal, A., Adamovic, I., Weiner, B., Karplus, M., and Kleckner, N. (2010) PR65, the HEAT-repeat scaffold of phosphatase PP2A, is an elastic connector that links force and catalysis. *Proceedings of the National Academy of Sciences of the United States of America* **107**, 2467-2472
48. Xu, Y., Chen, Y., Zhang, P., Jeffrey, P. D., and Shi, Y. (2008) Structure of a protein phosphatase 2A holoenzyme: insights into B55-mediated Tau dephosphorylation. in *Mol Cell*, United States. pp 873-885
49. Wlodarchak NJ, G. F., Satyshur KA, Jiang L, Jeffrey PD, Sun T, Stanevich V, Mumby MC, Xing Y. (2013) Structural mechanism of trimeric PR70 PP2A holoenzyme: insights into Cdc6 dephosphorylation. in *ASBMB Annual Meeting*, Boston
50. Janssens, V., Longin, S., and Goris, J. (2008) PP2A holoenzyme assembly: in cauda venenum (the sting is in the tail). *Trends in biochemical sciences* **33**, 113-121
51. Longin, S., Zwaenepoel, K., Louis, J. V., Dilworth, S., Goris, J., and Janssens, V. (2007) Selection of protein phosphatase 2A regulatory subunits is mediated by the C terminus of the catalytic Subunit. *The Journal of biological chemistry* **282**, 26971-26980
52. Guo, H., and Damuni, Z. (1993) Autophosphorylation-activated protein kinase phosphorylates and inactivates protein phosphatase 2A. *Proc Natl Acad Sci U S A* **90**, 2500-2504
53. Xiong, Y., Jing, X. P., Zhou, X. W., Wang, X. L., Yang, Y., Sun, X. Y., Qiu, M., Cao, F. Y., Lu, Y. M., Liu, R., and Wang, J. Z. (2013) Zinc induces protein phosphatase 2A inactivation and tau hyperphosphorylation through Src dependent PP2A (tyrosine 307) phosphorylation. *Neurobiol Aging* **34**, 745-756
54. Chen, J., Martin, B. L., and Brautigan, D. L. (1992) Regulation of protein serine-threonine phosphatase type-2A by tyrosine phosphorylation. *Science (New York, N.Y.)* **257**, 1261-1264
55. Lee, J., Chen, Y., Tolstykh, T., and Stock, J. (1996) A specific protein carboxyl methylesterase that demethylates phosphoprotein phosphatase 2A in bovine brain. *Proceedings of the National Academy of Sciences of the United States of America* **93**, 6043-6047
56. Lee, J., and Stock, J. (1993) Protein phosphatase 2A catalytic subunit is methyl-esterified at its carboxyl terminus by a novel methyltransferase. *The Journal of biological chemistry* **268**, 19192-19195
57. Wu, J., Tolstykh, T., Lee, J., Boyd, K., Stock, J. B., and Broach, J. R. (2000) Carboxyl methylation of the phosphoprotein phosphatase 2A catalytic subunit promotes its functional association with regulatory subunits in vivo. *The EMBO journal* **19**, 5672-5681

58. Tolstykh, T., Lee, J., Vafai, S., and Stock, J. B. (2000) Carboxyl methylation regulates phosphoprotein phosphatase 2A by controlling the association of regulatory B subunits. *The EMBO journal* **19**, 5682-5691
59. Yu, X. X., Du, X., Moreno, C. S., Green, R. E., Ogris, E., Feng, Q., Chou, L., McQuoid, M. J., and Pallas, D. C. (2001) Methylation of the protein phosphatase 2A catalytic subunit is essential for association of Balpha regulatory subunit but not SG2NA, striatin, or polyomavirus middle tumor antigen. *Molecular biology of the cell* **12**, 185-199
60. Lee, J. A., and Pallas, D. C. (2007) Leucine carboxyl methyltransferase-1 is necessary for normal progression through mitosis in mammalian cells. *The Journal of biological chemistry* **282**, 30974-30984
61. Nien, W. L., Dauphinee, S. M., Moffat, L. D., and Too, C. K. (2007) Overexpression of the mTOR alpha4 phosphoprotein activates protein phosphatase 2A and increases Stat1alpha binding to PIAS1. *Molecular and cellular endocrinology* **263**, 10-17
62. Ortega-Gutierrez, S., Leung, D., Ficarro, S., Peters, E. C., and Cravatt, B. F. (2008) Targeted disruption of the PME-1 gene causes loss of demethylated PP2A and perinatal lethality in mice. *PLoS One* **3**, e2486
63. Vafai, S. B., and Stock, J. B. (2002) Protein phosphatase 2A methylation: a link between elevated plasma homocysteine and Alzheimer's Disease. *FEBS letters* **518**, 1-4
64. Sontag, E., Nunbhakdi-Craig, V., Sontag, J. M., Diaz-Arrastia, R., Ogris, E., Dayal, S., Lentz, S. R., Arning, E., and Bottiglieri, T. (2007) Protein phosphatase 2A methyltransferase links homocysteine metabolism with tau and amyloid precursor protein regulation. *The Journal of neuroscience : the official journal of the Society for Neuroscience* **27**, 2751-2759
65. Sontag, J. M., Nunbhakdi-Craig, V., Montgomery, L., Arning, E., Bottiglieri, T., and Sontag, E. (2008) Folate deficiency induces in vitro and mouse brain region-specific downregulation of leucine carboxyl methyltransferase-1 and protein phosphatase 2A B(alpha) subunit expression that correlate with enhanced tau phosphorylation. in *J Neurosci*, United States. pp 11477-11487
66. Israel, M., and Schwartz, L. (2011) The metabolic advantage of tumor cells. in *Mol Cancer*, England. pp 70
67. Van Hoof, C., Janssens, V., De Baere, I., de Winde, J. H., Winderickx, J., Dumortier, F., Thevelein, J. M., Merlevede, W., and Goris, J. (2000) The Saccharomyces cerevisiae homologue YPA1 of the mammalian phosphotyrosyl phosphatase activator of protein phosphatase 2A controls progression through the G1 phase of the yeast cell cycle. in *J Mol Biol*, 2000 Academic Press., England. pp 103-120
68. Mitchell, D. A., and Sprague, G. F., Jr. (2001) The phosphotyrosyl phosphatase activator, Ncs1p (Rrd1p), functions with Cla4p to regulate the G(2)/M transition in Saccharomyces cerevisiae. *Mol Cell Biol* **21**, 488-500
69. Ramotar, D., Belanger, E., Brodeur, I., Masson, J. Y., and Drobetsky, E. A. (1998) A yeast homologue of the human phosphotyrosyl phosphatase activator PTPA is implicated in protection against oxidative DNA damage induced by the model carcinogen 4-nitroquinoline 1-oxide. *J Biol Chem* **273**, 21489-21496
70. Zhang, W., and Durocher, D. (2010) De novo telomere formation is suppressed by the Mec1-dependent inhibition of Cdc13 accumulation at DNA breaks. in *Genes Dev*, United States. pp 502-515
71. Van Hoof, C., Janssens, V., De Baere, I., Stark, M. J., de Winde, J. H., Winderickx, J., Thevelein, J. M., Merlevede, W., and Goris, J. (2001) The Saccharomyces cerevisiae phosphotyrosyl phosphatase activator proteins are required for a subset of the functions disrupted by protein phosphatase 2A mutations. in *Exp Cell Res*, 2001 Academic Press., United States. pp 372-387

72. Douville, J., David, J., Lemieux, K. M., Gaudreau, L., and Ramotar, D. (2006) The Saccharomyces cerevisiae phosphatase activator RRD1 is required to modulate gene expression in response to rapamycin exposure. in *Genetics*, United States. pp 1369-1372
73. Jouvet, N., Poschmann, J., Douville, J., Bulet, L., and Ramotar, D. (2010) Rrd1 isomerizes RNA polymerase II in response to rapamycin. in *BMC Mol Biol*, England. pp 92
74. Poschmann, J., Drouin, S., Jacques, P. E., El Fadili, K., Newmarch, M., Robert, F., and Ramotar, D. (2011) The peptidyl prolyl isomerase Rrd1 regulates the elongation of RNA polymerase II during transcriptional stresses. in *PLoS One*, United States. pp e23159
75. Douville, J., David, J., Fortier, P. K., and Ramotar, D. (2004) The yeast phosphotyrosyl phosphatase activator protein, yPtpa1/Rrd1, interacts with Sit4 phosphatase to mediate resistance to 4-nitroquinoline-1-oxide and UVA. *Curr Genet* **46**, 72-81
76. Van Hoof, C., Martens, E., Longin, S., Jordens, J., Stevens, I., Janssens, V., and Goris, J. (2005) Specific interactions of PP2A and PP2A-like phosphatases with the yeast PTPA homologues, Ypa1 and Ypa2. in *Biochem J*, England. pp 93-102
77. Fellner, T., Lackner, D. H., Hombauer, H., Piribauer, P., Mudrak, I., Zaragoza, K., Juno, C., and Ogris, E. (2003) A novel and essential mechanism determining specificity and activity of protein phosphatase 2A (PP2A) in vivo. in *Genes Dev*, United States. pp 2138-2150
78. Leulliot, N., Vicentini, G., Jordens, J., Quevillon-Cheruel, S., Schiltz, M., Barford, D., van Tilbeurgh, H., and Goris, J. (2006) Crystal structure of the PP2A phosphatase activator: implications for its PP2A-specific PPIase activity. *Molecular cell* **23**, 413-424
79. Chao, Y., Xing, Y., Chen, Y., Xu, Y., Lin, Z., Li, Z., Jeffrey, P. D., Stock, J. B., and Shi, Y. (2006) Structure and mechanism of the phosphotyrosyl phosphatase activator. *Molecular cell* **23**, 535-546
80. Cayla, X., Goris, J., Hermann, J., Jessus, C., Hendrix, P., and Merlevede, W. (1990) Phosphotyrosyl phosphatase activity of the polycation-stimulated protein. *Adv Enzyme Regul* **30**, 265-285
81. Guo F, S. V., Wlodarchak N, Li Y, Pallas DC, Sengupta R, Jiang L, Satyshur KA, Xing Y. (2013) Structural basis of PP2A phosphatase activator reveals a unique chaperone function in PP2A activation. in *ASBMB Annual Meeting*, Boston
82. Di Como, C. J., and Arndt, K. T. (1996) Nutrients, via the Tor proteins, stimulate the association of Tap42 with type 2A phosphatases. *Genes & development* **10**, 1904-1916
83. Gingras, A. C., Caballero, M., Zarske, M., Sanchez, A., Hazbun, T. R., Fields, S., Sonenberg, N., Hafen, E., Raught, B., and Aebersold, R. (2005) A novel, evolutionarily conserved protein phosphatase complex involved in cisplatin sensitivity. in *Mol Cell Proteomics*, United States. pp 1725-1740
84. Inui, S., Sanjo, H., Maeda, K., Yamamoto, H., Miyamoto, E., and Sakaguchi, N. (1998) Ig receptor binding protein 1 (alpha4) is associated with a rapamycin-sensitive signal transduction in lymphocytes through direct binding to the catalytic subunit of protein phosphatase 2A. *Blood* **92**, 539-546
85. Smetana, J. H., and Zanchin, N. I. (2007) Interaction analysis of the heterotrimer formed by the phosphatase 2A catalytic subunit, alpha4 and the mammalian ortholog of yeast Tip41 (TIPRL). *The FEBS journal* **274**, 5891-5904
86. Murata, K., Wu, J., and Brautigan, D. L. (1997) B cell receptor-associated protein alpha4 displays rapamycin-sensitive binding directly to the catalytic subunit of protein phosphatase 2A. *Proceedings of the National Academy of Sciences of the United States of America* **94**, 10624-10629
87. Kong, M., Ditsworth, D., Lindsten, T., and Thompson, C. B. (2009) Alpha4 is an essential regulator of PP2A phosphatase activity. *Molecular cell* **36**, 51-60

88. Jiang, Y., and Broach, J. R. (1999) Tor proteins and protein phosphatase 2A reciprocally regulate Tap42 in controlling cell growth in yeast. *The EMBO journal* **18**, 2782-2792
89. Yan, G., Shen, X., and Jiang, Y. (2006) Rapamycin activates Tap42-associated phosphatases by abrogating their association with Tor complex 1. in *EMBO J*, England. pp 3546-3555
90. Yamashita, T., Inui, S., Maeda, K., Hua, D. R., Takagi, K., Fukunaga, K., and Sakaguchi, N. (2006) Regulation of CaMKII by alpha4/PP2Ac contributes to learning and memory. *Brain research* **1082**, 1-10
91. Yoo, S. J., Jimenez, R. H., Sanders, J. A., Boylan, J. M., Brautigan, D. L., and Gruppuso, P. A. (2008) The alpha4-containing form of protein phosphatase 2A in liver and hepatic cells. *Journal of cellular biochemistry* **105**, 290-300
92. Nanahoshi, M., Nishiuma, T., Tsujishita, Y., Hara, K., Inui, S., Sakaguchi, N., and Yonezawa, K. (1998) Regulation of protein phosphatase 2A catalytic activity by alpha4 protein and its yeast homolog Tap42. *Biochemical and biophysical research communications* **251**, 520-526
93. Kloeker, S., Reed, R., McConnell, J. L., Chang, D., Tran, K., Westphal, R. S., Law, B. K., Colbran, R. J., Kamoun, M., Campbell, K. S., and Wadzinski, B. E. (2003) Parallel purification of three catalytic subunits of the protein serine/threonine phosphatase 2A family (PP2A(C), PP4(C), and PP6(C)) and analysis of the interaction of PP2A(C) with alpha4 protein. *Protein expression and purification* **31**, 19-33
94. Chen, J., Peterson, R. T., and Schreiber, S. L. (1998) Alpha 4 associates with protein phosphatases 2A, 4, and 6. *Biochemical and biophysical research communications* **247**, 827-832
95. Liu, J., Prickett, T. D., Elliott, E., Meroni, G., and Brautigan, D. L. (2001) Phosphorylation and microtubule association of the Opitz syndrome protein mid-1 is regulated by protein phosphatase 2A via binding to the regulatory subunit alpha 4. *Proceedings of the National Academy of Sciences of the United States of America* **98**, 6650-6655
96. Short, K. M., Hopwood, B., Yi, Z., and Cox, T. C. (2002) MID1 and MID2 homo- and heterodimerise to tether the rapamycin-sensitive PP2A regulatory subunit, alpha 4, to microtubules: implications for the clinical variability of X-linked Opitz GBBB syndrome and other developmental disorders. *BMC cell biology* **3**, 1
97. Prickett, T. D., and Brautigan, D. L. (2006) The alpha4 regulatory subunit exerts opposing allosteric effects on protein phosphatases PP6 and PP2A. *The Journal of biological chemistry* **281**, 30503-30511
98. Lizotte, D. L., Blakeslee, J. J., Siryaporn, A., Heath, J. T., and DeLong, A. (2008) A PP2A active site mutant impedes growth and causes misregulation of native catalytic subunit expression. *Journal of cellular biochemistry* **103**, 1309-1325
99. Trockenbacher, A., Suckow, V., Foerster, J., Winter, J., Krauss, S., Ropers, H. H., Schneider, R., and Schweiger, S. (2001) MID1, mutated in Opitz syndrome, encodes an ubiquitin ligase that targets phosphatase 2A for degradation. *Nature genetics* **29**, 287-294
100. McConnell, J. L., Watkins, G. R., Soss, S. E., Franz, H. S., McCorvey, L. R., Spiller, B. W., Chazin, W. J., and Wadzinski, B. E. (2010) Alpha4 is a ubiquitin-binding protein that regulates protein serine/threonine phosphatase 2A ubiquitination. *Biochemistry* **49**, 1713-1718
101. Xu, G., Paige, J. S., and Jaffrey, S. R. (2010) Global analysis of lysine ubiquitination by ubiquitin remnant immunoaffinity profiling. *Nature biotechnology* **28**, 868-873
102. De Baere, I., Derua, R., Janssens, V., Van Hoof, C., Waelkens, E., Merlevede, W., and Goris, J. (1999) Purification of porcine brain protein phosphatase 2A leucine carboxyl methyltransferase and cloning of the human homologue. *Biochemistry* **38**, 16539-16547
103. Xing, Y., Li, Z., Chen, Y., Stock, J. B., Jeffrey, P. D., and Shi, Y. (2008) Structural mechanism of demethylation and inactivation of protein phosphatase 2A. *Cell* **133**, 154-163
104. Leulliot, N., Quevillon-Cheruel, S., Sorel, I., de La Sierra-Gallay, I. L., Collinet, B., Graille, M., Blondeau, K., Bettache, N., Poupon, A., Janin, J., and van Tilbeurgh, H. (2004) Structure of

protein phosphatase methyltransferase 1 (PPM1), a leucine carboxyl methyltransferase involved in the regulation of protein phosphatase 2A activity. *The Journal of biological chemistry* **279**, 8351-8358

105. Bedford, M. T., and Clarke, S. G. (2009) Protein arginine methylation in mammals: who, what, and why. *Molecular cell* **33**, 1-13
106. Stanevich, V., Jiang, L., Satyshur, K. A., Li, Y., Jeffrey, P. D., Li, Z., Menden, P., Semmelhack, M. F., and Xing, Y. (2011) The Structural Basis for Tight Control of PP2A Methylation and Function by LCMT-1. *Molecular cell* **41**, 331-342
107. Otwinowski Z, M. W. (1997) Processing of X-ray Diffraction Data Collected in Oscillation Mode. *Methods in Enzymology* **276**, 307-326
108. Emsley, P., Lohkamp, B., Scott, W. G., and Cowtan, K. (2010) Features and development of Coot. *Acta crystallographica.Section D, Biological crystallography* **66**, 486-501
109. Winn, M. D. (2003) An overview of the CCP4 project in protein crystallography: an example of a collaborative project. in *J Synchrotron Radiat*, Denmark. pp 23-25
110. Schuttelkopf, A. W., and van Aalten, D. M. (2004) PRODRG: a tool for high-throughput crystallography of protein-ligand complexes. in *Acta Crystallogr D Biol Crystallogr*, Denmark. pp 1355-1363
111. Weller, R. L., and Rajski, S. R. (2006) Design, synthesis, and preliminary biological evaluation of a DNA methyltransferase-directed alkylating agent. *Chembiochem : a European journal of chemical biology* **7**, 243-245
112. Rao, R. K., and Clayton, L. W. (2002) Regulation of protein phosphatase 2A by hydrogen peroxide and glutathionylation. in *Biochem Biophys Res Commun*, United States. pp 610-616
113. Sommer, D., Coleman, S., Swanson, S. A., and Stemmer, P. M. (2002) Differential susceptibilities of serine/threonine phosphatases to oxidative and nitrosative stress. in *Arch Biochem Biophys*, 2002 Elsevier Science (USA). United States. pp 271-278
114. Foley, T. D., Petro, L. A., Stredny, C. M., and Coppa, T. M. (2007) Oxidative inhibition of protein phosphatase 2A activity: role of catalytic subunit disulfides. *Neurochem Res* **32**, 1957-1964
115. Foley, T. D., Melideo, S. L., Healey, A. E., Lucas, E. J., and Koval, J. A. (2011) Phenylarsine oxide binding reveals redox-active and potential regulatory vicinal thiols on the catalytic subunit of protein phosphatase 2A. *Neurochem Res* **36**, 232-240
116. Hermann, J., Cayla, X., Dumortier, K., Goris, J., Ozon, R., and Merlevede, W. (1988) Modulation of the substrate specificity of the polycation-stimulated protein phosphatase from Xenopus laevis oocytes. *Eur J Biochem* **173**, 17-25
117. Galadari, S., Kishikawa, K., Kamibayashi, C., Mumby, M. C., and Hannun, Y. A. (1998) Purification and characterization of ceramide-activated protein phosphatases. in *Biochemistry*, United States. pp 11232-11238
118. Xing, Y., Xu, Y., Chen, Y., Jeffrey, P. D., Chao, Y., Lin, Z., Li, Z., Strack, S., Stock, J. B., and Shi, Y. (2006) Structure of protein phosphatase 2A core enzyme bound to tumor-inducing toxins. *Cell* **127**, 341-353
119. Turowski, P., Fernandez, A., Favre, B., Lamb, N. J., and Hemmings, B. A. (1995) Differential methylation and altered conformation of cytoplasmic and nuclear forms of protein phosphatase 2A during cell cycle progression. *J Cell Biol* **129**, 397-410
120. Xing, Y., Xu, Y., Chen, Y., Jeffrey, P. D., Chao, Y., Lin, Z., Li, Z., Strack, S., Stock, J. B., and Shi, Y. (2006) Structure of protein phosphatase 2A core enzyme bound to tumor-inducing toxins. *Cell* **127**, 341-353
121. Ogris, E., Gibson, D. M., and Pallas, D. C. (1997) Protein phosphatase 2A subunit assembly: the catalytic subunit carboxy terminus is important for binding cellular B subunit but not polyomavirus middle tumor antigen. *Oncogene* **15**, 911-917

122. Bryant, J. C., Westphal, R. S., and Wadzinski, B. E. (1999) Methylated C-terminal leucine residue of PP2A catalytic subunit is important for binding of regulatory Balpha subunit. *The Biochemical journal* **339 (Pt 2)**, 241-246
123. Wei, H., Ashby, D. G., Moreno, C. S., Ogris, E., Yeong, F. M., Corbett, A. H., and Pallas, D. C. (2001) Carboxymethylation of the PP2A catalytic subunit in Saccharomyces cerevisiae is required for efficient interaction with the B-type subunits Cdc55p and Rts1p. *The Journal of biological chemistry* **276**, 1570-1577
124. Favre, B., Zolnierowicz, S., Turowski, P., and Hemmings, B. A. (1994) The catalytic subunit of protein phosphatase 2A is carboxyl-methylated in vivo. *The Journal of biological chemistry* **269**, 16311-16317
125. Jiang, L., Stanevich, V., Satyshur, K. A., Kong, M., Watkins, G. R., Wadzinski, B. E., Sengupta, R., and Xing, Y. (2013) Structural basis of protein phosphatase 2A stable latency. in *Nat Commun*, England. pp 1699
126. Colella, S., Ohgaki, H., Ruediger, R., Yang, F., Nakamura, M., Fujisawa, H., Kleihues, P., and Walter, G. (2001) Reduced expression of the Aalpha subunit of protein phosphatase 2A in human gliomas in the absence of mutations in the Aalpha and Abeta subunit genes. *International journal of cancer.Journal international du cancer* **93**, 798-804
127. Ruediger, R., Pham, H. T., and Walter, G. (2001) Disruption of protein phosphatase 2A subunit interaction in human cancers with mutations in the A alpha subunit gene. *Oncogene* **20**, 10-15
128. Pettersen, E. F., Goddard, T. D., Huang, C. C., Couch, G. S., Greenblatt, D. M., Meng, E. C., and Ferrin, T. E. (2004) UCSF Chimera--a visualization system for exploratory research and analysis. *J Comput Chem* **25**, 1605-1612
129. Schneider, C. A., Rasband, W. S., and Eliceiri, K. W. (2012) NIH Image to ImageJ: 25 years of image analysis. *Nat Methods* **9**, 671-675
130. Wang, H., Wang, X., and Jiang, Y. (2003) Interaction with Tap42 is required for the essential function of Sit4 and type 2A phosphatases. *Molecular biology of the cell* **14**, 4342-4351
131. Duvel, K., Santhanam, A., Garrett, S., Schneper, L., and Broach, J. R. (2003) Multiple roles of Tap42 in mediating rapamycin-induced transcriptional changes in yeast. *Molecular cell* **11**, 1467-1478
132. Smetana, J. H., Oliveira, C. L., Jablonka, W., Aguiar Pertinhez, T., Carneiro, F. R., Montero-Lomeli, M., Torriani, I., and Zanchin, N. I. (2006) Low resolution structure of the human alpha4 protein (IgBP1) and studies on the stability of alpha4 and of its yeast ortholog Tap42. *Biochimica et biophysica acta* **1764**, 724-734
133. Yang, J., Roe, S. M., Prickett, T. D., Brautigan, D. L., and Barford, D. (2007) The structure of Tap42/alpha4 reveals a tetratricopeptide repeat-like fold and provides insights into PP2A regulation. *Biochemistry* **46**, 8807-8815
134. Morrison, D. K. (2009) The 14-3-3 proteins: integrators of diverse signaling cues that impact cell fate and cancer development. *Trends in cell biology* **19**, 16-23
135. Allan, R. K., and Ratajczak, T. (2010) Versatile TPR domains accommodate different modes of target protein recognition and function. *Cell stress & chaperones*
136. Inui, S., Kuwahara, K., Mizutani, J., Maeda, K., Kawai, T., Nakayasu, H., and Sakaguchi, N. (1995) Molecular cloning of a cDNA clone encoding a phosphoprotein component related to the Ig receptor-mediated signal transduction. *J Immunol* **154**, 2714-2723
137. Ness, S. R., de Graaff, R. A., Abrahams, J. P., and Pannu, N. S. (2004) CRANK: new methods for automated macromolecular crystal structure solution. in *Structure*, 2004 Elsevier Ltd., United States. pp 1753-1761
138. Winn, M. D., Ballard, C. C., Cowtan, K. D., Dodson, E. J., Emsley, P., Evans, P. R., Keegan, R. M., Krissinel, E. B., Leslie, A. G., McCoy, A., McNicholas, S. J., Murshudov, G. N., Pannu, N. S., Potterton, E. A., Powell, H. R., Read, R. J., Vagin, A., and Wilson, K. S. (2011) Overview of

the CCP4 suite and current developments. in *Acta Crystallogr D Biol Crystallogr*, England. pp 235-242
139. Pannu, N. S., and Read, R. J. (2004) The application of multivariate statistical techniques improves single-wavelength anomalous diffraction phasing. in *Acta Crystallogr D Biol Crystallogr*, Denmark. pp 22-27
140. Cowtan, K. (2006) The Buccaneer software for automated model building. 1. Tracing protein chains. in *Acta Crystallogr D Biol Crystallogr*, Denmark. pp 1002-1011
141. Li, J., Dangott, L. J., and Fitzpatrick, P. F. (2010) Regulation of phenylalanine hydroxylase: conformational changes upon phenylalanine binding detected by hydrogen/deuterium exchange and mass spectrometry. *Biochemistry* **49**, 3327-3335
142. Weis, D. D., Engen, J. R., and Kass, I. J. (2006) Semi-automated data processing of hydrogen exchange mass spectra using HX-Express. in *J Am Soc Mass Spectrom*, United States. pp 1700-1703
143. Tao, H., Simmons, B. N., Singireddy, S., Jakkidi, M., Short, K. M., Cox, T. C., and Massiah, M. A. (2008) Structure of the MID1 tandem B-boxes reveals an interaction reminiscent of intermolecular ring heterodimers. *Biochemistry* **47**, 2450-2457
144. Massiah, M. A., Simmons, B. N., Short, K. M., and Cox, T. C. (2006) Solution structure of the RBCC/TRIM B-box1 domain of human MID1: B-box with a RING. in *J Mol Biol*, England. pp 532-545
145. Lenoue-Newton, M., Watkins, G. R., Zhou, P., Germane, K. L., McCorvey, L. R., Wadzinski, B. E., and Spiller, B. W. (2011) The E3 ubiquitin ligase and protein phosphatase 2A (PP2A) binding domains of Alpha4 are both required for Alpha4 to inhibit PP2A degradation. *The Journal of biological chemistry*
146. Prickett, T. D., and Brautigan, D. L. (2004) Overlapping binding sites in protein phosphatase 2A for association with regulatory A and alpha-4 (mTap42) subunits. *The Journal of biological chemistry* **279**, 38912-38920
147. Nanahoshi, M., Tsujishita, Y., Tokunaga, C., Inui, S., Sakaguchi, N., Hara, K., and Yonezawa, K. (1999) Alpha4 protein as a common regulator of type 2A-related serine/threonine protein phosphatases. *FEBS letters* **446**, 108-112
148. Herzog, F., Kahraman, A., Boehringer, D., Mak, R., Bracher, A., Walzthoeni, T., Leitner, A., Beck, M., Hartl, F. U., Ban, N., Malmstrom, L., and Aebersold, R. (2012) Structural probing of a protein phosphatase 2A network by chemical cross-linking and mass spectrometry. *Science* **337**, 1348-1352
149. Ikehara, T., Ikehara, S., Imamura, S., Shinjo, F., and Yasumoto, T. (2007) Methylation of the C-terminal leucine residue of the PP2A catalytic subunit is unnecessary for the catalytic activity and the binding of regulatory subunit (PR55/B). *Biochem Biophys Res Commun* **354**, 1052-1057
150. Jacinto, E., Guo, B., Arndt, K. T., Schmelzle, T., and Hall, M. N. (2001) TIP41 interacts with TAP42 and negatively regulates the TOR signaling pathway. *Mol Cell* **8**, 1017-1026
151. McConnell, J. L., Gomez, R. J., McCorvey, L. R., Law, B. K., and Wadzinski, B. E. (2007) Identification of a PP2A-interacting protein that functions as a negative regulator of phosphatase activity in the ATM/ATR signaling pathway. *Oncogene* **26**, 6021-6030
152. McCluskey, A., Bowyer, M. C., Collins, E., Sim, A. T. R., Sakoff, J. A., and Baldwin, M. L. (2000) Anhydride modified cantharidin analogues: synthesis, inhibition of protein phosphatases 1 and 2A and anticancer activity. *Bioorg Med Chem Lett* **10**, 1687-1690
153. Buck, S. B., Hardouin, C., Ichikawa, S., Soenen, D. R., Gauss, C. M., Hwang, I., Swingle, M. R., Bonness, K. M., Honkanen, R. E., and Boger, D. L. (2003) Fundamental role of the fostriecin unsaturated lactone and implications for selective protein phosphatase inhibition. *J Am Chem Soc* **125**, 15694-15695